จุฬาลงกรณ์มหาวิทยาลัย
ทุนวิจัย
กองทุนรัชดาภิเษกสมโภช

รายงานวิจัย

การเปลี่ยนรูปก๊าซธรรมชาติที่มีองค์ประกอบคาร์บอกไดออกไซด์เพื่อผลิตก๊าซสังเคราะห์ภายใต้ระบบพลาสมาอุณหภูมิต่ำแบบไฟร่อนแบบหลายขั้นตอน

โดย

สุเมธ ชวเดช
ธรรมนูญ ศรีทะวงศ์
กฤติยา พรใหม่

กุมภาพันธ์ 2555

จุฬาลงกรณ์มหาวิทยาลัย
ทุนวิจัย
กองทุนรัชดาภิเษกสมโภช

รายงานวิจัย

การเปลี่ยนรูปก๊าซธรรมชาติที่มีองค์ประกอบคาร์บอกไดออกไซด์ เพื่อผลิตก๊าซสังเคราะห์ภายใต้ระบบพลาสมาอุณหภูมิต่ำแบบไฟร่อนแบบหลายขั้นตอน

โดย

สุเมธ ชวเดช
ธรรมนูญ ศรีทะวงศ์
กฤติยา พรใหม่

กุมภาพันธ์ 2555

Acknowledgments

This project was financially supported by The Ratchada Pisak Sompot Fund, Chulalongkorn University. The Excellence Center for Petroleum, Petrochemical and Advanced Materials is also acknowledged for providing all research facilities.

ชื่อโครงการวิจัย: "การเปลี่ยนรูปก๊าซธรรมชาติที่มีองค์ประกอบคาร์บอกไดออกไซด์เพื่อผลิตก๊าซสังเคราะห์ภายใต้ระบบพลาสมาอุณหภูมิต่ำแบบไฟฟ้าร่อนแบบหลายขั้นตอน"

ชื่อผู้วิจัย: ศ. ดร. สุเมธ ชวเดช, ผศ. ดร. ธรรมนูญ ศรีทะวงศ์, นางสาวกฤติยา พรใหม่

เดือนและปีที่ทำการวิจัย: เมษายน 2553

บทคัดย่อ

ส่วนที่ 1: ได้ทำการศึกษาผลกระทบของจำนวนเครื่องปฏิกรณ์ของระบบพลาสมาประกายไฟฟ้าร่อนอุณหภูมิต่ำแบบหลายขั้นตอนต่อประสิทธิภาพระบบร่วมการเปลี่ยนรูปและการออกซิเดชันบางส่วนของก๊าซธรรมชาติจำลองที่มีคาร์บอนไดออกไซด์เป็นองค์ประกอบโดยมีอัตราส่วนโดยโมลของมีเทน, อีเทน, โพรเพน, และคาร์บอนไดออกไซด์ เป็น 70:5:5:20 สำหรับการทดลองปฏิกิริยาออกซิเดชันแบบบางส่วนนั้น ออกซิเจนบริสุทธิ์หรืออากาศถูกนำมาใช้เป็นแหล่งออกซิเจนโดยมีอัตราส่วนระหว่างไฮโดรคาร์บอนต่อออกซิเจนเป็น 2/1 จากการศึกษาพบว่า ในระบบที่ไม่มีการออกซิเดชันบางส่วนและมีอัตราการไหลของสารตั้งต้นคงที่ ค่าการเปลี่ยนแปลงของสารตั้งต้นทั้งหมดยกเว้นคาร์บอนไดออกไซด์เพิ่มขึ้นเมื่อเพิ่มจำนวนเครื่องปฏิกรณ์จาก 1 ถึง 3 เครื่อง แต่ถ้าเพิ่มจำนวนเครื่องปฏิกรณ์มากกว่า 3 เครื่อง ค่าการเปลี่ยนแปลงของสารตั้งต้นจะไม่เปลี่ยนแปลง แต่อย่างไรก็ตามสำหรับระบบที่มีการควบคุมให้มีเวลาในการเกิดปฏิกิริยาคงที่ เฉพาะค่าการเปลี่ยนแปลงของโพรเพนเท่านั้นที่เพิ่มขึ้นเล็กน้อย ในขณะที่ค่าการเปลี่ยนแปลงของสารตั้งต้นตัวอื่นๆไม่เปลี่ยนแปลงมากนักเมื่อจำนวนของเครื่องปฏิกรณ์เพิ่มขึ้น เมื่อทำการเติมออกซิเจนให้แก่ระบบ พบว่าช่วยเพิ่มประสิทธิภาพในการเปลี่ยนรูปของก๊าซธรรมชาติเป็นอย่างมาก การใช้อากาศเป็นแหล่งของออกซิเจนส่งผลดีต่อ

ประสิทธิภาพของระบบมากกว่าการใช้ออกซิเจนบริสุทธิ์ ทั้งในรูปของค่าการเปลี่ยนแปลงของสารตั้งต้น และค่าการเลือกเกิดของผลิตภัณฑ์ที่ต้องการ โดยพบว่าค่าการใช้พลังงานไฟฟ้าที่เหมาะสมสำหรับการเปลี่ยนแปลงสารตั้งต้น คือ 3.21×10^{-18} วัตต์ วินาที ต่อโมเลกุลของสารตั้งต้นที่เปลี่ยนแปลงไป และ 2.57×10^{-18} วัตต์ วินาที ต่อโมเลกุลของไฮโดรเจนที่ผลิตได้ ซึ่งได้จากระบบที่มีการใช้อากาศเป็นแหล่งของออกซิเจนและใช้เครื่องปฏิกรณ์จำนวน 3 เครื่อง ที่เวลาของการเกิดปฏิกิริยาคงที่ที่ 4.38 วินาที

ส่วนที่ 2: โดยปกติแล้วก๊าซธรรมชาติประกอบด้วยมีทนเป็นส่วนใหญ่และมีคาร์บอบไดออกไซด์สูงถึง ๒๐% การผลิตทางการค้าก๊าซสังเคราะห์ (มีองค์ประกอบของไฮโดรเจนและคาร์บอนมอนออกไซด์) มักใช้กระบวนการตัวเร่งปฏิกิริยาของมีเทนที่แยกจากก๊าซธรรมชาติร่วมกับการเปลี่ยนรูปด้วยไอน้ำ แต่อย่างไรก็ตามกระบวนการตัวเร่งปฏิกิริยานี้ต้องควบคุมภายใต้อุณหภูมิและความดันสูง ดังนั้นการควบรวมระหว่างการเปลี่ยนรูปไอน้ำและพลาสมาอุณหภูมิต่ำจึงถูกพิจารณาเป็นวิธีการที่เป็นไปได้ในการเปลี่ยนรูปก๊าซธรรมชาติที่อุณหภูมิห้องและความดันบรรยากาศ ในงานวิจัยนี้ ระบบพลาสมาอุณหภูมิต่ำแบบประกายไฟฟ้าร่อนได้ถูกนำมาใช้ในการศึกษาผลกระทบของปริมาณไอน้ำและค่าปัจจัยการควบคุมระบบต่างๆ อาทิ อัตราการไหลของสารตั้งต้น ค่าความต่างศักย์ และค่าความถี่กระแสไฟฟ้าที่มีผลต่อประสิทธิภาพการเปลี่ยนรูปก๊าซธรรมชาติที่มีองค์ประกอบคาร์บอนไดออกไซด์ ผลการศึกษาเปิดเผยว่าค่าการเปลี่ยนแปลงของสารตั้งต้นทั้งหมดและค่าผลิตผลของไฮโดรเจนและคาร์บอนไดออกไซด์มีค่าสูงสุดที่ปริมาณไอน้ำมีค่า 10 โมล% อัตราการไหลของสารตั้งต้น 100 ลูกบาศก์เซนติเมตรต่อนาที ค่าความต่างศักย์ 13.5 กิโลโวลท์ และค่าความถี่ 300 เฮิรตซ์ โดยที่สภาวะเหมาะดังกล่าวให้ค่าพลังงาน

ไฟฟ้าที่ใช้สำหรับการเปลี่ยนแปลงสารตั้งต้นคือ 2.26 x 10^{-18} วัตต์วินาทีต่อโมเลกุลของสารตั้งต้นที่เปลี่ยนไป และ 1.58 x 10^{-18} วัตต์วินาทีต่อโมเลกุลของไฮโดรเจนที่ผลิตได้

ส่วนที่ 3: ในการศึกษานี้ ได้ทำการทดลองวิธีการร่วมระหว่างการเปลี่ยนรูปโดยไอน้ำและการออกซิเดชันบางส่วนของก๊าซธรรมชาติที่มีคาร์บอนไดออกไซด์เป็นองค์ประกอบภายใต้ประกายไฟฟ้าแบบร่อน โดยได้ทำการศึกษาอิทธิพลของปัจจัยการควบคุมระบบต่างๆ ได้แก่ อัตราส่วนโมลที่เติมของไฮโดรคาร์บอนต่อออกซิเจน, ความต่างศักย์ไฟฟ้า, ความถี่กระแสไฟฟ้า, และระยะห่างระหว่างขั้วไฟฟ้า ที่มีผลต่อการเปลี่ยนแปลงสารตั้งต้น, การเลือกเกิดและผลิตผลของผลิตภัณฑ์ต่างๆ, และพลังงานที่ใช้ ผลการทดลองแสดงให้เห็นว่า การเพิ่มขึ้นของการเปลี่ยนแปลงของมีเทนหรือผลิตผลของก๊าซสังเคราะห์เมื่อมีการเพิ่มของความต่างศักย์ไฟฟ้าและระยะห่างระหว่างขั้วไฟฟ้า แต่ได้ผลตรงกันข้ามเมื่อมีการเพิ่มขึ้นของอัตราส่วนโมลที่เติมของไฮโดรคาร์บอนต่อออกซิเจนและความถี่กระแสไฟฟ้า ที่สภาวะเหมาะสมคือ อัตราส่วนโมลที่เติมของไฮโดรคาร์บอนต่อออกซิเจนเท่ากับ 2/1, ความต่างศักย์ไฟฟ้าเท่ากับ 14.5 กิโลโวลท์, ความถี่กระแสไฟฟ้าเท่ากับ 300 เฮิรตซ์, และระยะห่างระหว่างขั้วไฟฟ้าเท่ากับ 6 มม ให้การการเปลี่ยนแปลงทั้งออกซิเจนและมีเทนที่สูงกว่า การเลือกเกิดก๊าซสังเคราะห์ที่สูงกว่า และความต้องการพลังงานที่ต่ำกว่า เมื่อเปรียบเทียบกับกระบวนการอื่นๆ (การเปลี่ยนรูปของก๊าซธรรมชาติอย่างเดียว, การเปลี่ยนรูปของก๊าซธรรมชาติด้วยไอน้ำ, และการเปลี่ยนรูปของก๊าซธรรมชาติร่วมกับการออกซิเดชันบางส่วน)

Project Title: "Reforming of CO_2-Containing Natural Gas for Synthesis Gas Production in Low-Temperature Multistage Gliding Arc Plasma System"

Name of the Investigators: Prof. Dr. Sumaeth Chavadej, Asst. Prof. Dr. Thammanoon Sreethawong, and Ms. Krittiya Pornami

Year: April, 2010

Abstract

Part 1: The effect of stage number of multistage AC gliding arc discharge reactors on the process performance of the combined reforming and partial oxidation of simulated CO_2-containing natural gas having a CH_4:C_2H_6:C_3H_8:CO_2 molar ratio of 70:5:5:20 was investigated. For the experiments with partial oxidation, either pure oxygen or air was used as the oxygen source with a fixed hydrocarbon-to-oxygen molar ratio of 2/1. Without partial oxidation at a constant feed flow rate, all conversions of hydrocarbons, except CO_2, greatly increased with increasing number of stages from 1 to 3; but beyond 3 stages, the reactant conversions remained almost unchanged. However, for a constant residence time, only C_3H_8 conversion gradually increased, whereas the conversions of the other reactants remained almost unchanged. The addition of oxygen was found to significantly enhance the process performance of natural gas reforming. The utilization of air as an oxygen source showed a superior process performance to pure oxygen in terms of reactant conversion and desired product selectivity. The optimum energy consumption of 12.059×10^{24} eV per mole of reactants converted and 9.659×10^{24} eV per mole of hydrogen produced was obtained using air as an oxygen source and 3 stages of plasma reactors at a constant residence time of 4.38 s.

Part 2: Generally, natural gas mainly contains methane with a very high carbon dioxide content up to 20 %. Synthesis gas (a mixture of hydrogen and carbon monoxide) is produced commercially by using the conventional catalytic processes of methane separated from natural gas with steam reforming; however, the catalytic processes have to be operated under high temperatures and pressures. Therefore, the combination of steam reforming and non-thermal plasma is considered to be a new promising way for the reforming of natural gas at ambient temperature and atmospheric pressure without a catalyst required. In this present work, a low-temperature gliding arc discharge system was employed to investigate the effects of steam content and operational parameters, i.e. total feed flow rate, applied voltage, and input frequency, on the reforming performance of CO_2-containing natural gas. The results reveal that the reactant conversions and yields of hydrogen and carbon monoxide were found to reach maximum values at a steam content of 10 mol%, a total feed flow rate of 100 cm^3/min, an applied voltage 13.5 kV, and an input frequency 300 Hz. Under these optimum conditions, the power consumptions were as low as 2.26×10^{-18} Ws (14.10 eV) per reactant molecule converted and 1.58×10^{-18} Ws (9.85 eV) per molecule of produced hydrogen.

Part 3: In this study, a technique of combining steam reforming with partial oxidation of CO_2-containing natural gas In a gliding arc discharge plasma was investigated. The effects of several operating parameters including: hydrocarbons (HCs)/O_2 feed molar ratio; applied voltage; input frequency; and electrode gap distance; on reactant conversions, product selectivities and yields, and power consumptions were examined. The results showed an increase in either methane (CH_4) conversion or synthesis gas yield with increasing applied voltage and electrode gap distance, whereas the opposite trends

were observed with increasing HCs/O_2 feed molar ratio and input frequency. The optimum conditions were found at a HCs/O_2 feed molar ratio of 2/1, an applied voltage of 14.5 kV, an input frequency of 300 Hz, and an electrode gap distance of 6 mm, providing high CH_4 and O_2 conversions with high synthesis gas selectivity and relatively low power consumptions, as compared with the other processes (sole natural gas reforming, natural gas reforming with steam, and combined natural gas reforming with partial oxidation).

Table of Contents

List of Table

List of Figures

Part 1: Combined Reforming and Partial Oxidation of CO_2-Containing Natural Gas Using an AC Multistage Gliding Arc Discharge System: Effect of Stage Number of Plasma Reactors (published in *Plasma Chemistry and Plasma Processing*)

1.1 Introduction and Survey of Related Literature

In recent years, natural gas has become one of the most useful energy resources in the world due to the depletion of oil reserves. Therefore, the value of natural gas as an alternative fuel is currently increasing [1]. Generally, natural gas contains a large amount of methane and significant amounts of ethane, propane, carbon dioxide, and nitrogen, and its composition varies according to the geological conditions in different parts of the world. Because methane is not only an inexpensive fuel but also an environmentally safe fuel, attempts of converting methane to hydrogen and higher hydrocarbons with alternatives of new technology have been increasingly studied. Moreover, the direct utilization of methane and carbon dioxide has been area of great interest due to its environmentally friendly concept for decreasing greenhouse gas emission.

In carbon dioxide reforming of methane, the natural gas can be used as a potential feed to produce synthesis gas or syngas, a mixture of hydrogen and carbon monoxide, which is used in various petrochemical processes, such as methanol synthesis and the so-called Fischer-Tropsch synthesis to produce liquid hydrocarbons. It has raised interest in its use as an alternative energy source because of the two main advantages of producing the hydrogen energy and reducing the greenhouse effect simultaneously. Nevertheless, carbon dioxide reforming of methane, as shown in Eq. (1), using conventional catalytic methods often encounters two problems. It is a highly endothermic

reaction consuming much energy, and the deactivation of catalysts used due to coke deposition on the catalyst surface usually occurs under various reaction conditions [2].

Carbon dioxide reforming of methane;

$$CH_4 + CO_2 \longrightarrow 2CO + 2H_2 \qquad \Delta H_{298K} = 247 kJ/mol \qquad (1)$$

The second route for methane conversion to syngas is the steam reforming, as shown in Eq. (2). This reaction is also highly endothermic, which is the same as the carbon dioxide reforming, resulting in high energy consumption. Steam reactors generally run with excess amounts of water in order to prevent the deposition of carbon on catalysts [3]. Steam reforming of methane has poor selectivity to CO and produces syngas with a high H_2/CO ratio, while carbon dioxide reforming of methane gives a high CO selectivity [4].

Steam reforming of methane;

$$CH_4 + H_2O \longrightarrow CO + 3H_2 \qquad \Delta H_{298K} = 206.2 kJ/mol \qquad (2)$$

Another way to produce syngas is catalytic partial oxidation of methane as shown in Eq. (3). The catalysts investigated are mainly supported Ni and noble metal catalysts. The latter are more active but comparatively cost-ineffective, while nickel-based catalysts show high activity and selectivity with low cost but coke deposition on nickel occurs much easier than on noble metals [5]. This process gives high activity and selectivity but cannot be easily controlled because of the generation of hot spots in the catalytic bed due to its exothermic nature [4].

Partial oxidation of methane;

$$CH_4 + \tfrac{1}{2} O_2 \longrightarrow CO + 2H_2 \qquad \Delta H_{298K} = -38 kJ/mol \qquad (3)$$

The combination of these reactions can potentially provide good and synergistic results. For example, a combination of carbon dioxide reforming and steam reforming of methane can reduce the carbon formation on the catalyst surface because the C/H ratio, as well as the C/O ratio, in the feed decrease, resulting in a controlled and limited carbon formation [6]. In addition, a combination of carbon dioxide reforming and partial oxidation of methane has a benefit in terms of balancing the heat load [7, 8].

One attractive method for reforming hydrocarbon compounds is to use non-thermal plasma processes. The plasma contains highly active species, such as electron, ions, and radicals, which can catalyze conversions of feed into more valuable products. The non-thermal plasma processes basically generate energetic electrons by applying a high voltage across electrodes to create electric discharge. The electric discharge produced also provides heat to the system, apart from generating radical and excited species to initiate and enhance the plasma chemical reactions [9]. Furthermore, the plasma reforming processes can be operated at mild conditions with less power consumption, and they have been employed for many applications [10-13]. A gliding arc discharge is a new discharge type of non-thermal plasma, which successfully provides the most effective non-equilibrium plasma with high productivity and good selectivity. The gliding arc discharge has at least two diverging knife-shaped electrodes, which are placed in a rapid gas flow of feed gas. A high voltage is generated across the fast gas between the electrodes. The electric discharge initially forms at the narrowest gap and then spreads along the knife-edges of the electrodes and finally disappears. New discharges instantaneously reform at the initial point repeatedly. Therefore, there are several researches reporting the utilization of gliding arc discharge for many purposes, including natural gas and methane conversion for production of higher hydrocarbons and synthesis

gas [14-16].

The purpose of this study was to apply the multistage gliding arc plasma system for a combined reforming and partial oxidation of simulated natural gas, which contained a CH_4:C_2H_6:C_3H_8:CO_2 molar ratio of 70:5:5:20, to produce hydrogen and higher hydrocarbons. The effects of the stage number of plasma reactor was mainly investigated on the system performance under two series of system with fixed feed flow rate and fixed residence time. Both pure oxygen and air were comparatively used as the oxygen source. The optimum stage number with corresponding power consumption was obtained.

1.2 Procedure

1.2.1. Reactant Gases

Simulated natural gas containing methane, ethane, propane, and carbon dioxide, with a CH_4:C_2H_6:C_3H_8:CO_2 molar ratio of 70:5:5:20, was specially produced for this research by Thai Industry Gas (Public) Co., Ltd. Ultra-high purity oxygen, air zero, H_2 with 99.99% purity, and helium used for performing the combined plasma reforming and partial oxidation of the simulated natural gas with partial oxidation and GC analysis, were also supplied by Thai Industry Gas (Public) Co., Ltd.

1.2.2. Multistage Gliding Arc Discharge System

The experimental set-up of the AC multistage gliding arc discharge system with 4 stages in series and the configuration of each reactor are shown in Figures 1 and 2, respectively. The gliding arc reactors were made of a glass tube with 9 cm OD and an 8.5 cm ID. Each reactor had two diverging knife-shaped electrodes that were fabricated from stainless steel sheets with 1.2 cm width for each electrode. The gap distance between the pair of electrodes was fixed at 6 mm. Two Teflon sheets were placed at the top and

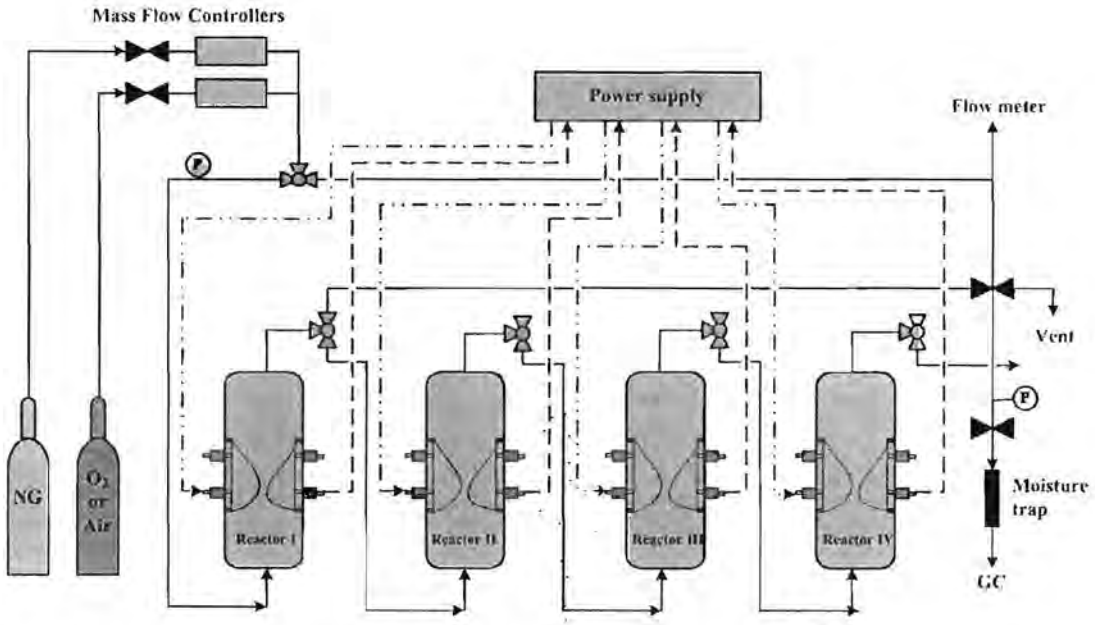

Figure 1.1 The schematic of the multistage gliding arc discharge system.

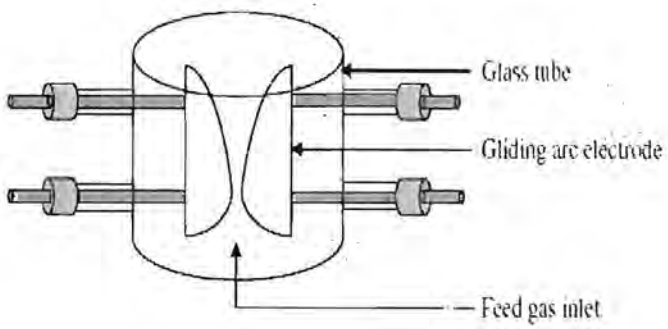

Figure 1.2 Schematic of the gliding arc reactor.

bottom of the electrodes to force the feed gas to pass through the reaction zone. The flow rates of the reactant gases were regulated by a set of mass flow controllers and transducers supplied by SIERRA® Instrument, Inc. The 7 μm stainless steel filters were placed upstream of all mass flow controllers in order to trap any solid particles in the

reactant gases. The check valves were also placed downstream of the mass flow controllers to prevent any back flow. All of the reactant gases and steam were well mixed and introduced upward into the first reactor at ambient temperature and atmospheric pressure. The compositions of the feed gas mixture and the effluent gases were analyzed by an on-line gas chromatograph (HP, 5890), equipped with Carboxen 1000 packed column and a thermal conductivity detector (TCD).

For any studied conditions, the feed gas mixture was first introduced into the gliding arc system without turning on the power supply unit. After the composition of outlet gas was constant, the power supply unit was turn on. The outlet gas composition was analyzed every 30 min by the on-line GC. After the system reached steady state, an analysis of outlet gas composition was taken at least few times every hour. The experimental data were averaged to evaluate the process performance. During the experiments, the temperature at the reactor wall was found to be in the range of 150-200°C. Since the volume of the reactor outlet zone was rather large, the outlet gas was cooled close to room temperature. It was observed that a small amount of water droplets appeared on the surrounding inner wall of the gliding arc reactor during the experiment of combined plasma reforming and partial oxidation of CO_2-containing natural gas. The flow rates of both the feed and the outlet gases were measured by using a bubble flow meter because of the gas volume change after the reaction.

A power supply unit used in this research was operated in three steps. For the first step, the domestic AC input of 220 V and 50 Hz was converted to a DC output of 70 V by a DC power supply converter. For the second step, a 500 W power amplifier with a function generator was used to convert the DC to AC with the sinusoidal waveform. For the final step, the output voltage was stepped up by using two transformers in series. The

output voltage and frequency were controlled by the function generator. Since the plasma generated in each plasma reactor is non-equilibrium in nature, it is not possible to measure the voltage across the electrodes of the reactor (high-side voltage). Therefore, the low-side voltage and current were measured instead, and the high-side voltage and current were then calculated by multiplying and dividing by a factor of 130, respectively. A power analyzer was used to measure power, power factor, current, frequency, and voltage at the low side of the power supply unit. Based on our previous work on the combined reforming and partial oxidation of CO_2-containing natural gas using a single-stage gliding arc discharge system[15], the obtained optimum operating conditions (an applied voltage of 17.5 kV, an input frequency of 300 Hz, and a hydrocarbons-to-oxygen molar ratio of 2/1) were used for the combined reaction under multistage gliding arc discharge in this study.

To evaluate the process performance, the conversions of reactant fee and the selectivities for product were considered.

In general, the conversion of reactant is defined as:

$$\% \text{ conversion} = \frac{(\text{moles of reactant in} - \text{moles of reactant out})(100)}{\text{moles of reactant in}} \qquad (4)$$

The percent selectivity of products containing carbon atoms is defined on the basis of the amount of carbon converted from the reactants into any specified products. In case of hydrogen product, the hydrogen selectivity is calculated based on hydrogen converted from the reactants.

$$\% \text{ selectivity of any hydrocarbon product} = [P](C_P)(100) / \sum[R](C_R) \qquad (5)$$

where [P] = moles of product in effluent;

[R] = moles of reactant in feed to be converted;

C_P = numbers of carbon atom in a product molecule;

C_R = numbers of carbon atom in a reactant molecule

$$\% \text{ selectivity of hydrogen} = [P](H_P)(100) / \sum[R](H_R) \quad (6)$$

where H_P = numbers of hydrogen atom in a product molecule;

H_R = numbers of hydrogen atom in a reactant molecule.

The product yield is formulated as follows:

$$\% \text{ yield of } C_2 \text{ hydrocarbons} = \sum(\% \text{ conversion of } CH_4, C_2H_6, C_3H_8, CO_2) \times \sum(\% \text{ selectivity of } C_2H_2, C_2H_4, C_2H_6) / (100) \quad (7)$$

$$\% \text{ yield of } H_2 = \sum(\% \text{ conversion of } CH_4, C_2H_6, C_3H_8) \times (\% \text{ selectivity of } H_2) / 100 \quad (8)$$

The specific energy consumption is calculated in a unit of Ws per a C-containing reactant molecule converted or per a hydrogen molecule produced (Ws/M) using the following equation:

$$\text{Specific energy consumption} = (P)\,(60) / (\tilde{N})\,(M) \quad (9)$$

where P = Power (W);

$\tilde{N}$ = Avogadro's number (6.02×10^{23} molecules·g-mole^{-1});

M = Rate of converted carbon in feed or rate of produced hydrogen molecule (g-mole·min^{-1})

1.3. Results and Discussion

In a plasma environment, the highly energetic electrons generated by gliding arc discharge collide with the gaseous molecules of hydrocarbons and CO_2, creating a variety of chemically active radicals. All the possibilities of chemical pathways occurring under the studied conditions were briefly described below to provided a better comprehensive understanding of the plasma reforming reactions of natural gas containing CO_2 under AC non-thermal gliding arc discharge, both without and with partial oxidation. In the absence of oxygen, the radicals of oxygen-active species are produced during the collisions between electrons and CO_2, as shown in Eqs. 10 and 11. Moreover, the produced CO can be further dissociated by the collisions with electrons to form coke and oxygen-active species (Eq. 12). In the case of added oxygen for partial oxidation, a large amount of oxygen-active species can be produced from the collisions between electrons and oxygen molecules, as described by Eqs. 13-15. Eqs. 16-28 show the collisions between electrons and all hydrocarbons presented in the feed to produce hydrogen and various hydrocarbon species for subsequent reactions.

Electron-carbon dioxide collisions:

Dissociation reactions of carbon dioxide;

$$e^- + CO_2 \rightarrow CO + O^- \quad (10)$$

$$e^- + CO_2 \rightarrow CO + O + e^- \quad (11)$$

$$e^- + CO \rightarrow C + O + e^- \quad (12)$$

Electron-oxygen collisions:

Dissociation attachment of oxygen;

$$e^- + O_2 \rightarrow 2O + e^- \rightarrow O^- + O \quad (13)$$

Attachment of oxygen;

$$e^- + O_2 \rightarrow O_2^- \quad (14)$$

Dissociation of oxygen;

$$e^- + O_2 \rightarrow 2O + e^- \quad (15)$$

Electron-methane collisions:

$$e^- + CH_4 \rightarrow CH_3 + H + e^- \quad (16)$$

$$e^- + CH_3 \rightarrow CH_2 + H + e^- \quad (17)$$

$$e^- + CH_2 \rightarrow CH + H + e^- \quad (18)$$

$$e^- + CH \rightarrow C + H + e^- \quad (19)$$

$$H + H \rightarrow H_2 \quad (20)$$

Electron-ethane collision:

$$e^- + C_2H_6 \rightarrow C_2H_5 + H + e^- \quad (21)$$

$$e^- + C_2H_5 \rightarrow C_2H_4 + H + e^- \quad (22)$$

$$e^- + C_2H_4 \rightarrow C_2H_3 + H + e^- \quad (23)$$

$$e^- + C_2H_3 \rightarrow C_2H_2 + H + e^- \quad (24)$$

$$e^- + C_2H_6 \rightarrow CH_3 + CH_3 + e^- \quad (25)$$

Electron-propane collision:

$$e^- + C_3H_8 \rightarrow C_3H_7 + H + e^- \quad (26)$$

$$e^- + C_3H_7 \rightarrow C_3H_6 + H + e^- \quad (27)$$

$$e^- + C_3H_8 \rightarrow C_2H_5 + CH_3 + e^- \quad (28)$$

The oxygen-active species derived from CO_2 and O_2 can further extract hydrogen atoms from the molecules of hydrocarbon gases via the oxidative dehydrogenation reactions (Eqs. 29-41), consequently producing several chemically active radicals and water.

Oxidative dehydrogenation reactions:

$$CH_4 + O \rightarrow CH_3 + OH \quad (29)$$

$$C_2H_6 + O \rightarrow C_2H_5 + OH \quad (30)$$

$$C_2H_5 + O \rightarrow C_2H_4 + OH \quad (31)$$

$$C_2H_4 + O \rightarrow C_2H_3 + OH \quad (32)$$

$$C_2H_3 + O \rightarrow C_2H_2 + OH \quad (33)$$

$$C_3H_8 + O \rightarrow C_3H_7 + OH \quad (34)$$

$$CH_4 + OH \rightarrow CH_3 + H_2O \quad (35)$$

$$C_2H_6 + OH \rightarrow C_2H_5 + H_2O \quad (36)$$

$$C_2H_5 + OH \rightarrow C_2H_4 + H_2O \quad (37)$$

$$C_2H_4 + OH \rightarrow C_2H_3 + H_2O \quad (38)$$

$$C_2H_3 + OH \rightarrow C_2H_2 + H_2O \quad (39)$$

$$C_3H_8 + OH \rightarrow C_3H_7 + H_2O \quad (40)$$

$$C_3H_7 + OH \rightarrow C_3H_6 + H_2O \quad (41)$$

The C_2H_5, C_2H_3, and C_3H_7 radicals can further react to form ethylene, acetylene, and propene either by electron collision (Eqs. 22-24, and 27) or by oxidative dehydrogenation reaction (Eqs. 31-33, 37-39, and 41). The extracted hydrogen atoms immediately form hydrogen gas according to Eq. 20. However, no propene was detected in the outlet gas stream. It is therefore believed that the propene species was unstable and may probably undergo further reactions (Eqs. 42 and 43).

Propene hydrogenation and cracking reactions:

$$C_3H_6 + H_2 \rightarrow C_3H_8 \quad (42)$$

$$C_3H_6 \rightarrow C_2H_2 + CH_4 \quad (43)$$

In addition, the radicals of hydrocarbons and hydrogen derived from the earlier reactions react further to combine with one another to form ethane, ethylene, acetylene,

propane, and butane, as shown in Eqs. 44-59. In addition, ethane can be further dehydrogenated to form ethylene, while ethylene can also be dehydrogenated to form acetylene by either electron collision or oxidative dehydrogenation (Eqs. 21, 22, 30, 31, 36, and 37 for ethylene formation; and, Eqs. 23, 24, 32, 33, 38, and 39 for acetylene formation).

Coupling reactions of active species:

Ethane formation;

$$CH_3 + CH_3 \rightarrow C_2H_6 \quad (44)$$

$$C_2H_5 + H \rightarrow C_2H_6 \quad (45)$$

$$C_2H_5 + C_2H_5 \rightarrow C_2H_6 + C_2H_4 \quad (46)$$

$$C_3H_7 + CH_3 \rightarrow C_2H_6 + C_2H_4 \quad (47)$$

Ethylene formation;

$$CH_2 + CH_2 \rightarrow C_2H_4 \quad (48)$$

$$CH_3 + CH_3 \rightarrow C_2H_4 + H_2 \quad (49)$$

$$C_2H_5 + H \rightarrow C_2H_4 + H_2 \quad (50)$$

$$C_3H_7 + H \rightarrow C_2H_4 + CH_4 \quad (51)$$

Acetylene formation;

$$CH + CH \rightarrow C_2H_2 \quad (52)$$

$$CH_2 + CH_2 \rightarrow C_2H_2 + H_2 \quad (53)$$

$$CH_3 + CH \rightarrow C_2H_2 + H_2 \quad (54)$$

$$C_2H_5 + H \rightarrow C_2H_2 + H_2 + H_2 \quad (55)$$

$$C_3H_7 + H \rightarrow C_2H_2 + CH_4 + H_2 \quad (56)$$

Propane formation;

$$C_2H_5 + CH_3 \rightarrow C_3H_8 \quad (57)$$

Butane formation;

$$C_2H_5 + C_2H_5 \rightarrow C_4H_{10} \quad (58)$$

$$C_3H_7 + CH_3 \rightarrow C_4H_{10} \quad (59)$$

Moreover, a significant amount of CO and a very small amount of water were

produced under the studied conditions, particularly in feed with high oxygen content. CO may be mainly formed via the partial oxidation reactions of the hydrocarbon reactants. Eqs. 60-64 show the partial oxidative pathways of methane to form CO and H_2 as the end products. The formation of water is believed to occur via the oxidative hydrocarbon reactions (Eqs. 35-41). In addition, water can be formed by the reactions between hydrogen or active hydrogen radical and active oxygen radical, as shown in Eqs. 65-67.

Carbon monoxide formation:

$$CH_3 + O \rightarrow HCHO + H \quad (60)$$

$$HCHO + O \rightarrow OH + CHO \quad (61)$$

$$CHO + O \rightarrow OH + CO \quad (62)$$

$$CHO + OH \rightarrow CO + H_2O \quad (63)$$

$$CHO + H \rightarrow H_2 + CO \quad (64)$$

Water formation:

$$2H + O \rightarrow H_2O \quad (65)$$

$$H_2 + O \rightarrow H_2O \quad (66)$$

$$H_2 + \tfrac{1}{2} O \rightarrow H_2O \quad (67)$$

Additionally, hydrocarbon molecules may crack to form carbon and hydrogen via thermal cracking reactions (Eqs. 68-70).

$$CH_4 \rightarrow C + 2H_2 \quad (68)$$

$$C_2H_6 \rightarrow 2C + 3H_2 \quad (69)$$

$$C_3H_8 \rightarrow 3C + 4H_2 \quad (70)$$

1.3.1 Reforming of Natural Gas without Partial Oxidation

1.3.1.1 Effect of Feed Flow Rate at Constant Residence Time

The effect of feed flow rate of reactant gases at a constant residence time was initially investigated to evaluate how it affected the process performance.

1.3.1.1.1 Effect on reactant conversion and product yield

The results of the reactant conversions and product yields as a function of stage number of plasma reactors when varying feed flow rate at a fixed residence time of 4.38 s are illustrated in Figure 1.3. The stage number of plasma reactors was varied from 1 to 4 stages. For each stage of plasma reactors, the feed flow rate was controlled at 31.25, 62.50, 93.75, and 125 cm^3/min, respectively, in order to maintain the same residence

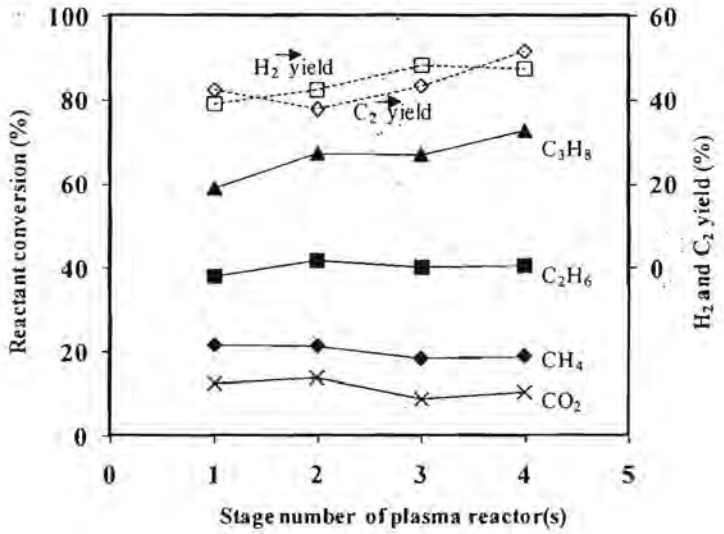

Figure 1.3 Effect of stage number of plasma reactors on reactant conversions and product yields for reforming of natural gas without partial oxidation in the case of varying feed flow rate (applied voltage, 17.5 kV; frequency, 300 Hz; electrode gap distance, 6 mm; and residence time, 4.38 s).

time. The results show that only the conversion of C_3H_8 gradually increased with increasing stage number, whereas the conversion of other reactant components remained almost unchanged. It can be confirmed by the concentrations of outlet gases, as presented in Figure 1.4, that the concentration of C_3H_8 sharply decreased, whereas the CH_4 concentration was nearly unchanged. The explanation is that the conversion of reactant gases depends upon the collision between the highly energetic electrons and reactant gases, which can be controlled by adjusting residence time. However, the plasma operation in this experimental part was performed at a constant residence time, so the probability of collision between reactant gas molecules and highly energetic electrons is

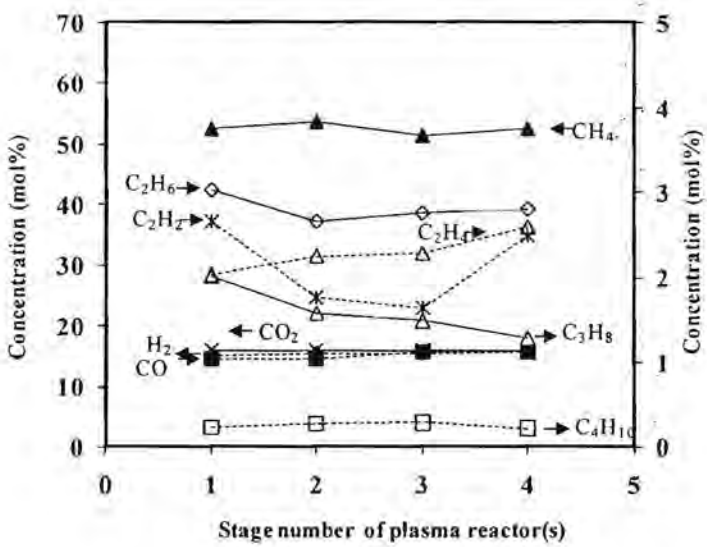

Figure 1.4 Effect of stage number of plasma reactors on concentrations of outlet gases for reforming of natural gas without partial oxidation in the case of varying feed flow rate (applied voltage, 17.5 kV; frequency, 300 Hz; electrode gap distance, 6 mm; and residence time, 4.38 s).

quite the same for all stages of plasma reactors, causing the slightly changed conversion of reactant gases. Therefore, when the residence time was fixed, the conversion of reactant gases in simulated natural gas was not much affected by the stage number of plasma reactors. Moreover, the H_2 and C_2 yields only slightly increased with increasing stage number of plasma reactors. It can be suggested that the coupling reactions of the active species and oxidative dehydrogenation reactions may not be significantly affected by the stage number as well.

1.3.1.1.2 Effect on product selectivity

The effect of stage number of plasma reactors on the selectivities for H_2, C_2H_2, C_2H_4, C_4H_{10}, and CO is depicted in Figure 1.5. The selectivities for H_2 and C_2H_4 tended to slightly increase with increasing stage number from 1 to 3 stages, and the

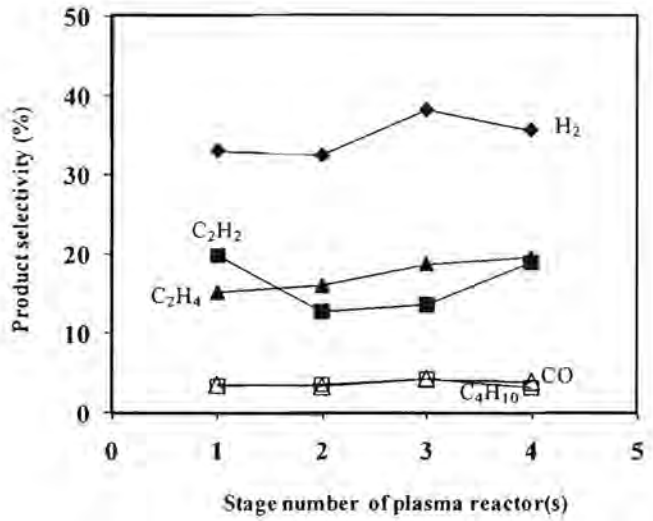

Figure 1.5 Effect of stage number of plasma reactors on product selectivities for reforming of natural gas without partial oxidation in the case of varying feed flow rate (applied voltage, 17.5 kV; frequency, 300 Hz; electrode gap distance, 6 mm; and residence time, 4.38 s).

selectivities for CO and C_4H_{10} were almost unchanged with the stage number of plasma reactors. The results are relevant to the molar ratios of H_2/C_2H_2 and C_2H_4/C_2H_2, as shown in Figure 1.6, while the molar ratio of H_2/C_2H_4 gradually decreased. This implies that the increase in C_2H_4 production exceeds the increase in H_2 production, resulting in the gradual decrease in H_2/C_2H_4 ratio. It should be therefore noted that the hydrogenation of C_2H_2 more favorably occurs than the coupling reaction of hydrocarbon active species with increasing stage number of plasma reactors from 1 to 3 stages, leading to the consumption of H_2 for some extent to produce C_2H_4. At 3 stages of the plasma reactors, the maximum selectivity for H_2 was obtained at approximately 38.23 %. From this point of view, it could be concluded that the increase in stage number of plasma reactors from 1

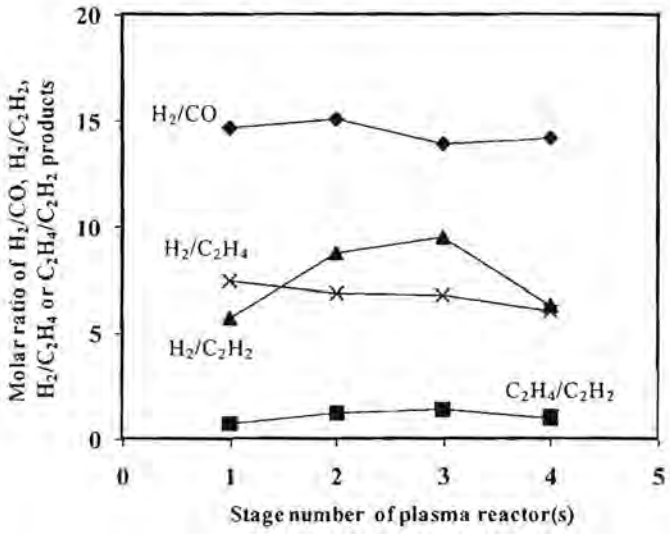

Figure 1.6 Effect of stage number of plasma reactors on product molar ratios for reforming of natural gas without partial oxidation in the case of varying feed flow rate (applied voltage, 17.5 kV; frequency, 300 Hz; electrode gap distance, 6 mm; and residence time, 4.38 s).

to 3 stages assists in improving the desired product selectivity, anyhow it did not provide the synergistic effect on the reactant conversion.

1.3.1.1.3 Effect on power consumption

The effect of stage number of plasma reactors on power consumptions per reactant molecule converted and per hydrogen molecule produced is shown in Figure 1.7. The power consumption per hydrogen molecule produced sharply declined from 1 to 2 stages of plasma reactors and then gradually decreased with increasing stage number from 2 to 4 stages, while the power consumption per reactant molecule converted also decreased in the same trend as the power consumption per hydrogen molecule produced when the stage number was increased from 1 to 2 stages but became almost unchanged The minimum power consumptions were about 2.75×10^{-18} Ws (17.18 eV) per molecule

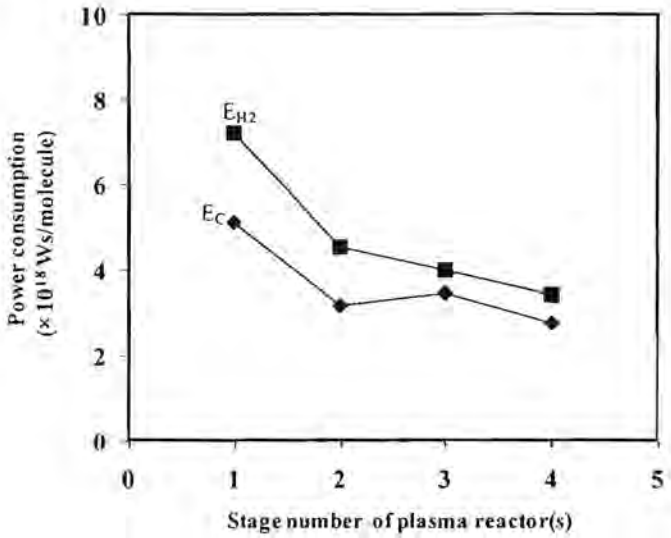

Figure 1.7 Effect of stage number of plasma reactors on power consumptions for reforming of natural gas without partial oxidation in the case of varying feed flow rate (applied voltage, 17.5 kV; frequency, 300 Hz; electrode gap distance, 6 mm; and residence time, 4.38 s).

with further increasing stage number to 4 stages. of converted reactant and 3.41×10^{-18} Ws (21.28 eV) per molecule of produced hydrogen at the stage number of 4 stages.

1.3.1.2 Effect of Residence Time at Constant Feed Flow Rate

Since the effect of feed flow rate at a constant residence time was found to insignificantly affect the process performance, the effect of residence time at a constant feed flow rate was next comparatively investigated.

1.3.1.2.1 Effect on reactant conversion and product yield

The results of the reactant conversions and product yields as a function of stage number of plasma reactors when varying residence time at a fixed feed flow rate of 125 cm^3/min are illustrated in Figure 1.8. For each stage of plasma reactors, the residence time was controlled at 1.09, 2.19, 3.29, and 4.38 s, respectively, in order to maintain the

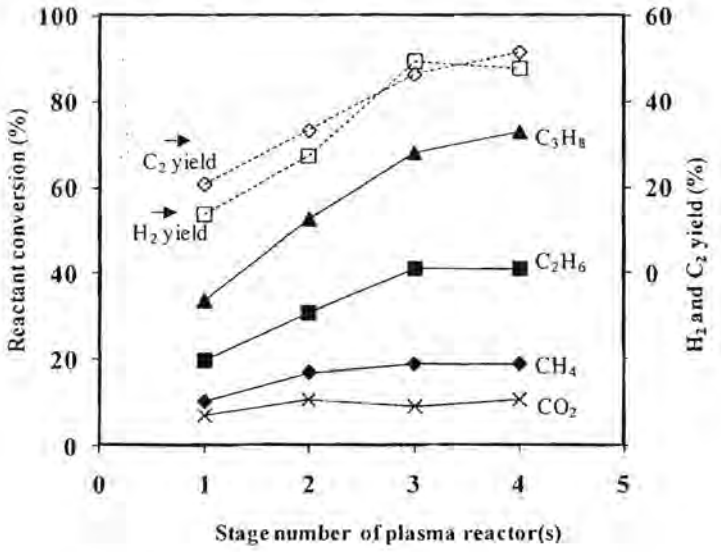

Figure 1.8 Effect of stage number of plasma reactors on reactant conversions and product yields for reforming of natural gas without partial oxidation in the case of varying residence time (applied voltage, 17.5 kV; frequency, 300 Hz; electrode gap distance, 6 mm; and feed flow rate, 125 cm^3/min).

same feed flow rate. The conversions of all hydrocarbons, except CO_2, considerably increased due to the longer residence time or contact time in the plasma reaction zone with increasing number of stage from 1 to 3 stages. Beyond the 3 stages, only propane conversion increased, but other reactant conversions remained almost unchanged. Comparatively, the propane conversion increased rapidly with increasing stage number of plasma reactors, whereas the methane conversion tended to slightly increase. The conversions of all reactant gases were in the following order: propane > ethane > methane > CO_2, resulting from their bond dissociation energies, which are 4.33, 4.35, 4.55, and 5.52 eV, respectively. The higher bond dissociation energy leads to more difficulty to be dissociated for further reacting to form other species (Dean, 1999). It can be supposed that the unchanged CO_2 conversion might be due to its relatively much higher bond dissociation energy. For the H_2 and C_2 yields, the increase in residence time due to the increase in the stage number of plasma reactors enhances the conversion of all reactants, as aforementioned, and consequently leads to increasing production yields. The outlet concentrations of all reactant gases shown in Figure 1.9 significantly decreased with increasing stage number of reactors from 1 to 3 stages except that the concentration of CO_2 remained unchanged due to the almost constant CO_2 conversion.

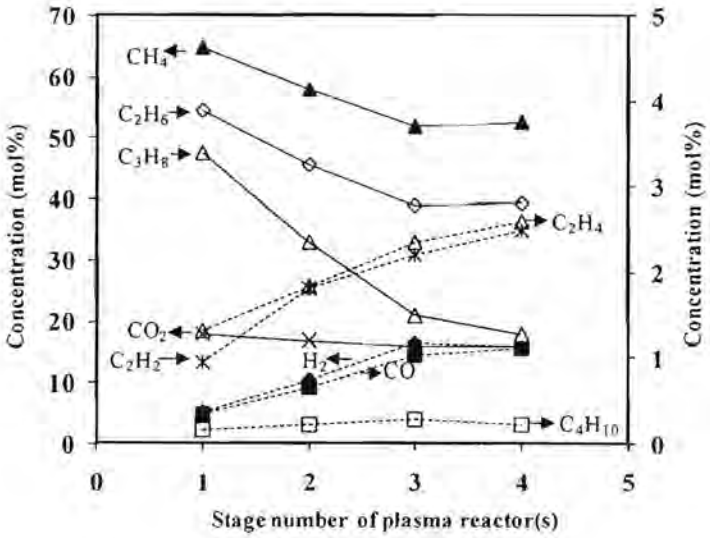

Figure 1.9 Effect of stage number of plasma reactors on concentrations of outlet gases for reforming of natural gas without partial oxidation in the case of varying residence time (applied voltage, 17.5 kV; frequency, 300 Hz; electrode gap distance, 6 mm; and feed flow rate, 125 cm^3/min).

1.3.1.2.2 Effect on product selectivity

Figure 1.10 illustrates the effect of stage number of plasma reactors on the product selectivities. The experimental results reveal that the selectivities for H_2 and C_2H_2 tended to increase with increasing stage number of plasma reactors, whereas those for C_2H_4, C_4H_{10}, and CO remained almost unchanged. This implies that the oxidative dehydrogenation is preferable at high residence time. As confirmed by the product molar ratios in Figure 1.11, the H_2/C_2H_4 ratio increased with increasing stage number of plasma reactors from 1 to 3 stages, and also the molar ratio of C_2H_4/C_2H_2 slightly decreased, suggesting that the dehydrogenation of C_2H_4 is likely to occur when the stage number of plasma reactors is increased. Moreover, the coupling reaction of hydrogen radicals could occur and resulted in the great increase in the selectivity for H_2 at 3 stages

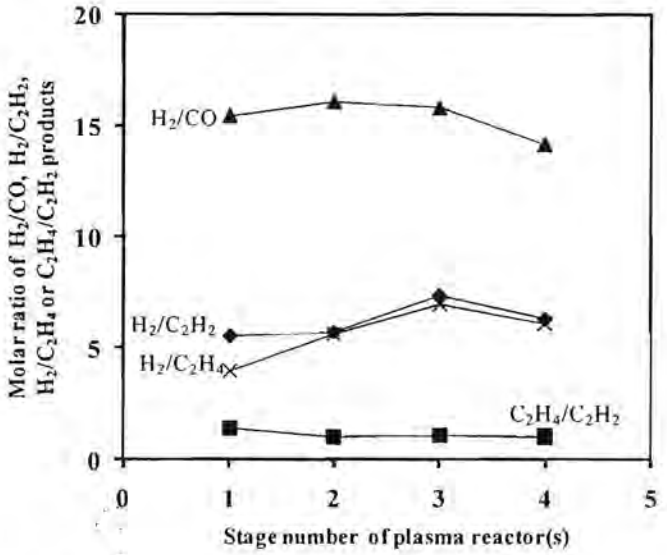

Figure 1.10 Effect of stage number of plasma reactors on product selectivities for reforming of natural gas without partial oxidation in the case of varying residence time (applied voltage, 17.5 kV; frequency, 300 Hz; electrode gap distance, 6 mm; and feed flow rate, 125 cm^3/min).

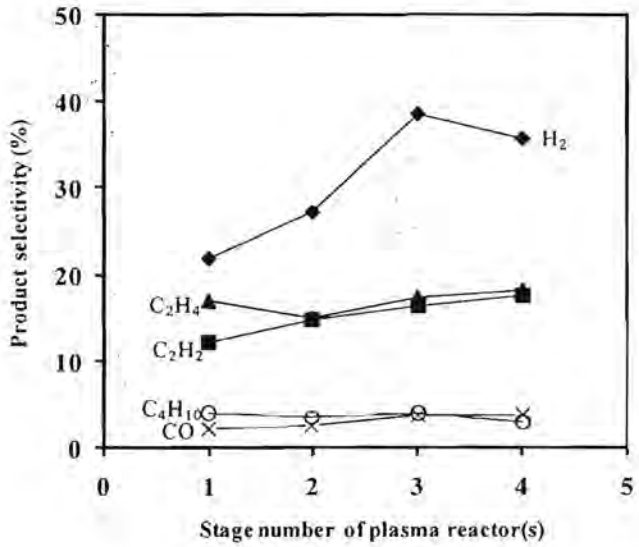

Figure 1.11 Effect of stage number of plasma reactors on product molar ratios for reforming of natural gas without partial oxidation in the case of varying residence time (applied voltage, 17.5 kV; frequency, 300 Hz; electrode gap distance, 6 mm; and feed flow rate, 125 cm^3/min).

of plasma reactors. In contrast, the selectivities for C_2H_4, C_4H_{10}, and CO remained almost unchanged. From these experimental results, it can be concluded that the rate of dehydrogenation increases with increasing stage number of plasma reactors when the multistage system is operated at constant feed flow rate.

1.3.1.2.3 Effect on power consumption

The effect of stage number of plasma reactors on power consumptions per reactant molecule converted and per hydrogen produced is depicted in Figure 12. The power consumption per hydrogen molecule produced substantially decreased when the stage number of plasma reactors was increased from 1 to 3 stages, but the power consumption per reactant molecule converted was insignificantly changed. At the 3

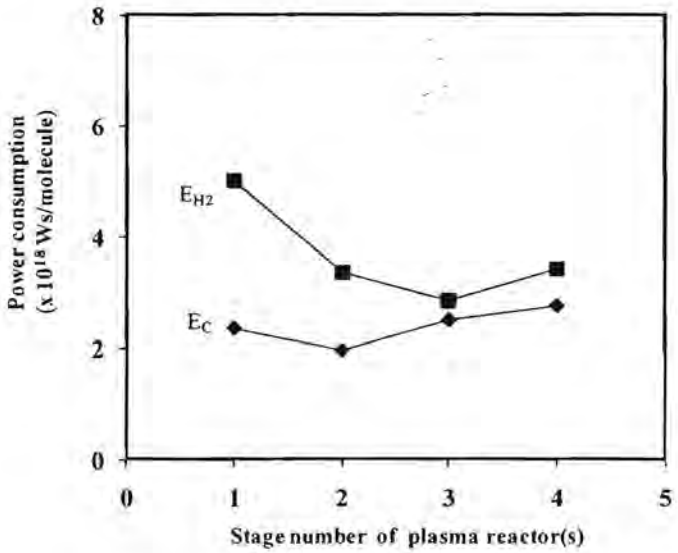

Figure 1.12 Effect of stage number of plasma reactors on power consumptions for reforming of natural gas without partial oxidation in the case of varying residence time (applied voltage, 17.5 kV; frequency, 300 Hz; electrode gap distance, 6 mm; and feed flow rate, 125 cm^3/min).

stages, the minimum power consumption about 2.85×10^{-18} Ws (17.77 eV) per molecule of produced hydrogen was achieved.

1.3.2 Reforming of Natural Gas with Partial Oxidation

For the combined plasma reforming and partial oxidation of the simulated natural gas, the effect of feed flow rate and residence time were systematically investigated to determine whether or not the addition of oxygen to the natural gas feed improved the system performance by using two different oxygen sources: pure oxygen and air.

1.3.2.1 Reforming of Natural Gas with Partial Oxidation by Using Pure Oxygen

1.3.2.1.1 Effect of Feed Flow Rate at Constant Residence Time

1.3.2.1.1.1 Effect on reactant conversion

The combined reforming and partial oxidation of natural gas by using pure oxygen as an oxygen source at a constant residence time under multistage gliding arc discharge was operated at the hydrocarbons-to-oxygen molar ratio of 2/1, which was the optimum ratio in the previous work [15]. Figure 1.13 shows that all reactant conversions only slightly increased with increasing stage number from 1 to 2 stages. Beyond 2 stages, those remained almost unchanged. The H_2 and C_2 yields gradually increased with the stage number of plasma reactors. The value of H_2 yield was somewhat greater than 100 due to the complexity of the reaction, of which both forward and backward reactions simultaneously occurred in the plasma reactors. The concentrations of the outlet gases are shown in Figure 1.14. The outlet concentrations of all reactants decreased with increasing

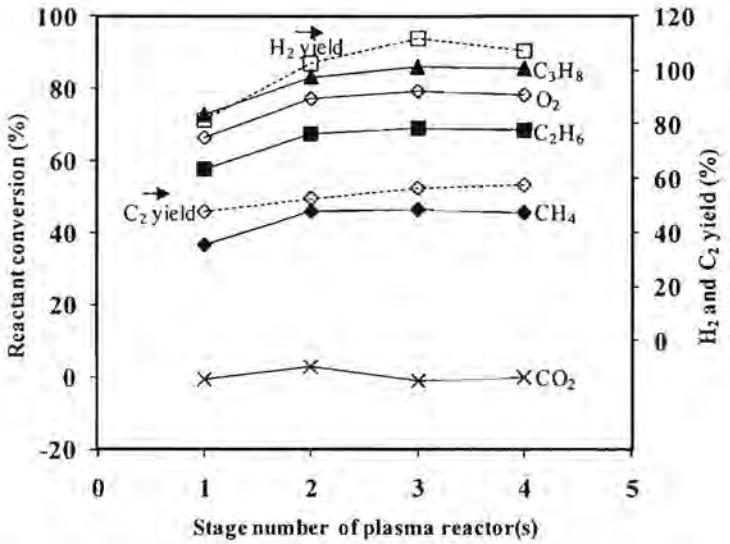

Figure 1.13 Effect of stage number of plasma reactors on reactant conversions and product yields for reforming of natural gas with pure O_2 addition in the case of varying feed flow rate (applied voltage, 17.5 kV; frequency, 300 Hz; electrode gap distance, 6 mm; and residence time, 4.38 s).

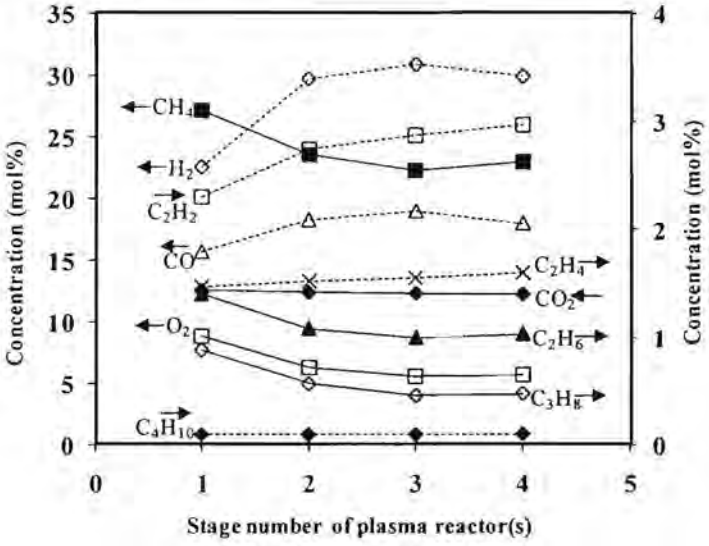

Figure 1.14 Effect of stage number of plasma reactors on concentrations of outlet gases for reforming of natural gas with pure O_2 addition in the case of varying feed flow rate (applied voltage, 17.5 kV; frequency, 300 Hz; electrode gap distance, 6 mm; and residence time, 4.38 s).

stage number of plasma reactors, except that the outlet concentration of CO_2 remained unchanged, which might result from the high bond energy dissociation, as mentioned previously.

1.3.2.1.1.2 Effect on product selectivity

Figure 1.15 shows that most product selectivities did not significantly change when the stage number of plasma reactors was increased except that the selectivity for H_2 tended to slightly increase. The molar ratio of H_2/C_2H_4 increased as the number of plasma reactors increased from 1 to 2 stages and then remained almost unchanged with further increasing stage number, whereas other product molar ratios were almost constant, as shown in Figure 1.16. This can be explained in that both the dehydrogenation reactions and the coupling reaction of hydrogen radicals to produce H_2 have high possibility to occur owing to the high opportunity to collide with the active species at the early stages of plasma reactors at the residence time of 4.38 s.

1.3.2.1.2.3 Effect on power consumption

As shown in Figure 1.17, the decrease in the power consumptions per both reactant molecule converted and hydrogen produced with increasing stage number of plasma reactors was observed, as previously obtained. The optimum power consumptions were 2.02×10^{-18} Ws (12.58 eV) per molecule of hydrocarbon converted and 1.61×10^{-18} Ws (10.09 eV) per molecule of hydrogen produced at the 4 stages of plasma reactors.

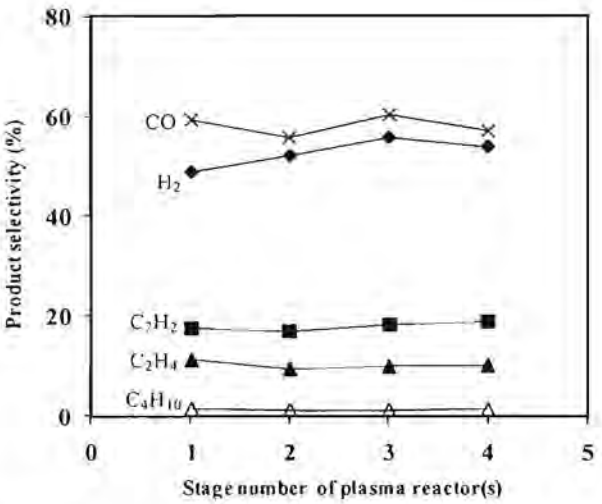

Figure 1.15 Effect of stage number of plasma reactors on product selectivities for reforming of natural gas with pure O_2 addition in the case of varying feed flow rate (applied voltage, 17.5 kV; frequency, 300 Hz; electrode gap distance, 6 mm; and residence time, 4.38 s).

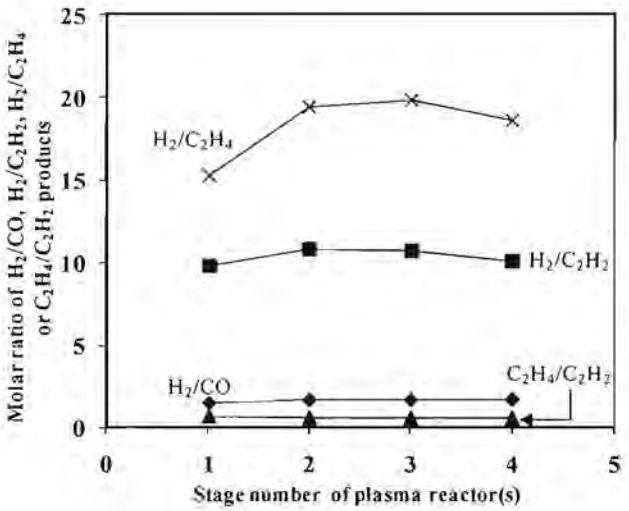

Figure 1.16 Effect of stage number of plasma reactors on product molar ratios for reforming of natural gas with pure O_2 addition in the case of varying feed flow rate (applied voltage, 17.5 kV; frequency, 300 Hz; electrode gap distance, 6 mm; and residence time, 4.38 s).

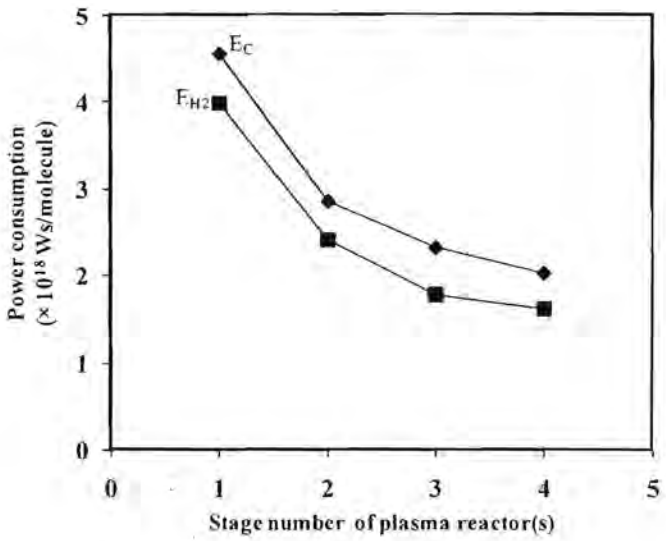

Figure 1.17 Effect of stage number of plasma reactors on power consumptions for reforming of natural gas with pure O_2 addition in the case of varying feed flow rate (applied voltage, 17.5 kV; frequency, 300 Hz; electrode gap distance, 6 mm; and residence time, 4.38 s).

1.3.2.1.2 Effect of Residence Time at Constant Feed Flow Rate

1.3.2.1.2.1 Effect on reactant conversion and product yield

As shown in Figure 1.18, the conversion of all reactants, except CO_2, considerably increased when the stage number of plasma reactors was increased from 1 to 3 stages, and remained almost unchanged with further increasing stage number to 4 stages, probably due to the small amounts of oxygen active species left, which can be clearly confirmed from the outlet gas concentration, as shown in Figure 1.19. For the CO_2 conversion, the minus value of the CO_2 conversion at the HCs/O_2 molar ratio of 2/1 was observed. It can be explained that the formation rate of CO_2 by the hydrocarbon oxidation is higher than the CO_2 consumption rate by the reforming reactions [15]. The H_2 yield

also significantly increased with increasing stage number of plasma reactors to reach the maximum at 3 stages, and after that it greatly decreased. In the meantime, the C_2 yield slightly increased with increasing stage number. Moreover, the H_2 yield was found to be much higher than the C_2 yield. At the 3 stages of plasma reactors, the most significant difference between H_2 and C_2 yields was noticed. This implies that at higher stage number of plasma reactors up to 3 stages, the production of H_2 via the dehydrogenation reactions occurs more favorably than the production of C_2 via the coupling reactions. However, at much higher stage number of 4 stages, the less H_2 production due to less reactant conversion, as well as its higher consumption for hydrogenation reactions, might occur instead.

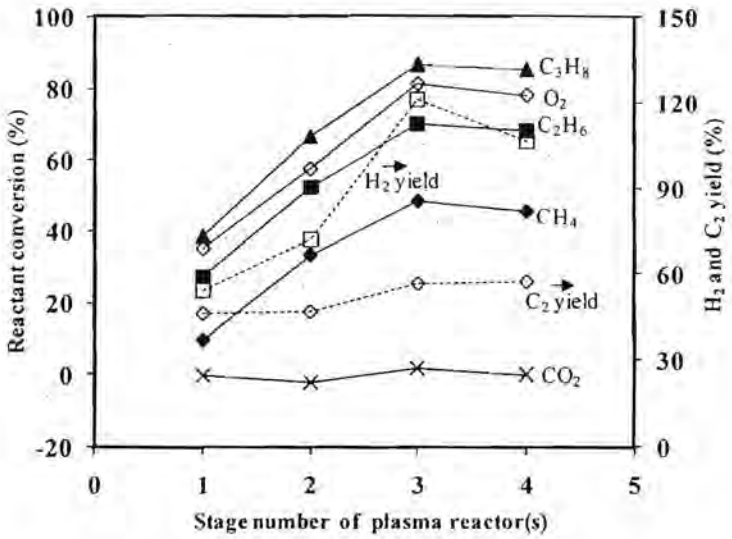

Figure 1.18 Effect of stage number of plasma reactors on reactant conversions and product yields for reforming of natural gas with pure O_2 addition in the case of varying residence time (applied voltage, 17.5 kV; frequency, 300 Hz; electrode gap distance, 6 mm; and feed flow rate, 125 cm^3/min).

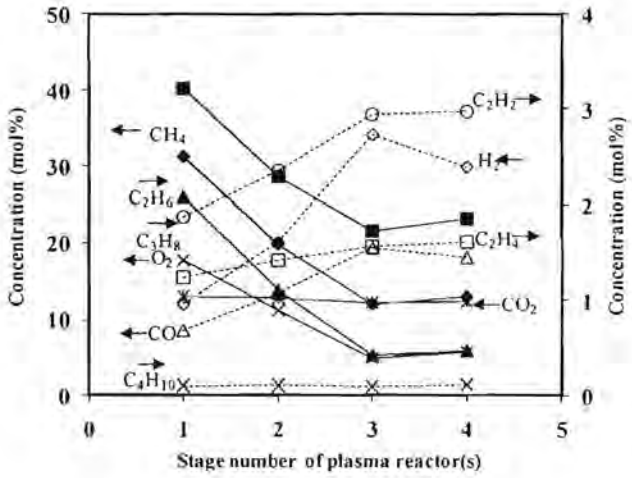

Figure 1.19 Effect of stage number of plasma reactors on concentrations of outlet gases for reforming of natural gas with pure O_2 addition in the case of varying residence time (applied voltage, 17.5 kV; frequency, 300 Hz; electrode gap distance, 6 mm; and feed flow rate, 125 cm^3/min).

1.3.2.1.2.2 Effect on product selectivity

All of product selectivities gradually decreased with increasing stage number of plasma reactors, as illustrated in Figure 1.20. The decreased selectivity for CO is due to the fact that with increasing stage number of plasma reactors, the residence time is enhanced. Therefore, CO has more opportunity to oxidize to CO_2 when increasing stage number of plasma reactors and accordingly the residence time.

However, the outlet concentration of CO_2, as shown in Figure 1.19, was almost unchanged probably because of the equivalent rates of formation and consumption of CO_2. Moreover, the declines of other product selectivities when increasing stage number from 1 to 2 stages were affected from the extraction of oxygen-active species in the system. As presented in Figure 1.21, the molar ratio of H_2/C_2 products dramatically

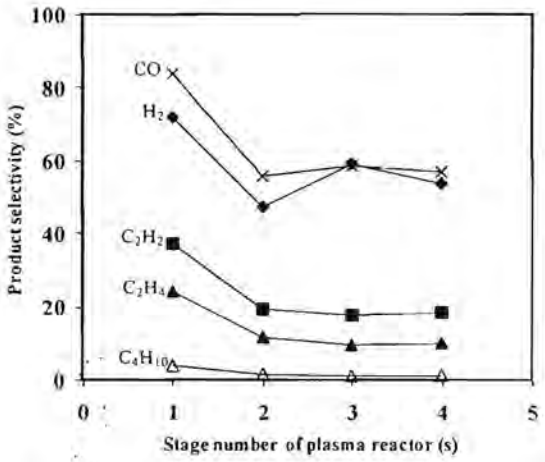

Figure 1.20 Effect of stage number of plasma reactors on product selectivities for reforming of natural gas with pure O_2 addition in the case of varying residence time (applied voltage, 17.5 kV; frequency, 300 Hz; electrode gap distance, 6 mm; and feed flow rate, 125 cm^3/min).

increased with increasing stage number from 1 to 3 stages and then decreased when the stage number of plasma reactors was further increased, whereas the H_2/CO molar ratio did not much change. These also imply that the dehydrogenation and coupling reaction were favorable to take place at high residence time, but not higher than 3.29 s at 3 stages.

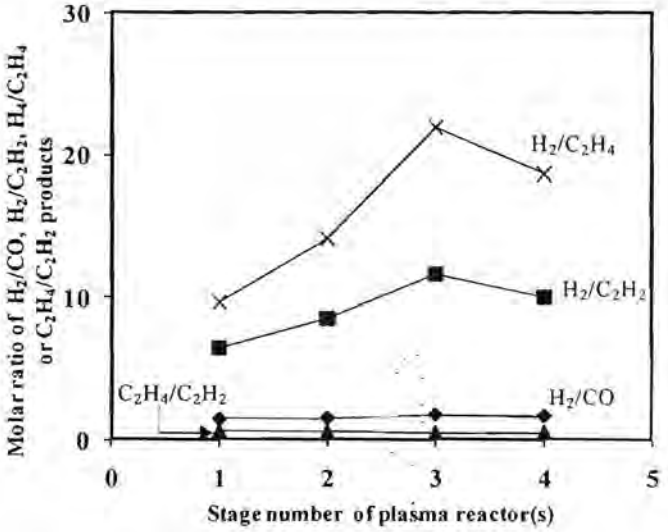

Figure 1.21 Effect of stage number of plasma reactors on product molar ratios for reforming of natural gas with pure O_2 addition in the case of varying residence time (applied voltage, 17.5 kV; frequency, 300 Hz; electrode gap distance, 6 mm; and feed flow rate, 125 cm^3/min).

1.3.2.1.2.3 Effect on power consumption

The power consumption per hydrocarbon converted rapidly declined with increasing stage number of reactors from 1 to 2 stages, and after that it remained almost constant, as depicted in Figure 1.22. Moreover, the power consumption per molecule of hydrogen produced dropped until the 3 stages, and then it slightly increased at the 4 stages. The optimum power consumptions were observed about 1.75×10^{-18} Ws (10.93 eV) per molecule of hydrocarbon converted at 2 stage numbers of plasma reactors and 1.31×10^{-18} Ws (8.15 eV) per molecule of hydrogen produced at 3 stages of plasma reactors.

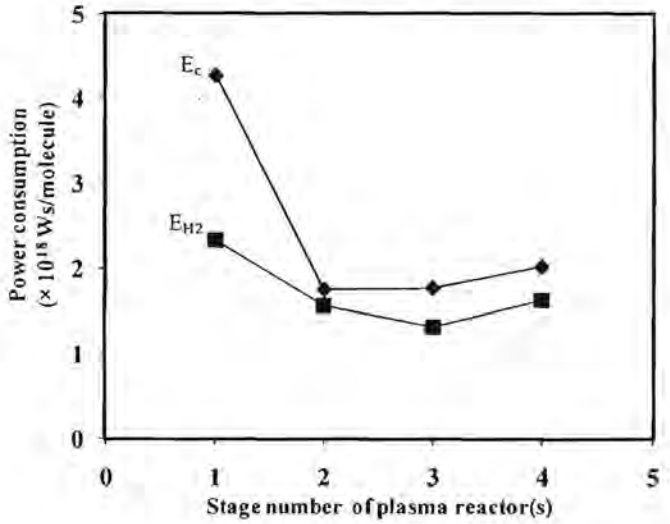

Figure 1.22 Effect of stage number of plasma reactors on power consumptions for reforming of natural gas with pure O_2 addition in the case of varying residence time (applied voltage, 17.5 kV; frequency, 300 Hz; electrode gap distance, 6 mm; and feed flow rate, 125 cm^3/min).

1.3.2.2 Reforming of Natural Gas with Partial Oxidation by Using Air

1.3.2.2.1 Effect of Feed Flow Rate at Constant Residence Time

1.3.2.2.1.1 Effect on reactant conversion and product yield

The conversions of all reactants slightly increased with increasing stage number from 1 to 3 stages, like the yields of H_2 and C_2, as presented in Figure 1.23. These suggest that the increase in all reactant conversions at 2-3 stages of plasma reactors may be because some highly energetic products and active species, which were generated in the plasma zone of the first stage, easily induced further reactions in the successive stages, resulting in the higher conversions. However, at the 4 stages, the conversions adversely decreased. This may be proposed that the backward reactions of some products may take

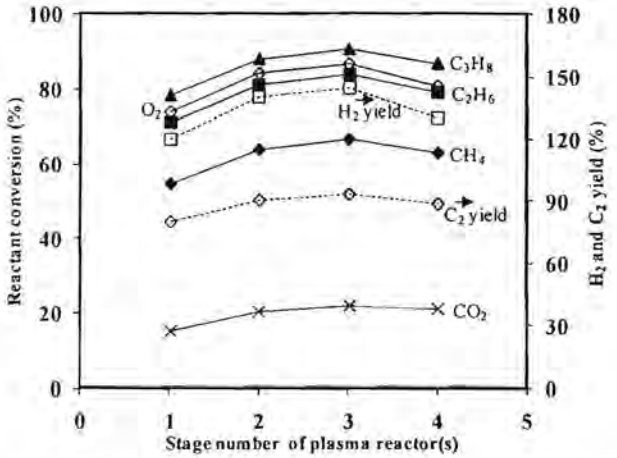

Figure 1.23 Effect of stage number of plasma reactors on reactant conversions and product yields for reforming of natural gas with air addition in the case of varying feed flow rate (applied voltage, 17.5 kV; frequency, 300 Hz; electrode gap distance, 6 mm; and residence time, 4.38 s).

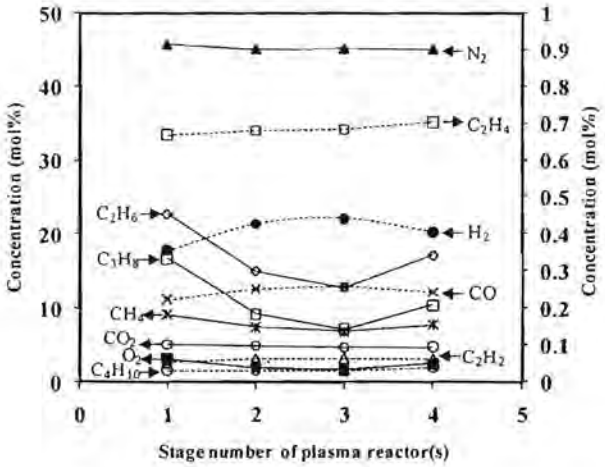

Figure 1.24 Effect of stage number of plasma reactors on concentrations of outlet gases for reforming of natural gas with air addition in the case of varying feed flow rate (applied voltage, 17.5 kV; frequency, 300 Hz; electrode gap distance, 6 mm; and residence time, 4.38 s).

place. In contrast, the CO_2 conversion slightly increased when the stage number of plasma reactors was increased. The concentrations of outlet gases shown in Figure 1.24 also well agree with the values of conversions.

1.3.2.2.1.2 Effect on product selectivity

The selectivities for C_2H_2, C_2H_4, and C_4H_{10} were nearly unchanged while the selectivity for CO slightly declined, with increasing stage number of plasma reactors, as shown in Figure 1.25. It can be explained that increasing the stage number of plasma reactors resulted in less opportunity of CO formation, causing from the less availability of $\bar{O}$ active species. For the molar ratio of H_2/C_2H_4 shown in Figure 1.26, it increased with the stage number of plasma reactors from 1 to 3 stages; however, after that it tended to decrease. This suggests that the oxidative dehydrogenation of C_2H_4 is likely to occur, leading to the increase in the H_2 selectivity with increasing stage number of plasma reactors from 1 to 3 stages, as shown in Figure 1.25.

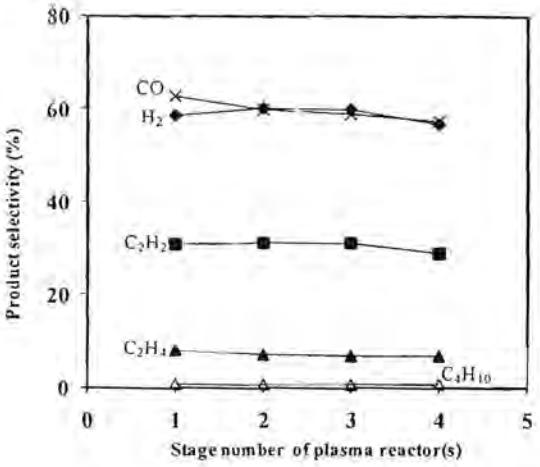

Figure 1.25 Effect of stage number of plasma reactors on product selectivities for reforming of natural gas with air addition in the case of varying feed flow rate (applied voltage, 17.5 kV; frequency, 300 Hz; electrode gap distance, 6 mm; and residence time, 4.38 s).

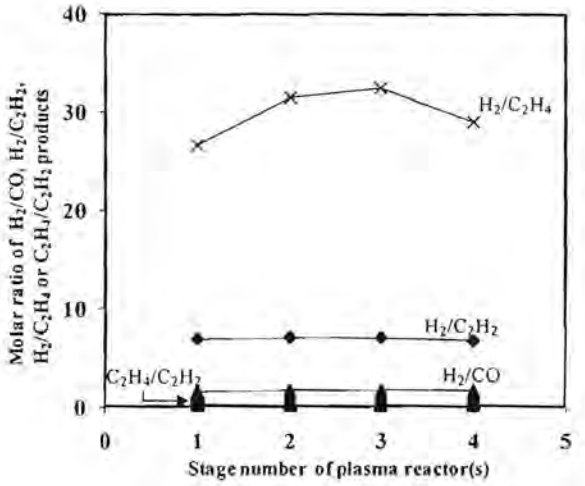

Figure 1.26 Effect of stage number of plasma reactors on product molar raios for reforming of natural gas with air addition in the case of varying feed flow rate (applied voltage, 17.5 kV; frequency, 300 Hz; electrode gap distance, 6 mm; and residence time, 4.38 s).

1.3.2.2.1.3 Effect on power consumption

Figure 1.27 shows the same tendency of the power consumptions per hydrocarbon molecule converted and per hydrogen molecule produced, as previously observed. It was found that they tended to rapidly decline from 1 to 2 stages, but after that they became almost unchanged.

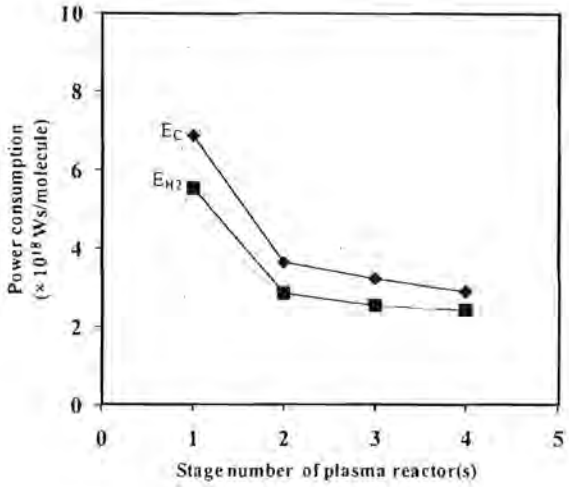

Figure 1.27 Effect of stage number of plasma reactors on power consumptions for reforming of natural gas with air addition in the case of varying feed flow rate (applied voltage, 17.5 kV; frequency, 300 Hz; electrode gap distance, 6 mm; and residence time, 4.38 s).

1.3.2.2.2 Effect of Residence Time at Constant Feed Flow Rate

1.3.2.2.2.1 Effect on reactant conversion and product yield

As depicted in Figure 1.28, both reactant conversions and product yields markedly increased as the stage number of plasma reactors was increased. It can be concluded that the higher stage number of plasma reactors or longer residence time allows more chance for highly energetic electrons to collide with reactants for subsequent

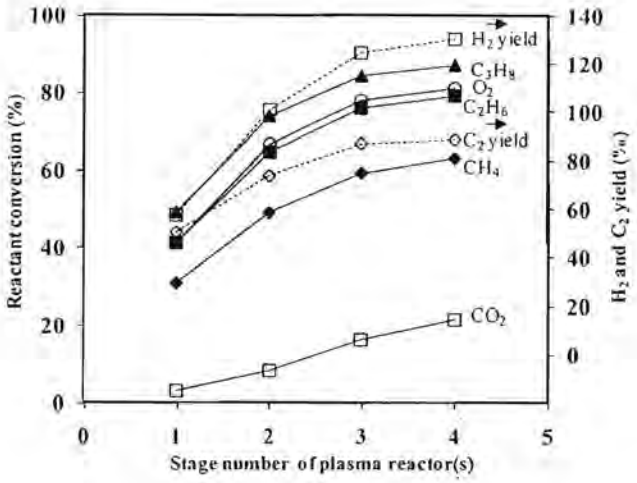

Figure 1.28 Effect of stage number of plasma reactors on reactant conversions and product yields for reforming of natural gas with air addition in the case of varying residence time (applied voltage, 17.5 kV; frequency, 300 Hz; electrode gap distance, 6 mm; and feed flow rate, 125 cm^3/min).

reactions, leading to higher reactant conversions and product yields. It can be noticed that the H_2 yield became much higher than the C_2 yield at a higher stage number of plasma reactors, indicating that the dehydrogenations and oxidative dehydrogenations to produce hydrogen are more favorable to occur than the coupling reactions at a longer residence time. Moreover, the concentrations of outlet gases are depicted in Figure 1.29. It can be described that the outlet concentrations of C_2H_6 and C_3H_8 tremendously dropped when the stage number of plasma reactors increased, corresponding to their conversions.

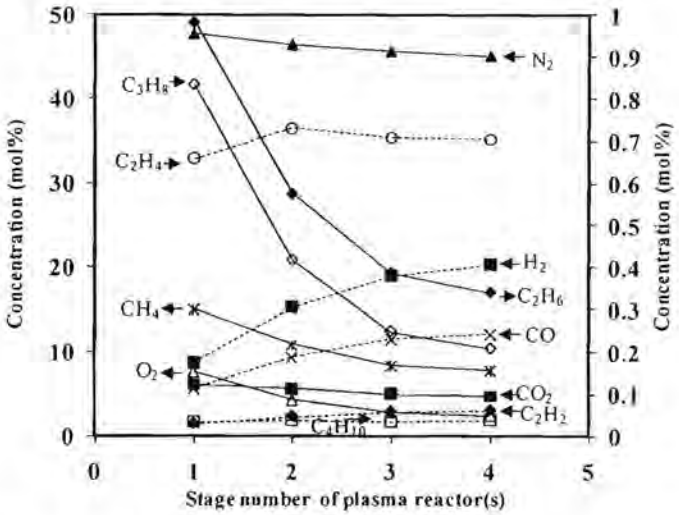

Figure 1.29 Effect of stage number of plasma reactors on concentrations of outlet gases for reforming of natural gas with air addition in the case of varying residence time (applied voltage, 17.5 kV; frequency, 300 Hz; electrode gap distance, 6 mm; and feed flow rate, 125 cm^3/min).

1.3.2.2.2.2 Effect on product selectivity

The selectivities for CO, H_2, and C_2H_2 slightly increased with increasing stage number of plasma reactors, whereas the selectivity for C_2H_4 tended to decrease, and the selectivity for C_4H_{10} remained unchanged, as shown in Figure 1.30. Figure 1.31 shows the rapid increase in the molar ratio of H_2/C_2H_4, while the molar ratios of the others nearly unchanged. These results can be explained in that with increasing stage number of plasma reactors, the oxidative dehydrogenation reactions more favorably occur, as previously stated.

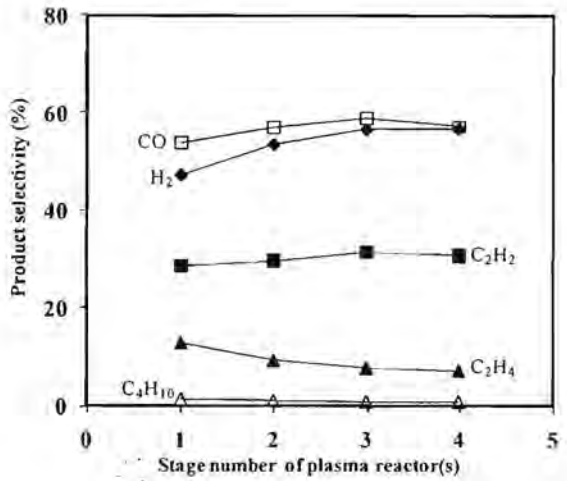

Figure 1.30 Effect of stage number of plasma reactors on product selectivities for reforming of natural gas with air addition in the case of varying residence time (applied voltage, 17.5 kV; frequency, 300 Hz; electrode gap distance, 6 mm; and feed flow rate, 125 cm^3/min).

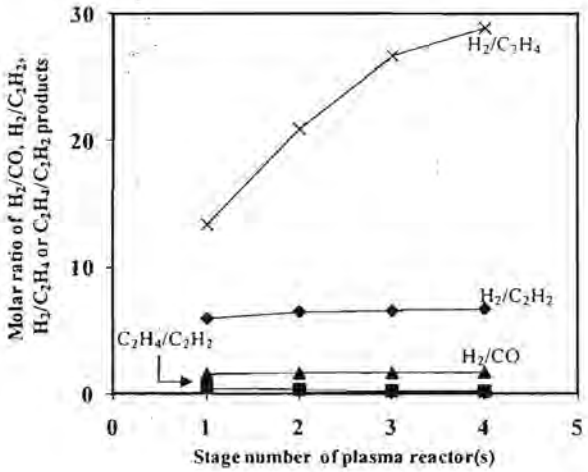

Figure 1.31 Effect of stage number of plasma reactors on product molar ratios for reforming of natural gas with air addition in the case of varying residence time (applied voltage, 17.5 kV; frequency, 300 Hz; electrode gap distance, 6 mm; and feed flow rate, 125 cm^3/min).

1.3.2.2.2.3 Effect on power consumption

The power consumptions are presented in Figure 1.32. The decreases in the power consumptions both per hydrogen molecule produced and per hydrocarbon molecule converted were obtained with increasing stage number of plasma reactors from 1 to 3 stages, but beyond 3 stages, they conversely increased. The optimum power consumptions were 1.96×10^{-18} Ws (12.26 eV) per molecule of hydrogen produced and 2.36×10^{-18} Ws (14.73 eV) per molecule of hydrocarbon converted at the 3 stages of plasma reactors. At the 4 stages, the higher power consumptions were observed due to less reactant conversion and too much input power, despite higher H_2 production as compared with the 3 stages of plasma reactors.

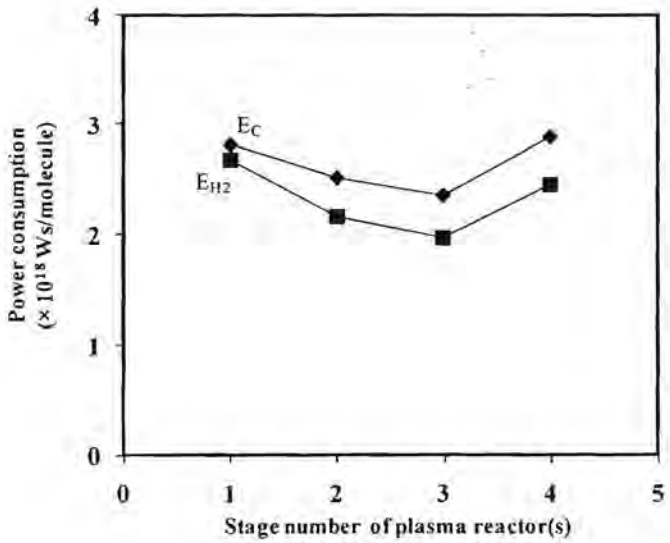

Figure 1.32 Effect of stage number of plasma reactors on power consumptions for reforming of natural gas with air addition in the case of varying residence time (applied voltage, 17.5 kV; frequency, 300 Hz; electrode gap distance, 6 mm; and feed flow rate, 125 cm^3/min).

1.3.3 Comparison of Reforming of Natural Gas without and with Partial Oxidation Using either Oxygen or Air

Two series of systems with a constant residence time and a constant feed flow rate were so far investigated. Even though the system operated at a constant feed flow rate provided more distinguishable, but expectable, results than that operated at a constant residence time when changing the stage number of plasma reactors, the system operated at a constant residence time under different conditions without and with oxygen addition was more interesting for comparison. Therefore, to obtain more understanding, the comparative results of the CO_2-containing natural gas reforming without and with addition of either pure oxygen or air at a constant residence time using the multistage plasma system are shown in Figures 33-36, under operating conditions of a fixed residence time of 4.38 s, an applied voltage of 17.5 kV, a frequency of 300 Hz, an electrode gap distance of 6 mm, and a HCs/O_2 molar ratio of 2/1 in the case of addition of pure oxygen or air as an oxygen source.

Figure 1.33 illustrates that the conversions of all reactants, except CO_2, increased substantially when oxygen was added into the natural gas feed because oxygen is believed to assist in improving the performance of the reaction, especially via the oxidative dehydrogenation to produce hydrogen. In comparison between the two oxygen sources, air provided a better process performance in terms of reactant conversions than pure oxygen. The results reveal that the addition of air in the feed potentially contributes the positive effect to the activation of reactant gases for the reforming of CO_2-containing natural gas. For the CO_2 conversion in the case of adding pure oxygen, the comparatively low values at all stages of plasma reactors are plausibly because the formation rate of CO_2 due to the complete hydrocarbon oxidations is higher than the consumption rate due

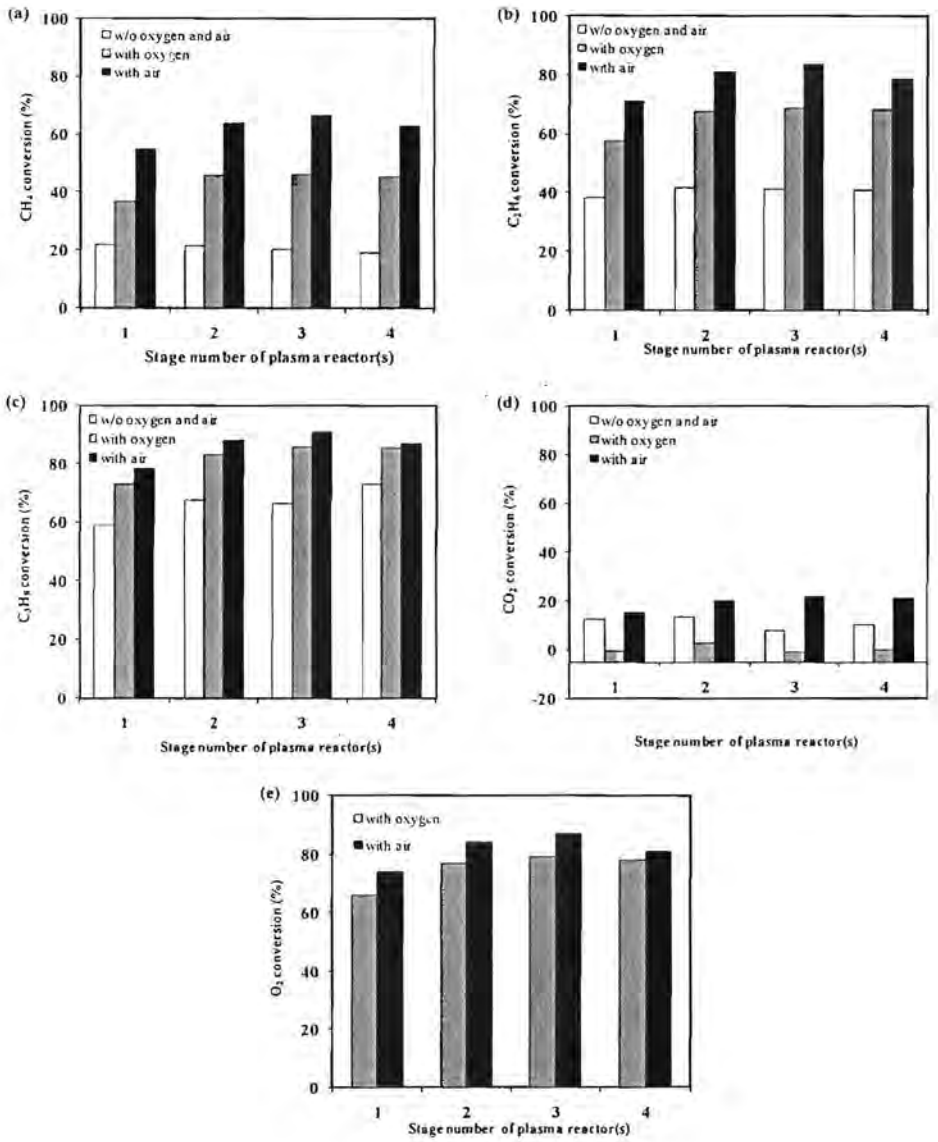

Figure 1.33 Comparison of conversions of (a) CH_4, (b) C_2H_6, (c) C_3H_8, (d) CO_2, and (e) O_2 for combined reforming and partial oxidation of natural gas in the case of varying feed flow rate (applied voltage, 17.5 kV; frequency, 300 Hz; electrode gap distance, 6 mm; and residence time, 4.38 s).

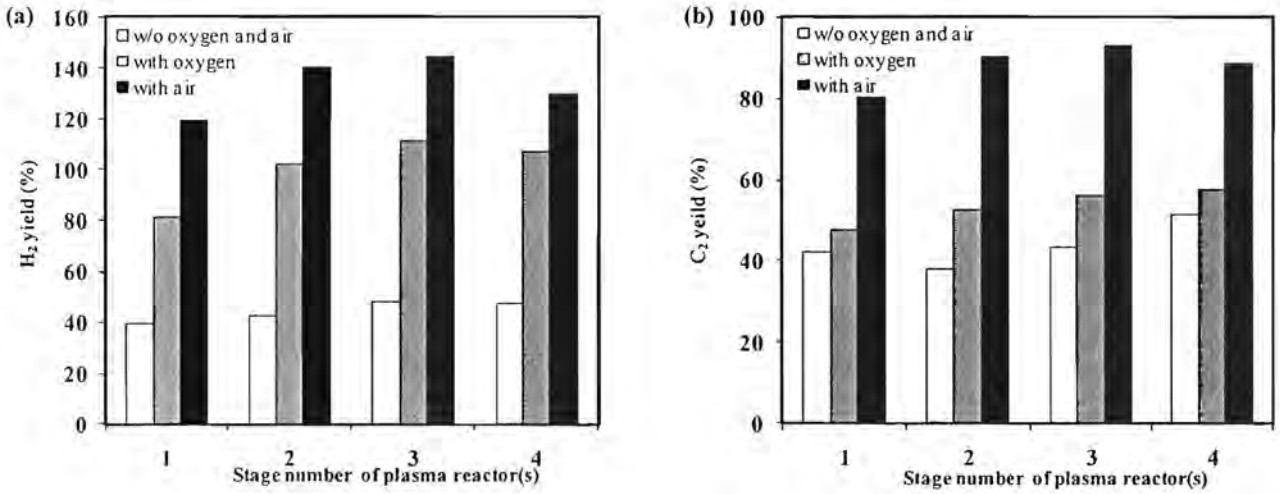

Figure 1.34 Comparison of yields of (a) H_2 and (b) C_2 for combined reforming and partial oxidation of natural gas in the case of varying feed flow rate (applied voltage, 17.5 kV; frequency, 300 Hz; electrode gap distance, 6 mm; and residence time, 4.38).

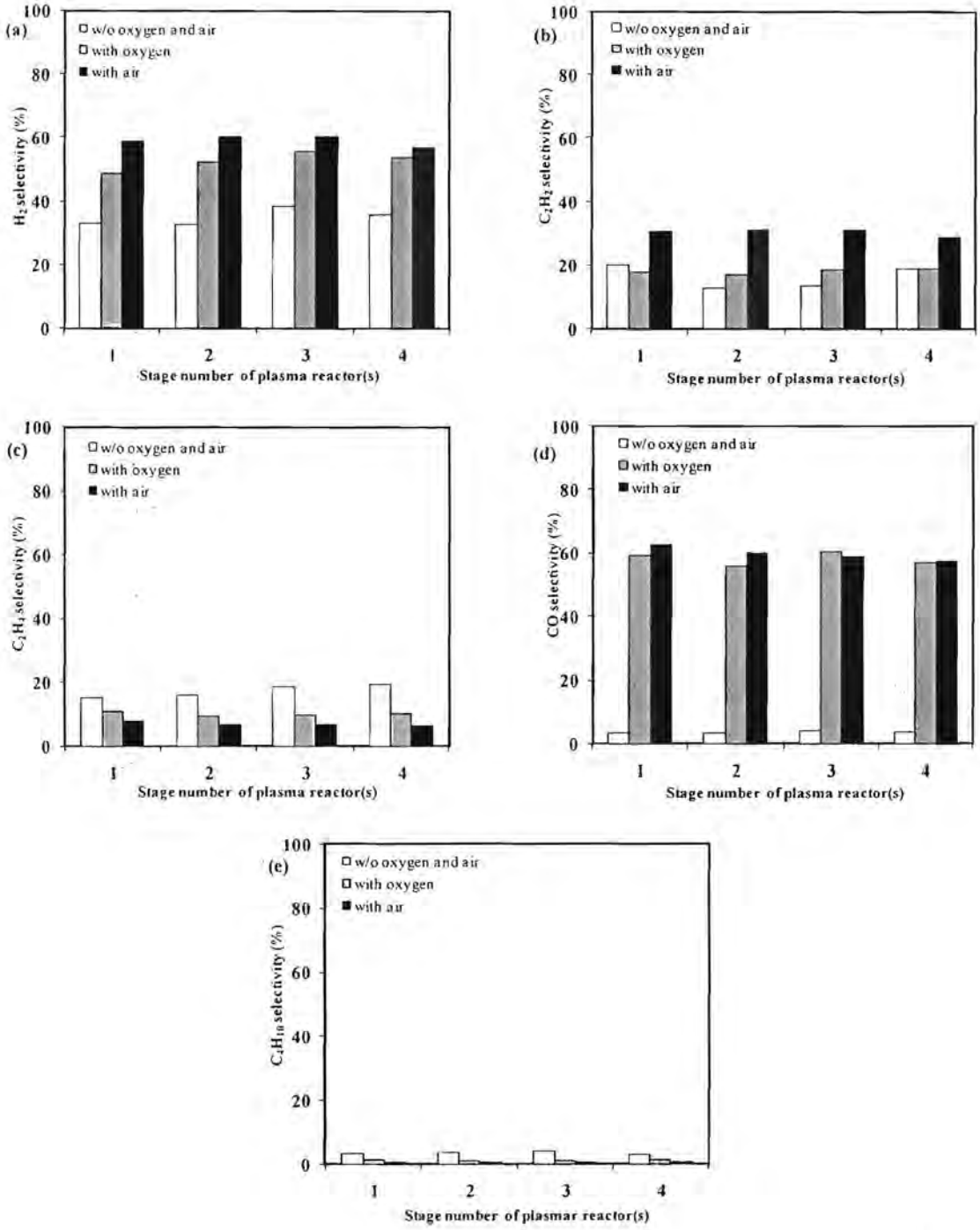

Figure 1.35 Comparison of selectivities for (a) H_2, (b) C_2H_2, (c) C_2H_4, (d) CO, and (e) C_4H_{10} for combined reforming and partial oxidation of natural gas in the case of varying feed flow rate.

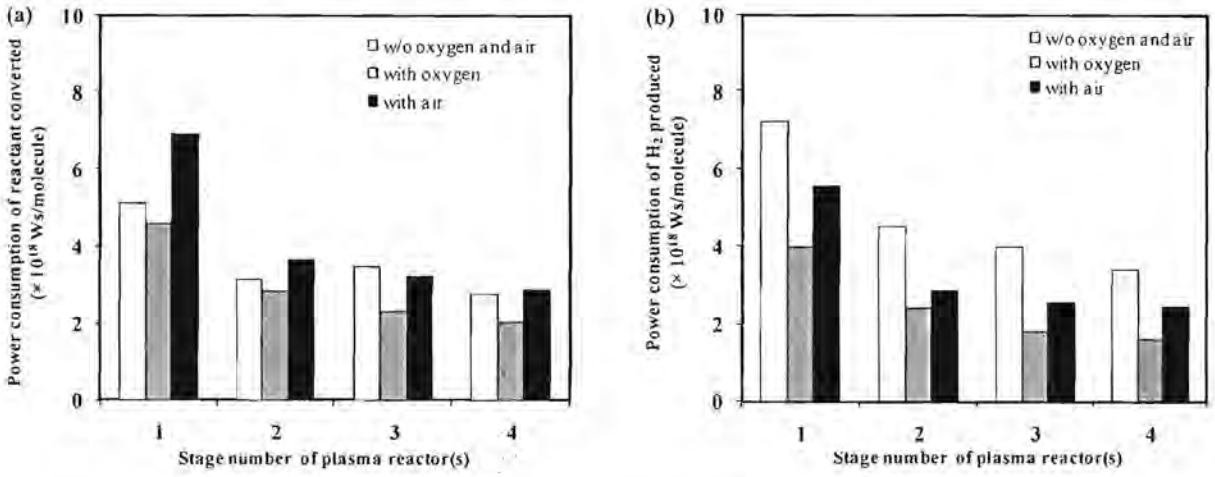

Figure 1.36 Comparison of power consumptions for combined reforming and partial oxidation of natural gas in the case of varying feed flow rate: (a) power consumption per reactant molecule converted, (b) power consumption per hydrogen molecule produced) (applied voltage, 17.5 kV; frequency, 300 Hz; electrode gap distance, 6 mm; and residence time, 4.38 s).

to the plasma-induced dissociation reactions, as mentioned previously. It can be observed that the highest reactant conversions were attained at 3 stages of plasma reactors when using air as an oxygen source.

Regarding the results of H_2 and C_2 yields as presented in Figure 1.34, the system with oxygen addition provided higher product yields than the system without oxygen addition because the oxygen molecules can be easily activated by the plasma and provide the oxygen active species for extracting the H atom from the hydrocarbons, as aforementioned. Interestingly, for the case of adding oxygen, the results show that the use of air as an oxygen source also provided significantly higher product yields than that of pure oxygen. These could be explained in that nitrogen in air could possibly act as the

third body in the reaction to receive the excessive energy of the products and make them stable. Therefore, it might bear the responsibility in promoting the plasma-chemical reactions. Moreover, the 3 stages of plasma reactors were clearly observed to provide the highest yields, an additional advantage to the highest reaction conversions as above mentioned.

The product selectivities are comparatively shown in Figure 1.35. Most product selectivities, except C_2H_4 and C_4H_{10}, significantly increased, especially for the CO selectivity, when adding both oxygen sources to the system. However, the addition of oxygen into the system did not provide the positive effect on the C_2H_4 and C_4H_{10} selectivities because the presence of the oxygen active species led to more probability of the oxidative dehydrogenations of both reactants and intermediates to form H_2 and C_2H_2 products instead of more saturated C_2H_4 and C_4H_{10} products. Particularly, this might be the main reason in achieving more H_2 formation under O_2-containing system. Moreover, when comparing the ability to induce the H_2 formation between pure oxygen and air, it was clearly observed that using air as an oxygen source provided the superior performance.

The power consumptions of the investigated systems are comparatively shown in Figure 1.36. The power consumption for converting reactant for the system with oxygen addition tended to become lower than that without oxygen addition at the stage numbers more than 3 stages. However, the power consumption for producing hydrogen for the system with oxygen addition was obviously lower than that without oxygen addition at all stage numbers of plasma reactors. When considering the power consumptions at higher stage numbers in the case of adding pure oxygen and air, even though using pure oxygen as an oxygen source consumed slightly lower power for the

plasma system operation, the difference in both the power consumptions between the cases of two oxygen sources seemed to be plausibly insignificant and negligible due to their extremely small values.

From these comparative results, it can be concluded that the addition of oxygen into the feed provided the positive effects on the reforming of CO_2-containing natural gas with not only enhancing the reactant conversions, the desired product yield and selectivity, but also consuming comparatively lower energy consumption for producing hydrogen, as compared with the system without oxygen addition. In addition, the utilization of air as an oxygen source assisted in improving the reforming of CO_2-containing natural gas more effectively than pure oxygen because it provided the better reactant conversions and better desired product yield and selectivity. Finally, from careful consideration of the overall results, it can also be reasonably concluded that the 3 stages of plasma reactors were satisfactorily sufficient to achieve excellent process performance. The operation with a higher stage number was not required due to the insignificant enhancement of the performance.

1.4. Conclusions

The combined reforming and partial oxidation of CO_2-containing natural gas was investigated under two series of system with a constant feed flow rate and a constant residence time by using non-thermal multistage gliding arc discharge. The major products were mainly hydrogen and C_2 hydrocarbons. In the case of the system without partial oxidation operated at a fixed flow rate, all reactant conversions, except CO_2 conversion, as well as product yields and product selectivities, increased with increasing stage number of plasma reactors. This is because when increasing stage number of plasma

reactors, the reactants had longer residence time to collide with highly energetic electrons. For the system operated at a fixed residence time, the stage number of plasma reactors slightly affected the reactant conversions, product yields, and product selectivities because the reaction time of each stage number was the same, thereby resulting in the similar possibility of the reactants to collide with the highly energetic electrons. In the case of the system with partial oxidation, the number of plasma reactors provided the positive effects on the reactant conversions, product yields, and product selectivities, and also lower power consumption was consumed as compared with the system without partial oxidation. These can suggest that the oxygen molecules could be activated by the plasma and provide the oxygen active species for extracting the H atom from the hydrocarbons via oxidative dehydrogenation, resulting in higher reactant conversions, desired product yields, and selectivities. The addition of air as oxygen source provided the better process performance for the CO_2-containing natural gas reforming than that of pure oxygen. Moreover, the plasma system operated with 3 stages of plasma reactors led to the good process performance with acceptably high reactant conversions, high desired product yields, and low power consumptions.

References

1. Jeong, H.K., Kim, S.C., Han, C., Lee, H., Song, H.K., and Na, B.K. (2001). Conversion of methane to higher hydrocarbons in pulsed DC barrier discharge at atmospheric pressure. Korean Journal Chemical Engineering, 18(2), 196-201.
2. Li, M.W., Xu, G.H., Tian, Y.L., Chen, L., and Fu, H.F. (2004). Carbon dioxide reforming of methane using DC corona discharge plasma reaction. Journal of Physical Chemistry A, 108(10), 1687-1693.
3. Hwang, B.B., Yeo, Y.K., and Na, B.K. (2003). Conversion of CH_4 and CO_2 to syngas and higher hydrocarbons using dielectric barrier discharge. Korean Journal of Chemical Engineering, 20(4), 631-634.
4. Xu, H., Shi, K., Shang, Y., Zhang, Y., Xu, G., and Wei, Y. (1999). A study on the reforming of natural gas with steam, oxygen and carbon dioxide to produce syngas for methanol feedstock. Journal of Molecular Catalysis A: Chemical, 147, 41-46.
5. Juan-Juan, J., Roman-Martinez, M.C., and Illan-Gomez, M.J. (2004). Catalytic activity and characterization of Ni/Al_2O_3 and NiK/Al_2O_3 catalysts for CO_2 methane reforming. Applied Catalysis A: General, 264, 169-174.
6. Effendi, A., Zhang, Z.G., Hellgardt, K., Honda, K., and Yoshida, T. (2002) Steam reforming of a clean model biogas over Ni/Al_2O_3 in fluidized- and fixed-bed reactors. Catalysis Today, 77, 181-189.
7. Supat, K., Chavadej, S., Lobban L.L, and Millinson G.R. (2003). Combined steam reforming and partial oxidation of methane to synthesis gas under electrical discharge. Industrial & Engineering Chemistry Research, 42, 1654-1661.

8. Supat, K., Kruapong, A., Chavadej, S., Lobbon, L.L., and Mallinson, R.G. (2003). Synthesis gas production from partial oxidation of methane with air in AC electric gas discharge. Energy & Fuels, 17, 474-418.

9. Paulmier, T., and Fulcheri, L. (2005). Use of non-thermal plasma for hydrocarbon reforming. Chemical Engineering Journal, 106, 59-71.

10. Chavadej, S., Kiatubolpaiboon, W., Rangsunvigit, P., and Sreethawong, T. (2007). A combined multistage corona discharge and catalytic system for gaseous benzene removal. Journal of Molecular Catalysis A: Chemical, 263, 128-136.

11. Eliasson, B., Hirth, M., and Kogeischatz, U. (1987). Ozone synthesis from oxygen in dielectric barrier discharge. Journal of Applied Physics, 20, 1421-1437.

12. Krawczyk, K., and Młotek, M. (2001). Combined plasma-catalytic processing of nitrous oxide. Applied Catalysis B: Environmental, 30, 233-245.

13. Rosacha, L.A., Anderson, G.K.. bechtold, L.A., Coogan, J.J., Heck, H.G., Kang, M., McCulla, W.H., Tennant, R.A., and Wantuck, P.J. (1993). Treatment of hazardous organic wastes using silent discharge plasma. NATO ASI Series, 34, Part B.

14. Rueangjitt, N., Akarawitoo, C., Sreethawong, T., and Chavadej, S. (2007). Reforming of CO_2-containing natural gas using an AC gliding arc system: Effect of gas component in natural gas. Plasma Chemistry and Plasma Processing, 27, 559-576.

15. Rueangjitt, N., Sreethawong, T., and Chavadej, S. (2008). Reforming of CO_2-containing natural gas using an AC gliding arc system: Effects of operational parameters and oxygen addition in feed. Plasma Chemistry and Plasma Processing, 28, 49-67.

16. Sreethawong, T., Thakonpatthanakun, P., and Chavadej, S. (2007). Partial oxidation of methane with air for synthesis gas production in a multistage gliding arc discharge system. International Journal of Hydrogen Energy, 32, 1067-1079.

Part 2: Synthesis Gas Production from Reforming of CO_2-Containing Natural Gas with Steam Using an AC Gliding Arc Discharge System: Effects of Steam Addition in Feed and Operational Parameters (submitted to *Plasma Chemistry and Plasma Processing*)

2.1 Introduction and Survey of Related Literature

In recent years, the energy demand around the world has markedly increased. As a result, many countries are aware of the shortage of fuels in the near future and have tried to encourage the use of alternative energy sources in order to reduce the demand for fossil fuels. Among the available fossil fuels, natural gas is currently considered to be an economical and substantial available resource, and it is becoming the most interesting alternative fuel for both community and industry. However, conventional natural gas reforming process (methane (CH_4) reforming) is usually operated at elevated temperatures (600–800°C), which requires an intense energy input [1]. Moreover, metal catalysts are required for the enhancement of the reaction rates, and these catalysts are seriously deactivated by the impurities in feed hydrocarbons and by carbon deposits during the reactions. Non-thermal plasma has been proposed by several studies as an alternative technique to convert natural gas to more valuable products [2-9], because of its ability to induce chemical reactions at relatively low temperatures, leading to lowering energy consumption [10]. Gliding arc discharge is one of the effective types of non-thermal plasma, and it provides the most effective non-equilibrium characteristics with simultaneous high productivity and good selectivity [11]. Therefore, gilding arc discharge was considered to be promising non-thermal plasma for reforming natural gas

in this study.

In our previous work [12,13], the challenging concept of the direct utilization of raw natural gas with a high CO_2 content was explored by using an AC low-temperature gilding arc discharge system, where the effects of each gas component in a simulated natural gas, operational parameters, and oxygen addition in feed were investigated. The results interestingly showed that the addition of a small amount of oxygen effectively minimized the carbon deposit on the electrode surface and inside the reactor wall, and also enhanced the performance of CO_2-containing natural gas reforming in terms of reactant conversion, desired product selectivity, desired product yield, and power consumption. Additionally, it was revealed that the addition of water in the form of steam to gaseous hydrocarbon feeds (e.g. methane and aliphatic hydrocarbons) improved the reaction rate, reactant conversion, product selectivity, and the ratio of hydrogen to carbon monoxide [14,15]. However, to our knowledge, the steam reforming of CO_2-containing natural gas with imitated compositions of real natural gas found in reservoirs using a gliding arc discharge system has never been investigated. Therefore, this present work aimed, for the first time, to examine the effects of hydrocarbons-to-steam molar ratio (steam content), total feed flow rate, applied voltage, and input frequency on reactant conversion, product selectivity, product yield, and power consumption for the reforming of CO_2-containing natural gas with steam using a gliding arc discharge system.

2.2 Procedure

2.2.1. Reactant Gases

The simulated natural gas used in this work consisted of CH_4, C_2H_6, C_3H_8, and CO_2, with a CH_4:C_2H_6:C_3H_8:CO_2 molar ratio of 70:5:5:20, and was specially manufactured by Thai Industry Gas (Public) Co., Ltd.

2.2.2. AC Gliding Arc Discharge System

The schematic of a low-temperature gliding arc system used in this work is shown in Figure 2.1.

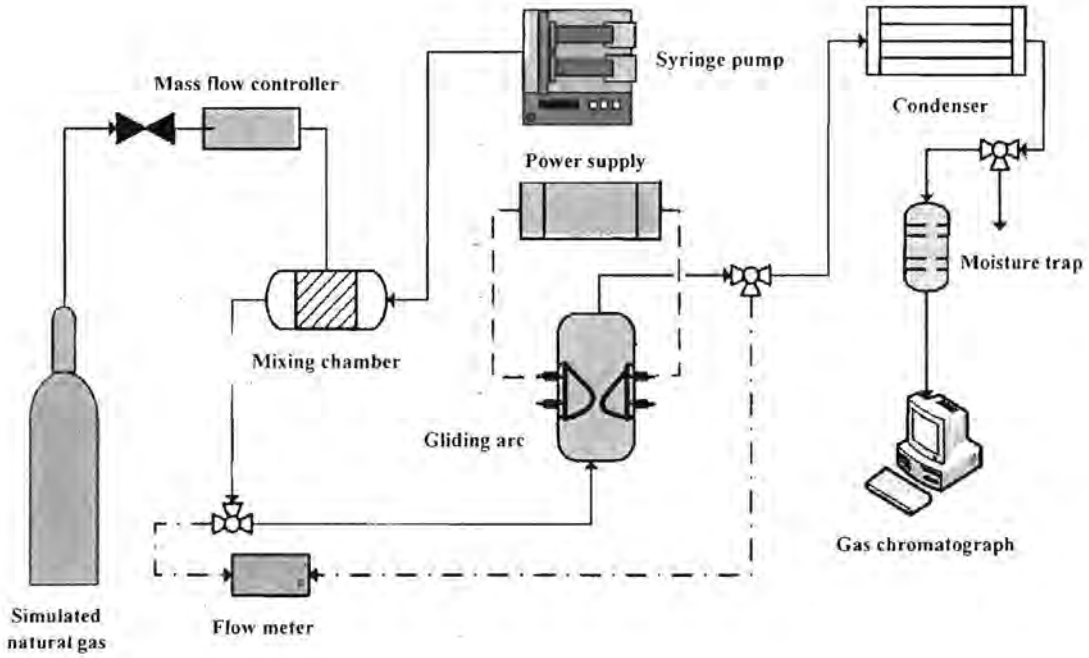

Figure 2.1 Schematic of gliding arc discharge system.

The detail of the gliding arc reactor configuration was described in our previous work [12]. A glass tube with 9 cm OD and 8.5 cm ID was used as the gliding arc reactor, which consisted of two diverging knife-shaped electrodes. The electrodes were made of stainless steel sheets with a 1.2 cm width. The gap distance between the pair of electrodes was fixed at 6 mm. The steam fed into the system was achieved by vaporizing water at a controlled temperature of 120 °C. A water flow rate was controlled by a syringe pump (Cole-Parmer). To prevent the water condensation in the feed line, the temperature of

stainless tube from the syringe pump to a mixing chamber was maintained at 120 °C by using a heating tape. The flow rate of the simulated natural gas was controlled by a mass flow controller with a transducer (AALBORG). A 7-μm stainless steel filter was placed upstream of the mass flow controller in order to trap any solid particles in the reactant gas. The check valve was also placed downstream of the mass flow controller to prevent any backflow. The reactant gas and steam were well mixed in the mixing chamber controlled at 120 °C before being introduced upward into the reactor at atmospheric pressure. The compositions of the feed gas mixture and the outlet gas were quantitatively analyzed by an on-line gas chromatograph (HP, 5890) equipped with two separate columns, i.e. a Carboxen 1000 packed column and a PLOT Al_2O_3 "s" capillary column, which were adequate to detect all hydrocarbons, CO, CO_2, and H_2.

The power supply unit consisted of three steps. For the first step, the domestic AC input of 220 V and 50 Hz was converted to a DC output of 70 V by a DC power supply converter. For the second step, a 500 W power amplifier with a function generator was used to transform the DC into AC current with a sinusoidal waveform and different frequencies. For the third step, the outlet voltage was stepped up by using a high voltage transformer. The output voltage and frequency were controlled by the function generator. The voltage and current at the low voltage side were measured instead of those at the high voltage side since the plasma generated is non-equilibrium in nature. The high side voltage and current were thereby calculated by multiplying and dividing by a factor of 130, respectively. A power analyzer was used to measure power, current, frequency, and voltage at the low voltage side of the power supply unit.

The feed gas mixture was first introduced into the gliding arc reactor without turning on the power supply unit for any studied conditions. After the compositions of

outlet gas became invariant, the power supply unit was turned on. The flow rate of the outlet gas was also measured by using a bubble flow meter. The outlet gas was analyzed by the on-line GC every 30 min. After the plasma system reached steady state with invariant outlet gas concentrations, the outlet gas was taken for analysis at least a few times every hour. The average data were used to assess the process performance of the studied gliding arc discharge system.

The plasma system performance was evaluated from reactant conversions, product selectivities, H_2 and C_2 yields, and power consumptions, as follows:

The reactant conversion is defined as:

$$\% \text{ Reactant conversion} = \frac{(\text{Moles of reactant in} - \text{Moles of reactant out}) \times (100)}{\text{Moles of reactant in}} \quad (1)$$

The selectivities of C-containing products are defined on the basis of the amount of C-containing reactants converted to any specified product, as stated in Equation 2. In the case of hydrogen product, its selectivity is calculated based on H-containing reactants converted, as stated in Equation 3:

$$\% \text{ Selectivity for any hydrocarbon product} = \frac{[P](C_P)(100)}{\Sigma[R](C_R)} \quad (2)$$

$$\% \text{ Selectivity for hydrogen} = \frac{[P](H_P)(100)}{\Sigma[R](H_R)} \quad (3)$$

where $[P]$ = moles of product in the outlet gas stream

$[R]$ = moles of each reactant in the feed stream to be converted

C_p = number of carbon atoms in a product molecule

C_R = number of carbon atom in each reactant molecule

H_p = number of hydrogen atoms in a product molecule

H_R = number of hydrogen atoms in each reactant molecule

The yields of various products are calculated using the following equations:

$$\%\ C_2 \text{ hydrocarbon yield} = \frac{[\Sigma(\%\ CH_4, \%\ C_2H_6, \%\ C_3H_8, \%\ CO_2 \text{ conversions})][\Sigma(\%\ C_2H_2, \%\ C_2H_4 \text{ selectivities})]}{(100)} \quad (4)$$

$$\%\ H_2 \text{ yield} = \frac{[\Sigma(\%\ CH_4, \%\ C_2H_6, \%\ C_3H_8 \text{ conversions})][\%\ H_2 \text{ selectivity}]}{(100)} \quad (5)$$

$$\%\ CO \text{ yield} = \frac{[\Sigma(\%\ CH_4, \%\ C_2H_6, \%\ C_3H_8, \%\ CO_2 \text{ conversions})][\%\ CO \text{ selectivity}]}{(100)} \quad (6)$$

The power consumption is calculated in a unit of Ws per C-containing reactant molecule converted and Ws per hydrogen molecule produced using the following equation:

$$\text{Power consumption} = \frac{P \times 60}{N \times M} \quad (7)$$

where P = power (W)

N = Avogadro's number (6.02×10^{23} molecule g mole^{-1})

M = rate of converted carbon in the rate of produced hydrogen molecules (g mole min^{-1})

2.3 Results and Discussion

In a plasma environment, the highly energetic electrons generated by gliding arc discharge collide with various gaseous molecules of hydrocarbons and CO_2, creating a variety of chemically active radicals. All the possibilities of chemical pathways occurring under the studied conditions are expressed below to provide a better comprehensible understanding about the plasma reforming reactions of a CO_2-containing natural gas with steam under AC non-thermal gliding arc discharge [12,13]. The radicals of oxygen active species and hydroxyl active species, as well as hydrogen, are produced during the water dissociation reactions by the collisions with electrons (Equations 8-9).

Electron-water collisions:

$$e^- + H_2O \rightarrow O^- + H_2 \quad (8)$$

$$e^- + H_2O \rightarrow OH^- + H \quad (9)$$

Additionally, the radicals of oxygen active species can be produced during the collisions of electrons on CO_2, as shown in Equations 10 and 11. Moreover, the produced CO can be further dissociated by the collisions with electrons to form coke and oxygen active species (Equation 12). The simultaneous collisions between electrons and all hydrocarbons present in the feed to produce hydrogen and various hydrocarbon species for subsequent reactions are described by Equations 13-25.

Electron-carbon dioxide collisions:

Dissociation reactions of carbon dioxide;

$$e^- + CO_2 \rightarrow CO + O^- \quad (10)$$

$$e^- + CO_2 \rightarrow CO + O + e^- \quad (11)$$

$$e^- + CO \rightarrow C + O + e^- \quad (12)$$

Electron-methane collisions:

$$e^- + CH_4 \rightarrow CH_3 + H + e^- \quad (13)$$

$$e^- + CH_3 \rightarrow CH_2 + H + e^- \quad (14)$$

$$e^- + CH_2 \rightarrow CH + H + e^- \quad (15)$$

$$e^- + CH \rightarrow C + H + e^- \quad (16)$$

$$H + H \rightarrow H_2 \quad (17)$$

Electron-ethane collisions:

$$e^- + C_2H_6 \rightarrow C_2H_5 + H + e^- \quad (18)$$

$$e^- + C_2H_5 \rightarrow C_2H_4 + H + e^- \quad (19)$$

$$e^- + C_2H_4 \rightarrow C_2H_3 + H + e^- \quad (20)$$

$$e^- + C_2H_3 \rightarrow C_2H_2 + H + e^- \quad (21)$$

$$e^- + C_2H_6 \rightarrow CH_3 + CH_3 + e^- \quad (22)$$

Electron-propane collisions:

$$e^- + C_3H_8 \rightarrow C_3H_7 + H + e^- \quad (23)$$

$$e^- + C_3H_7 \rightarrow C_3H_6 + H + e^- \quad (24)$$

$$e^- + C_3H_8 \rightarrow C_2H_5 + CH_3 + e^- \quad (25)$$

The oxygen active species derived from the CO_2 dissociation reaction can further extract hydrogen atoms from the molecules of hydrocarbon gases via the oxidative dehydrogenation reactions (Equations 26-39), consequently producing several chemically active radicals and water.

Oxidative dehydrogenation reactions:

$$CH_4 + O \rightarrow CH_3 + OH \quad (26)$$

$$C_2H_6 + O \rightarrow C_2H_5 + OH \quad (27)$$

$$C_2H_5 + O \rightarrow C_2H_4 + OH \quad (28)$$

$$C_2H_4 + O \rightarrow C_2H_3 + OH \quad (29)$$

$$C_2H_3 + O \rightarrow C_2H_2 + OH \quad (30)$$

$$C_3H_8 + O \rightarrow C_3H_7 + OH \quad (31)$$

$$C_3H_7 + O \rightarrow C_3H_6 + OH \quad (32)$$

$$CH_4 + OH \rightarrow CH_3 + H_2O \quad (33)$$

$$C_2H_6 + OH \rightarrow C_2H_5 + H_2O \quad (34)$$

$$C_2H_5 + OH \rightarrow C_2H_4 + H_2O \quad (35)$$

$$C_2H_4 + OH \rightarrow C_2H_3 + H_2O \quad (36)$$

$$C_2H_3 + OH \rightarrow C_2H_2 + H_2O \quad (37)$$

$$C_3H_8 + OH \rightarrow C_3H_7 + H_2O \quad (38)$$

$$C_3H_7 + OH \rightarrow C_3H_6 + H_2O \quad (39)$$

The C_2H_5, C_2H_3, and C_3H_7 radicals can be further converted to form ethylene, acetylene, and propane either by electron collisions (Equations 19-21, and 24) or by the oxidative dehydrogenation reactions (Equations 28-30, 32-35, 37, and 39). The extracted hydrogen atoms immediately form hydrogen gas according to Equation 17. However, no propene is detected in the outlet gas stream [13]. It is, therefore, believed that the propene species is unstable and may possibly undergo further reactions (Equations 40 and 41).

Propene hydrogenation and cracking reactions:

$$C_3H_6 + H_2 \rightarrow C_3H_8 \quad (40)$$

$$C_3H_6 \rightarrow C_2H_2 + CH_4 \quad (41)$$

In addition, the radicals of hydrocarbons and hydrogen derived from the earlier reactions further react with themselves and the other radicals to form ethane, ethylene, acetylene, propane, and butane, as shown in Equations 42-57. In addition, ethane can be further dehydrogenated to form ethylene, while ethylene can also be dehydrogenated to form acetylene by either electron collision or oxidative dehydrogenation (Equations 18, 19, 27, 28, 34, and 35 for ethylene formation; and, Equations 20, 21, 29, 30, 36, and 37 for acetylene formation).

Coupling reactions of active species:

Ethane formation reactions;

$$CH_3 + CH_3 \rightarrow C_2H_6 \quad (42)$$

$$C_2H_5 + H \rightarrow C_2H_6 \quad (43)$$

$$C_2H_5 + C_2H_5 \rightarrow C_2H_6 + C_2H_4 \quad (44)$$

$$C_3H_7 + CH_3 \rightarrow C_2H_6 + C_2H_4 \quad (45)$$

Ethylene formation reactions;

$$CH_2 + CH_2 \rightarrow C_2H_4 \quad (46)$$

$$CH_3 + CH_3 \rightarrow C_2H_4 + H_2 \quad (47)$$

$$C_2H_5 + H \rightarrow C_2H_4 + H_2 \quad (48)$$

$$C_3H_7 + H \rightarrow C_2H_4 + CH_4 \quad (49)$$

Acetylene formation reactions;

$$CH + CH \rightarrow C_2H_2 \quad (50)$$

$$CH_2 + CH_2 \rightarrow C_2H_2 + H_2 \quad (51)$$

$$CH_3 + CH \rightarrow C_2H_2 + H_2 \quad (52)$$

$$C_2H_5 + H \rightarrow C_2H_2 + H_2 + H_2 \quad (53)$$

$$C_3H_7 + H \rightarrow C_2H_2 + CH_4 + H_2 \quad (54)$$

Propane formation reactions;

$$C_2H_5 + CH_3 \rightarrow C_3H_8 \quad (55)$$

Butane formation reactions;

$$C_2H_5 + C_2H_5 \rightarrow C_4H_{10} \quad (56)$$

$$C_3H_7 + CH_3 \rightarrow C_4H_{10} \quad (57)$$

Moreover, CO can be produced under the studied conditions, particularly in feed with high oxygen content. CO may be mainly formed via the CO_2 dissociation (Equations 10 and 11). Equations 58-62 show the partial oxidative pathways of methane to form CO and H_2 as the end products. The formation of water is believed to occur via the oxidative hydrogenation reactions (Equations 33-39). In addition, water can be formed by the reactions between hydrogen or hydrogen active radical and oxygen active radical, as shown in Equations 63-65.

Carbon monoxide formation reactions:

$$CH_3 + O \rightarrow HCHO \quad (58)$$

$$HCHO + O \rightarrow OH + CHO \quad (59)$$

$$CHO + O \rightarrow OH + CO \quad (60)$$

$$CHO + OH \rightarrow CO + H_2O \quad (61)$$

$$CHO + H \rightarrow H_2 + CO \quad (62)$$

Water formation reactions:

$$2H + O \rightarrow H_2O \quad (63)$$

$$H_2 + O \rightarrow H_2O \quad (64)$$

$$H_2 + \tfrac{1}{2} O \rightarrow H_2O \quad (65)$$

Additionally, hydrocarbon molecules may crack to form carbon and hydrogen via cracking reactions (Equations 66-68).

$$CH_4 \rightarrow C + 2H_2 \quad (66)$$

$$C_2H_6 \rightarrow 2C + 3H_2 \quad (67)$$

$$C_3H_8 \rightarrow 3C + 4H_2 \quad (68)$$

2.3.1. Effect of Hydrocarbons-to-Steam Molar Ratio

The experiments were performed to initially investigate the effect of hydrocarbons-to-steam molar ratio by varying steam content in feed in the range of 0-30 mol%, while the other operating parameters were controlled at the base conditions [12]: a total feed flow rate of 100 cm^3/min, an input frequency of 300 Hz, an applied voltage of 17.5 kV, and an electrode gap distance of 6 mm. Table 1 shows the corresponding hydrocarbons-to-steam molar ratios at various steam contents used in this work.

Table 2.1 The corresponding steam contents at various hydrocarbons-to steam molar ratio

Hydrocarbons-to-steam molar ratio	Steam content (mol%)
no steam	0
9/1	10
8.5/1.5	15
8/2	20
7/3	25

The effect of steam content on reactant conversions and product yields is shown in Figure 2.2a. When the steam content increased to 10 mol%, the conversions of CH_4, C_2H_6, C_3H_8, and CO_2, as well as the H_2 yield, were remarkably enhanced as compared to the system without steam addition. Basically, in the plasma system, the steam plays an important role in providing several active species, such as OH, H, and O, from its dissociation reactions resulted from the collision by electrons (Equations 8-9). These active species can activate all reactants to form various products, leading to increasing the rates of oxidative dehydrogenation reactions and coupling reactions (Equations 26-39 and 42-57), as well as the increases in the conversions of CH_4, C_2H_6, C_3H_8, and CO_2. However, a further increase in steam content greater than 10 mol% was found to exhibit negative effects on the process performance. It should be noted that the high-energy electrons directly collide with both hydrocarbons mixture and steam, with the amount directly relative to their concentrations. As a result there are the competitive collision reactions of electrons with both hydrocarbons and steam, leading to lowering the

possibility of electron-hydrocarbon collisions at a large steam content [15]. Hence, the conversions of CH_4, C_2H_6, and CO_2, as well as the H_2 yield, decreased. Moreover, a large steam content can alter the plasma characteristics and also reduce the stability of plasma, which was directly observed from the discharge appearance and its behaviors (e.g. a smaller number of arcs produced with unsmooth arc patterns along the knife-shaped electrode pairs).

Figure 2.2b shows the outlet gas concentrations as a function of steam content. The concentrations of CH_4, C_2H_6, and CO_2 in the outlet gas tended to increase with increasing steam content from 10 to 30 mol%, corresponding to the decreases in CH_4, C_2H_6, and CO_2 conversions (Figure 2.2a). Interestingly, the concentration of C_3H_8 decreased with increasing steam content from 0-20 mol%, and increased with further increasing steam content, which corresponded well with the C_3H_8 conversion. In comparisons of all reactant conversions, the conversion was found in the following order: $C_3H_8 > C_2H_6 > CH_4 > CO_2$. These results can be explained by the differences in the bond dissociation energies of C_3H_8, C_2H_6, CH_4, and CO_2, which are 395, 410, 431, and 532 kJ/mol, respectively [12]. The higher the value of the bond dissociation energy, the lower the conversion. Thus, the C_3H_8 molecule can be much more easily converted in the plasma zone as compared to the other reactant components, even though the plasma characteristics and stability became more fluctuated at a large steam content.

Figure 2.2c shows the effect of steam content on the product selectivities. The H_2 selectivity rapidly increased with increasing steam content up to 10 mol%, and then it gradually dropped in the steam content range of 10-30 mol%. These results indicate the significant effect of the presence of steam in the plasma system, as stated above. Both the selectivities for CO and C_4H_{10} were found to slightly change with increasing steam

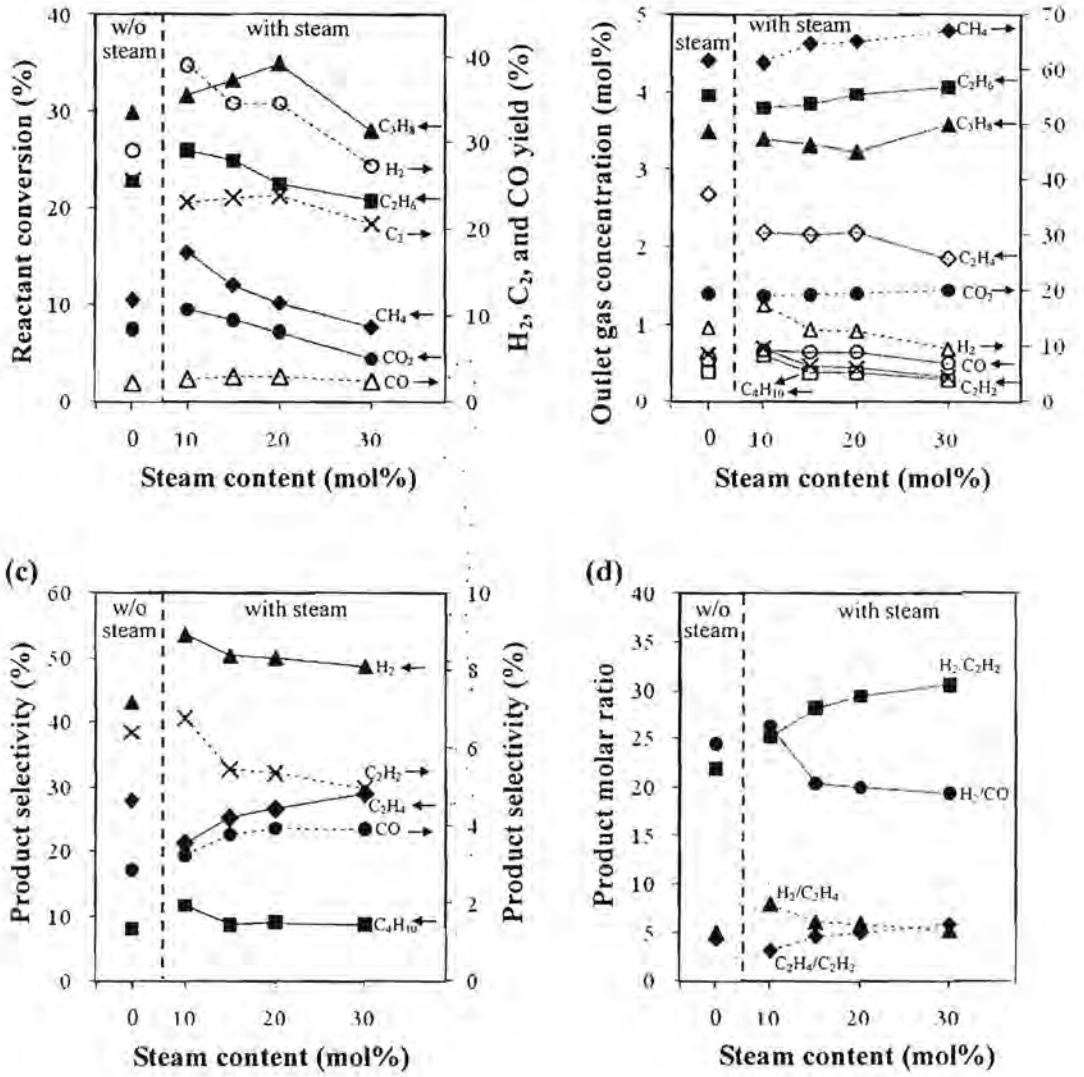

Figure 2.2 Effect of steam content on (a) reactant conversions and product yields, (b) concentrations of outlet gas, (c) product selectivities, and (d) product molar ratios for the reforming of natural gas with steam (total feed flow rate, 100 cm^3/min; applied voltage, 17.5 kV; input frequency, 300 Hz; and electrode gap distance, 6 mm).

content. The insignificant change of the CO selectivity agrees well with the CO yield, as shown in Figure 2.2a. The C_2H_2 selectivity slightly increased with increasing steam content up to 10 mol% and tended to decrease with further increasing steam content. On the other hand, the C_2H_4 selectivity showed an opposite trend. The results are well related to the molar ratios of C_2H_4/C_2H_2, H_2/C_2H_2, and H_2/C_2H_4, as shown in Figure 2.2d. The molar ratio of C_2H_4/C_2H_2 moderately decreased with increasing steam content to 10 mol%, whereas the rapid increases in both the H_2/C_2H_2 and H_2/C_2H_4 molar ratios were observed. These results indicate that the increase in H_2 production exceeds the increases in C_2H_2 and C_2H_4 production, partly due to the dehydrogenation of C_2H_4 to form H_2 and C_2H_2. It can also suggest that at the steam content of 10 mol%, the dehydrogenation of C_2H_4 is more dominant than the coupling reactions of hydrocarbon active species, leading to the consumption of C_2H_4 for a large extent to produce H_2. This possibly led to an overall decrease in the C_2 yield when increasing steam content from 0 to 10 mol % (Figure 2.2a). As mentioned above, the contradictory selectivities for C_2H_2 and C_2H_4 imply that the decrease in C_2H_4 selectivity had a more impact on the C_2 yield than the C_2H_2 selectivity in the steam content range of 0 to 10 mol%. When the steam content increased from 10 to 20 mol%, the C_2 yield remained almost unchanged (Figure 2.2a). A possible explanation is that the dehydrogenation of C_2H_4 and the coupling reactions of hydrocarbon active species simultaneously occurred at approximately the same rate. Moreover, the further increase in steam content from 20 to 30 mol% decreased the C_2 yield. It can be explained by the fact that when the steam content increased, the system had lower electrons available to collide with the reactants.

In comparisons of the H_2/CO ratios, the H_2 and CO concentrations in the outlet gas and the selectivities for H_2 and CO at different steam contents, at the steam content of

10 mol%, the system provided the highest selectivity for H_2 and the maximum molar ratios of H_2/CO and H_2/C_2H_4, suggesting the synergistic effect of steam addition on both the reactant conversions and H_2 yield, as indicated by the smoother and more stable gliding arc discharge phenomena. Therefore, the steam content of 10 mol% was preliminarily considered to be an optimum value for the reforming of CO_2-containing natural gas using gliding arc.

The effect of steam content on the power consumptions per reactant molecule converted and per H_2 molecule produced is shown in Figure 2.3. Both power consumptions first rapidly decreased with increasing steam content to 10 mol%, but dramatically increased with further increasing steam content from 10 to 30 mol%. The minimum power consumptions were about 2.12×10^{-18} Ws (13.23 eV) per reactant molecule converted and 1.95×10^{-18} Ws (12.15 eV) per H_2 molecule produced at the steam content of 10 mol%. Interestingly, it can be clearly seen that at any steam content, the power consumption per H_2 molecule produced was lower than that per reactant molecule converted, implying that the studied plasma system can be considered to be effective for producing hydrogen from the steam reforming of CO_2-containing natural gas. From the overall results, the steam content of 10 mol% was selected for further investigation.

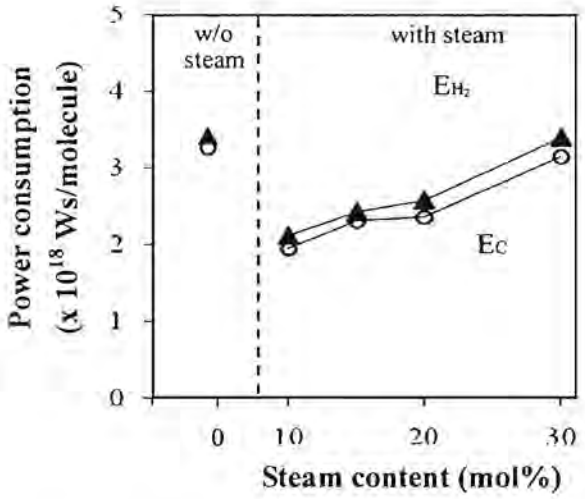

Figure 2.3 Effect of steam content on power consumptions for the reforming of natural gas with steam (total feed flow rate, 100 cm^3/min; applied voltage, 17.5 kV; input frequency, 300 Hz; and electrode gap distance, 6 mm) (E_C: power per reactant molecule converted; E_{H2}: power per H_2 molecule produced).

2.3.2. Effect of Total Feed Flow Rate and Residence Time

The effect of total feed flow rate (or residence time) on reactant conversions and product yields at a constant steam content of 10 mol% is illustrated in Figure 2.4a. The corresponding residence times at various total feed flow rates of 75, 100, 125, and 150 cm^3/min were 1.83, 1.37, 1.10, and 0.91 s, respectively. An increase in the total feed flow rate results in decreasing the residence time in the plasma reaction zone, leading to decreasing the probability of collisions between reactant molecules and highly energetic electrons. As expected, the conversions of CH_4, C_2H_6, C_3H_8, and CO_2 tended to decrease with increasing total feed flow rate or decreasing residence time. Interestingly, the H_2 yield rapidly increased with increasing total feed flow rate from 75 to 100 cm^3/min, and then sharply decreased with further increasing total feed flow rate from 100 to 150

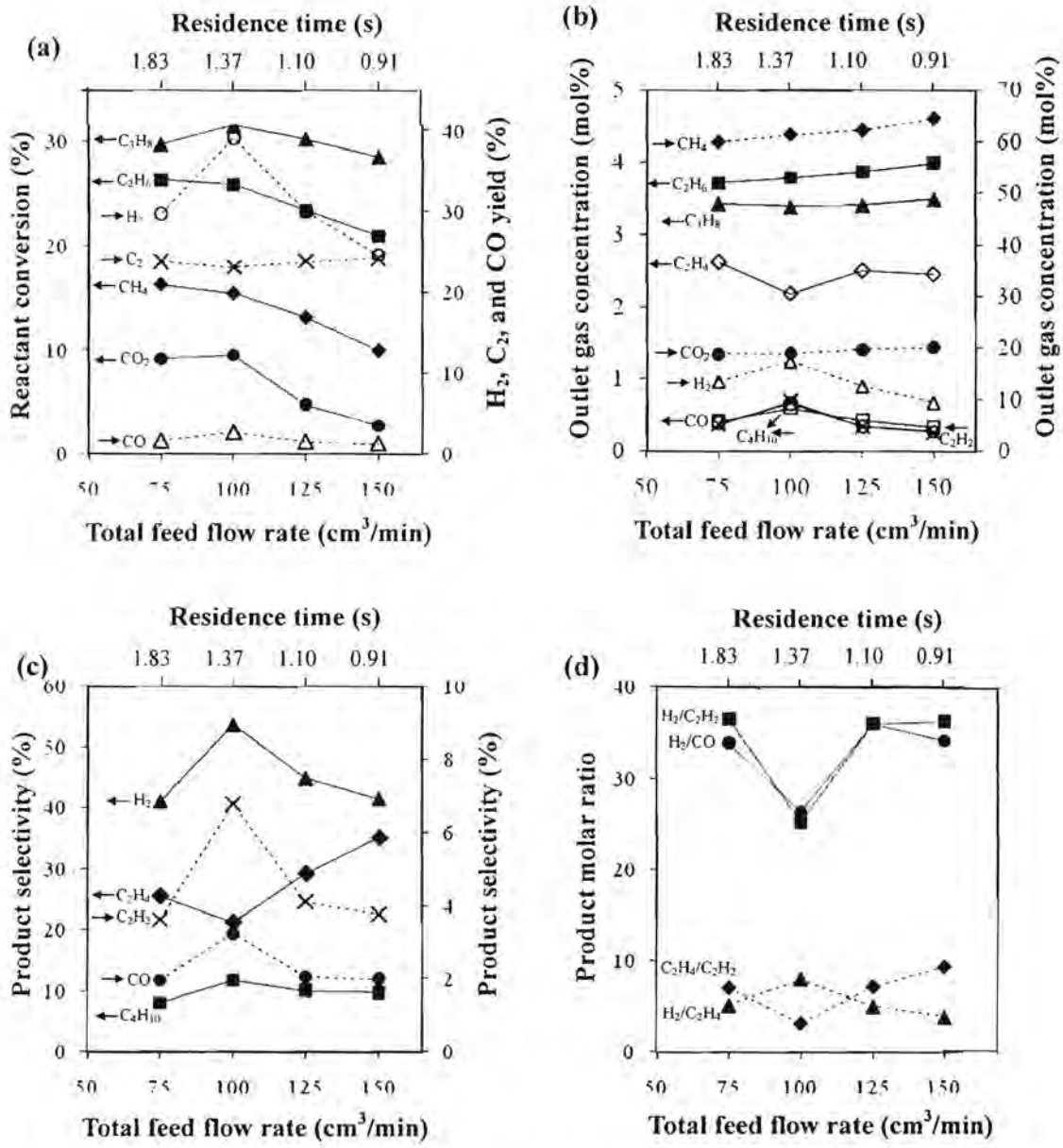

Figure 2.4 Effect of total feed flow rate on (a) reactant conversions and product yields, (b) concentrations of outlet gas, (c) product selectivities, and (d) product molar ratios for the reforming of natural gas with steam (steam content, 10 mol%; applied voltage, 17.5 kV; input frequency, 300 Hz; and electrode gap distance, 6 mm).

cm^3/min. These results well relate to the concentrations of outlet gases, particularly the H_2 concentration, as shown in Figure 2.4b. However, the increase in total feed flow rate has an insignificant impact on the C_2 and CO yields, as shown in Figure 2.4a. The concentrations of CH_4, C_2H_6, C_3H_8, and CO_2 tended to increase with increasing total feed flow rate, whereas the concentrations of H_2, CO, and C_2H_2 increased with increasing total feed flow rate from 75 to 100 cm^3/min and then decreased with further increasing total feed flow rate from 100 to 150 cm^3/min.

Figure 2.4c shows the effect of total feed flow rate or residence time on the product selectivities at a constant steam content of 10 mol%. The selectivities for H_2, CO, C_2H_2, and C_4H_{10}, initially increased with increasing total feed flow rate from 75 to 100 cm^3/min, and then sharply decreased with further increasing total feed flow rate from 100 to 150 cm^3/min. In contrast, the C_2H_4 selectivity initially decreased with increasing total feed flow rate from 75 to 100 cm^3/min and then greatly increased with further increasing total feed flow rate from 100 to 150 cm^3/min. These results also agree well with the concentrations of outlet gases, as shown in Figure 2.4b. The concentrations of H_2, CO, C_2H_2, and C_4H_{10} were found to increase with increasing total feed flow rate from 75 to 100 cm^3/min and then decreased with further increasing total feed flow rate from 100 to 150 cm^3/min. On the other hand, the concentration of C_2H_4 exhibited the opposite trend. This finding can be explained in that at a lower total feed flow rate, a greater number of energetic electrons, as well as various active species, essentially provided a comparatively higher possibility of the plasma-chemical dehydrogenation of hydrocarbon species (e.g. C_2H_4 and C_2H_6) to be converted to smaller molecules (e.g. C_2H_2, H_2, and CO), as shown in Equations 27-30, 34-37, 53, 58-62. In contrast, at a higher total feed

flow rate, the possibility of secondary dehydrogenation of hydrocarbon species decreased because of the decreasing residence time in the plasma zone. However, a further decrease in feed flow rate from 100 to 75 cm^3/min resulted in lowering all the product selectivities and the product concentrations, except C_2H_4. This result indicates that at the feed flow rate of 75 cm^3/min, the system had a very long residence time, leading to increasing the probability for the hydrogenation, or the reverse of the oxidative dehydrogenation, of C_2H_2 and the CO oxidation reaction. The maximum H_2 and C_2H_2 selectivities were observed at the total feed flow rate of 100 cm^3/min (the residence time of 1.37 s), suggesting that the dehydrogenation reaction of C_2H_4 to form C_2H_2 and H_2 preferably occurred and was maximized at this optimum total feed flow rate.

The effect of total feed flow rate on the product molar ratios is illustrated in Figure 2.4d. With increasing total feed flow rate from 75 to 100 cm^3/min, the molar ratios of H_2/CO and H_2/C_2H_2 sharply decreased, then rapidly increased with increasing total feed flow rate from 100 to 125 cm^3/min and finally remained almost unchanged with further increasing total feed flow rate from 125 to 150 cm^3/min. The molar ratio of C_2H_4/C_2H_2 slightly decreased with increasing total feed flow rate from 75 to 100 cm^3/min and then gradually increased with further increasing total feed flow rate to 150 cm^3/min. In contrast, the molar ratio of H_2/C_2H_4 slightly increased with increasing total feed flow rate from 75 to 100 cm^3/min and then decreased with further increasing total feed flow rate to 150 cm^3/min, which was in the opposite trend to the molar ratios of H_2/CO, H_2/C_2H_2, and C_2H_4/C_2H_2. These results can be correlated well with the plasma-chemical dehydrogenation behavior as stated above that the dehydrogenation reaction of C_2H_4 to form C_2H_2 and H_2, as well as the CO formation, preferably occurred at the total feed flow rate of 100 cm^3/min.

The effect of total feed flow rate on the power consumptions per reactant molecule converted and per H_2 molecule produced is shown in Figure 2.5. With increasing total feed flow rate from 75 to 100 cm^3/min, the power consumed to convert hydrogen reactant molecules and to produce hydrogen molecule significantly decreased, probably resulting from the observed good characteristic and high stability of plasma generated at the total feed flow rate of 100 cm^3/min. At a lower total feed flow rate (75 cm^3/min), the steam in the reactant feed can change the dielectric property of the system, which subsequently led to a decrease in the stability of plasma, as above mentioned. However, with further increasing total feed flow rate from 100 to 150 cm^3/min, the input power sharply increased. The increases in power consumptions at too high feed flow rates can be explained by the decreases in both reactant conversions and hydrogen production when the total feed flow rate was too high (too short residence time). Because, the minimum power consumptions were found at the total feed flow rate of 100 cm^3/min, this total feed flow rate was selected for further investigation.

2.3.3. Effect of Applied Voltage

In this present work, the effect of applied voltage was investigated by varying in the range of 12.5 to 18.5 kV. The corresponding input power at various applied voltages of 12.5, 13.5, 15.5, 17.5, and 18.5 kV were 22.1, 26.0, 26.2, 28.3, and 28.5 W, respectively, noting that the amount of input power was given from the calculation. The highest operationable applied voltage of 18.5 kV was limited by the abrupt formation of coke filament on the surfaces of the two electrodes in a relatively short operation period, which resulted in a significant decrease in the stability of plasma, while the lowest operationable applied voltage of 12.5 kV was limited by the breakdown voltage of the studied plasma system, which is a minimum voltage value required to generate a steady plasma

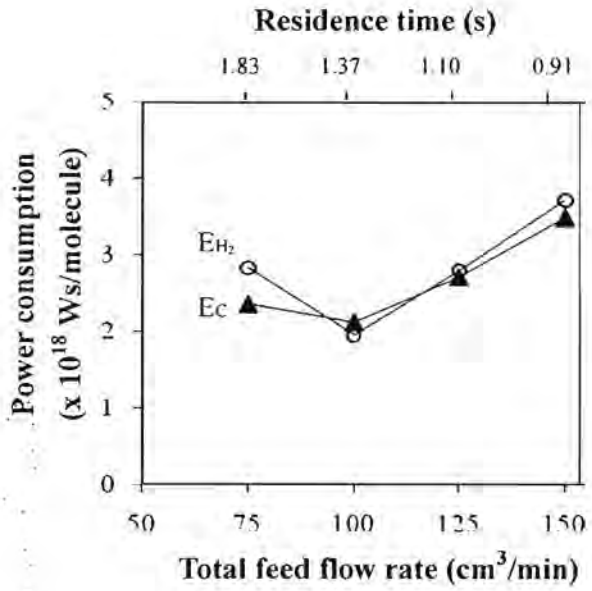

Figure 2.5 Effect of total feed flow rate on power consumptions for the reforming of natural gas with steam (steam content, 10 mol%; applied voltage, 17.5 kV; input frequency, 300 Hz; and electrode gap distance, 6 mm) (E_C: power per reactant molecule converted; E_{H2}: power per H_2 molecule produced).

discharges.

Figure 2.6a shows the effect of applied voltage on the reactant conversions and product yields at a constant steam content of 10 mol%, an input frequency of 300 Hz, and electrode gap distance of 6 mm, and a constant total feed flow rate of 100 cm^3/min. The results showed that the conversions of CH_4, C_2H_6, C_3H_8, and CO_2, as well as the H_2 and C_2 yields, tended to increase with increasing applied voltage except the CO yield remained almost unchanged. It could be clearly observed that an increase in applied voltage induces a stronger electric field strength across the electrodes, as experimentally

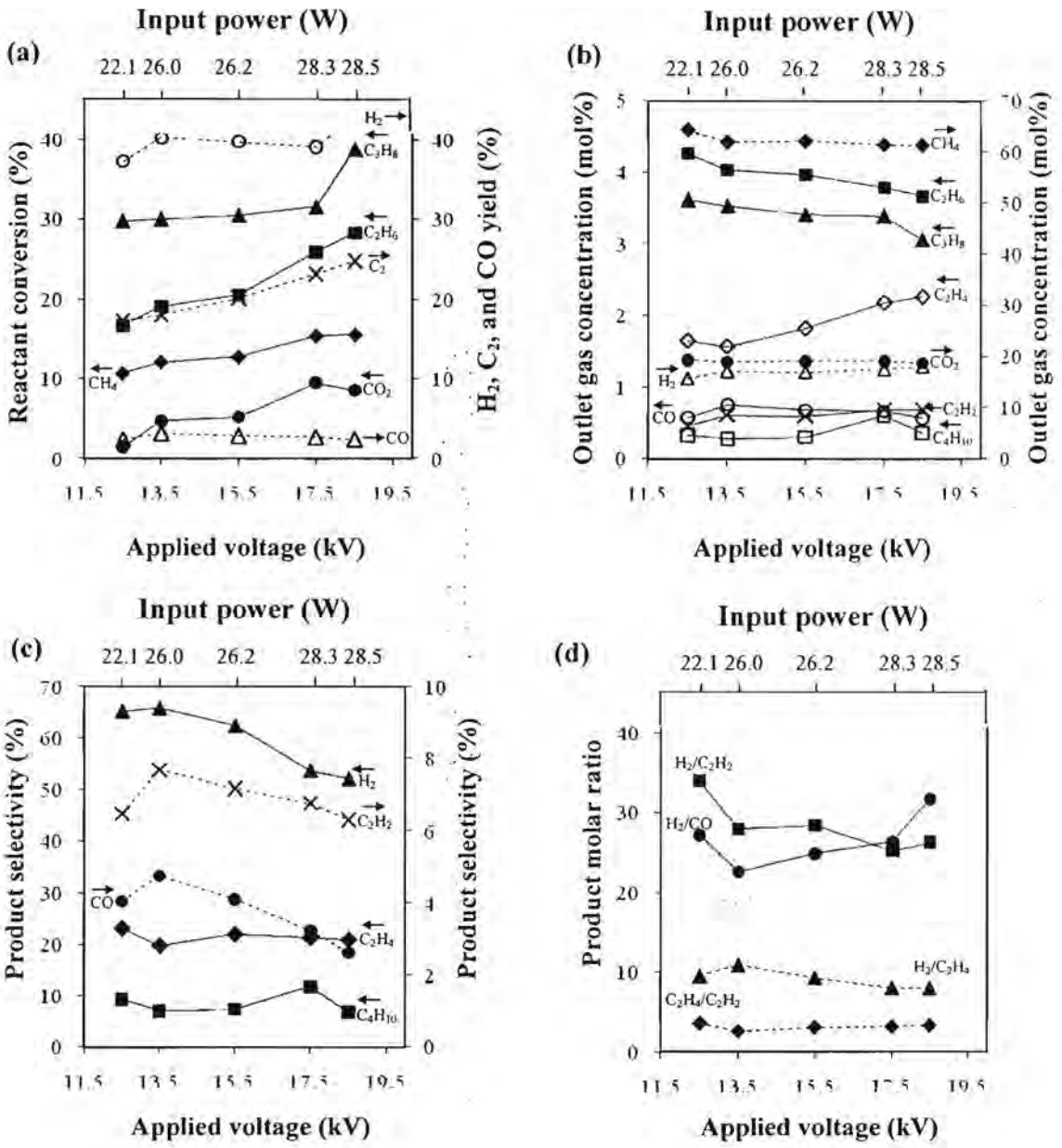

Figure 2.6 Effect of applied voltage on (a) reactant conversions and product yields, (b) concentrations of outlet gas, (c) product selectivities, and (d) product molar ratios for the reforming of natural gas with steam (steam content, 10 mol%; total feed flow rate, 100 cm^3/min; input frequency, 300 Hz; and electrode gap distance, 6 mm).

observed by an increase in input current and power. More specifically, the electric field strength is simply proportional to the mean electron energy intensity and electron temperature in the plasma [13]. Thereby, at a higher voltage, the higher input power, the generated plasma contains not only electrons with a higher average energy and temperature but also has a higher electron density. Hence, as expected, the opportunity for the occurrence of elementary chemical reactions by electron collisions (mainly ionization, excitation, and dissociation of gaseous molecules) is increased (Equations 8-25), resulting in an increase in the number of chemically active species being formed and sub-sequentially used to activate the plasma-chemical reactions [13-15, 17]. However, it was observed that the CO yield was insignificantly affected by an increase in applied voltage (Figure 2.6a). These results suggest that the partial oxidation pathways of methane to form CO and the dissociation reactions of carbon dioxide to form CO cannot complete with the other reactions.

The effect of applied voltage on the concentrations of outlet gases is illustrated in Figure 2.6b. The concentrations of CH_4, C_2H_6, C_3H_8, and CO_2 gradually decreased with increasing applied voltage, whereas the concentration of H_2 slightly increased. These results well agree with the CH_4, C_2H_6, C_3H_8, and CO_2 conversions and the H_2 yield. Figure 2.6c shows the effect of applied voltage on the product selectivities. The C_2H_2, H_2, and CO selectivities initially increased with increasing applied voltage from 12.5 to 13.5 kV and then decreased significantly with further increasing applied voltage from 13.5 to 18.5 kV. On the contrary, the selectivities for C_2H_4 and C_4H_{10} slightly decreased with increasing applied voltage from 12.5 to 13.5 kV and then tended to slightly increased with further increasing applied voltage. When considering the applied voltage range of 12.5-13.5 kV, the selectivities for C_2H_2 and H_2 increased, whereas the selectivities for

C_2H_4 and C_4H_{10} showed the opposite trends, indicating that the C_2H_2 and H_2 were preferentially produced from the dehydrogenation reactions of C_2H_4 and C_4H_{10}. A possible explanation is that at a higher applied voltage of 13.5 kV, a higher electron density, as well as a subsequent more number of active species, led to the increase in opportunity for the secondary plasma-chemical dehydrogenations of C_2H_4 and C_4H_{10}, resulting in the increase in the C_2H_2 and H_2 selectivities. However, in the applied voltage range of 13.5-18.5 kV, the decreases in the H_2 and C_2H_2 selectivities with increasing applied voltage. This is because the amount of coke deposit on the electrode surfaces was found to increase with increasing applied voltage in this studied range (7.46 % of coke at 12.5 kV, 9.15 % at 13.5 kV, 9.74 % at 15.5 kV, 10.92 % at 17.5 kV, and 13.22 % at 18.5 kV). This is possibly because at very high applied voltage, a large number of active species increased an opportunity for the secondary-dissociation reaction of CO_2 to form coke (Equation 12). In addition, the increasing tendency of the C_2H_4 and C_4H_{10} selectivities in this high applied voltage range implies that the dehydrogenation reactions are less likely to occur than the coupling reactions with increasing applied voltage.

The effect of applied voltage on the product molar ratios is shown in Figure 2.6d. The molar ratio of H_2/CO initially decreased with increasing applied voltage from 12.5 to 13.5 kV and then significantly increased with further increasing applied voltage. In the applied voltage range of 12.5-13.5 kV, the selectivity of CO rapidly increased, as mentioned above, indicating that the increase in applied voltage enhanced the dissociation reactions of CO_2 (Equations 10-11). Additionally, the result implies that, in the low applied voltage range, the CO_2 dissociation has a higher possibility to occur, as compared to the cracking of hydrocarbons to produce H_2 and coke (Equations 66-68). In the applied voltage range of 13.5-18.5 kV, the substantial increase in the molar ratio of

H_2/CO was found with increasing applied voltage because both the CO dissociation, the cracking of hydrocarbons, and the dehydrogenation reactions of hydrocarbons have higher possibilities to simultaneously occur, as compared to the CO_2 dissociation. These possible pathways are well confirmed by the observed increase in the amount of coke with increasing applied voltage. The molar ratio of H_2/C_2H_4 slightly increased with increasing applied voltage from 12.5 to 13.5 kV and then tended to decrease with further increasing applied voltage. This can be explained in that in the low applied voltage range of 12.5-13.5 kV, C_2H_4 can be selectively dehydrogenated to form H_2 via the secondary plasma-chemical dehydrogenation reaction due to the increase in the number of active species. However, at an applied voltage higher than 13.5 kV, the H_2 selectivity was found to drastically decrease (Figure 2.6c). This led to the decreases in both the molar ratios of H_2/C_2H_2 and H_2/C_2H_4 (Figure 2.6c). Interestingly, the C_2H_4/C_2H_2 molar ratio tended to slightly increase with increasing applied voltage from 13.5 to 18.5 kV (Figure 2.6d), implying that the coupling reactions preferably occur than the dehydrogenation reactions. These results were confirmed by the increase in C_2H_4 concentration (Figure 2.6b).

Figure 2.7 shows the effect of applied voltage on the power consumptions. The power consumption per reactant molecule converted (E_C) remained almost constant with increasing applied voltage from 12.5 to 13.5 kV, and it slightly increased with increasing applied voltage from 13.5 to 15.5 kV, and finally decreased with further increasing applied voltage. The decrease in power consumption per reactant molecule converted at high applied voltage range is possibly due to the rapid increase in CH_4, C_2H_6, and C_3H_8 conversions (Figure 2.6a). The power consumption per H_2 molecule produced (E_{H2})

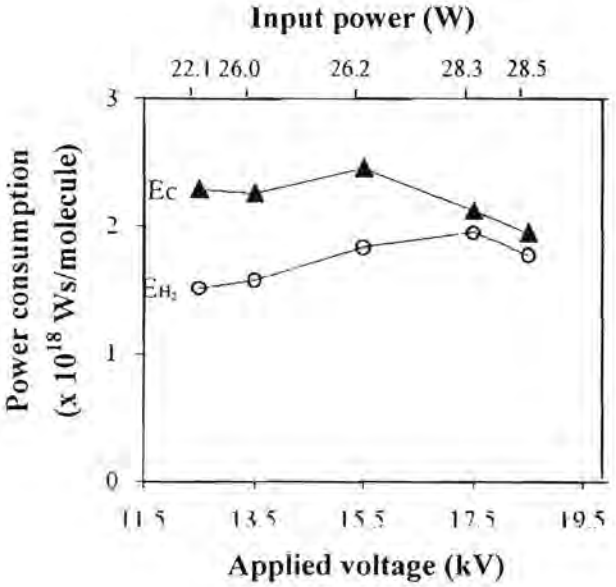

Figure 2.7 Effect of applied voltage on power consumptions for the reforming of natural gas with steam (steam content, 10 mol%; total feed flow rate, 100 cm^3/min; input frequency, 300 Hz; and electrode gap distance, 6 mm) (E_C: power per reactant molecule converted; E_{H2}: power per H_2 molecule produced).

tended to increase with increasing applied voltage from 12.5 to 17.5 kV and then decreased with further increasing applied voltage. The initial increase in the power consumption per H_2 molecule produced can be explained by the decrease in hydrogen production (Figure 2.6c). From the overall results, the optimum voltage of 13.5 kV, which reasonably provided both high selectivities for H_2 and CO and relatively low power consumptions, was selected for further experiments.

2.3.4. Effect of Input Frequency

In this present work, the input frequency was experimentally varied in the range of 300-600 Hz. The corresponding input power at various input frequencies of 300, 400,

500, and 600 Hz were 26.0, 21.7, 19.7, and 19.2 watt, respectively. The limitation of the operationable lowest frequency of 300 Hz was due to the rapid formation of coke on the electrode surfaces, leading to the interruption of the plasma generation and stability, whereas the operationable highest frequency of 600 Hz was limited by the insufficient and unstable gliding arc discharges (i.e. the extremely small number of arc produced with unsmooth arc patterns along the electrode pairs).

Figure 2.8a illustrates the effect of input frequency on the reactant conversions and product yields at a constant steam content of 10 mol%, a total feed flow rate of 100 cm^3/min, and an applied voltage of 13.5 kV, and an electrode gap distance of 6 mm. The experimental results clearly reveal that all of reactant conversions and product yields tended to decrease with increasing input frequency, corresponding to the increase in all reactant concentrations and the decrease in H_2, C_2H_2, C_2H_4, and CO concentrations in the outlet gas (Figure 2.8b). The measured current across the electrodes and input power were found to gradually decrease with increasing input frequency from 300 to 600 Hz. It is widely accepted that in an alternating current discharge system, each electrode acts alternately as an anode and cathode, due to the reversal in polarity of the electric field, and the current periodically reverse in direction. A higher frequency and a faster reversal rate in the current can cause a slower decay rate of space charges (electrons and ions) [13,17-19]. According to this reason, when employing a constant applied voltage and a fixed electrode gap distance, the current consumed to continuously activate and maintain the plasma discharge is reduced with increasing input frequency. As a result, the higher the input frequency, the lower the current, the lower the number of generated electrons and the lower the number of generated active species to initiate the plasma-chemical reactions. Based on the aforementioned phenomena relating to the input frequency, the

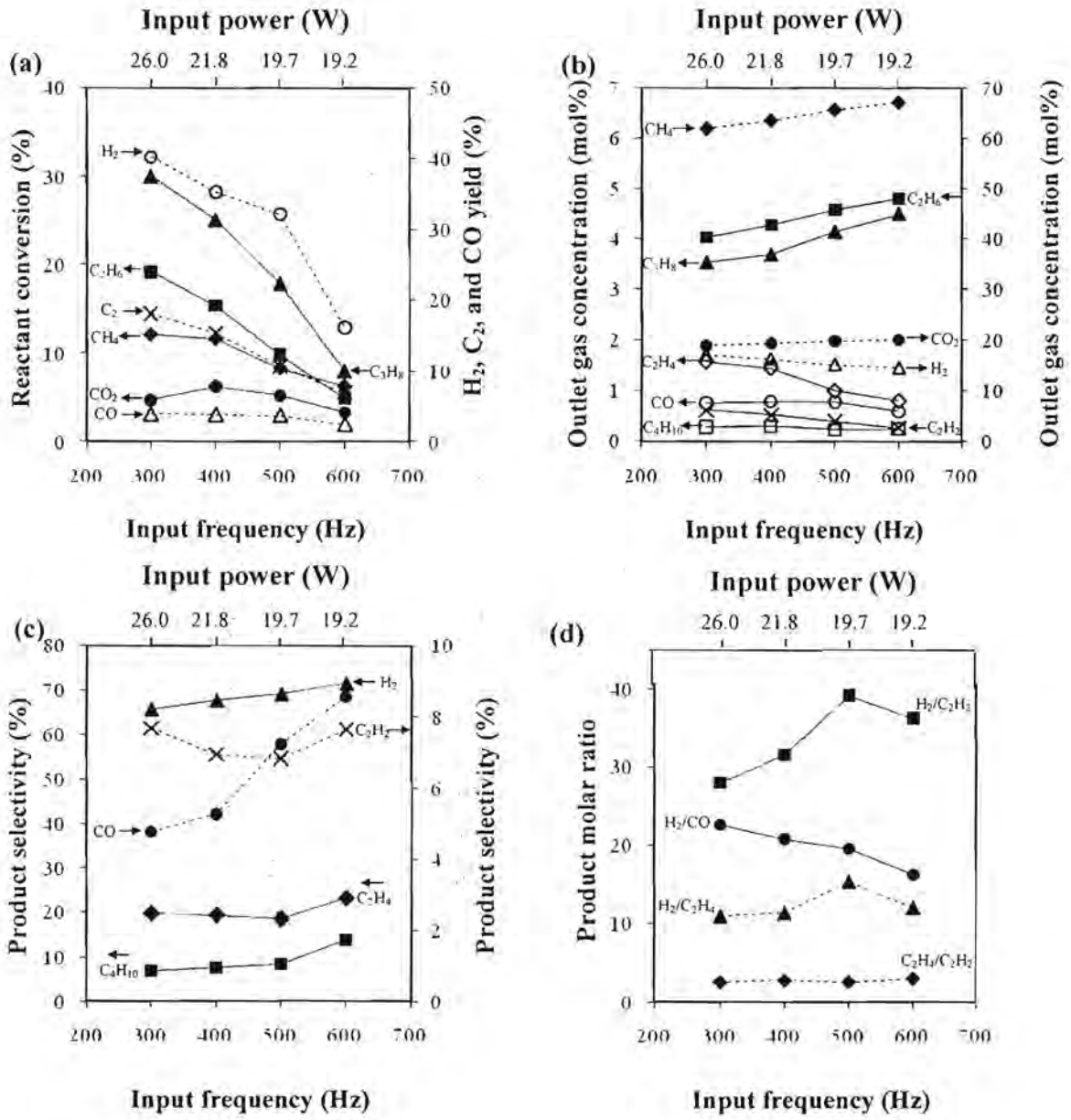

Figure 2.8 Effect of input frequency on (a) reactant conversions and product yields, (b) concentrations of outlet gas, (c) product selectivities, and (d) product molar ratios for the reforming of natural gas with steam (steam content, 10 mol%; total feed flow rate, 100 cm^3/min; applied voltage 13.5 kV; and electrode gap distance, 6 mm).

space charge characteristic of the alternating current discharge is a decisive factor that greatly influences the behaviors of discharge and the efficiency of the plasma-chemical reactions. By taking this reason into account, when the input frequency was increased, the decreases in all reactant conversions and product yields possibly resulted from the reduction of the number of generated electrons to activate the chemically active species [14,21].

The effect of input frequency on the product selectivities is shown in Figure 2.8c. With increasing input frequency, all the product selectivities except C_2H_2 tended to increase, especially the CO selectivity. However, when correlatively considering H_2, C_2H_4, and C_4H_{10} concentrations (Figure 2.8b), they slightly decreased with increasing input frequency. These results suggest that even though the reactant conversions were found to decrease, the reactants tended to be converted more selectively to H_2, CO, C_2H_4, and C_4H_{10}. For the C_2H_2 selectivity, it initially decreased with the increasing input frequency from 300 to 500 Hz and then increased with increasing input frequency from 500 to 600 Hz. The initial decrease in the C_2H_2 selectivity in the input frequency range of 300 to 500 Hz corresponded well to the decrease in the C_2H_2 concentration (Figure 2.8b). The decrease in C_2H_2 selectivity implies that the electron collisions with C_2H_4, C_2H_6, and C_3H_8 (Equations 13-24) and oxidative dehydrogenation reactions (Equations 21-39) are preferable to occur at a lower frequency (i.e. 300 Hz). For the CO concentration, it slightly increased with increasing input frequency from 300 to 500 Hz and then decreased with further increasing input frequency. These results suggest that increasing input frequency in the range of 300 to 500 Hz enabled the occurrence of carbon dioxide dissociation reactions and the oxidative dehydrogenation reactions of methane to form CO. Afterwards, at the higher input frequency range of 500-600 Hz, the number of active

species was reduced due to the undesired phenomena of space charge characteristic, as mentioned above, causing the reduction of input power. Therefore, all of the product concentrations tended to decrease.

Figure 2.8d shows the effect of input frequency on the product molar ratios. The H_2/C_2H_2 and H_2/C_2H_4 molar ratios gradually increased with increasing input frequency from 300 to 500 Hz and then rapidly decreased with further increasing input frequency. These results imply that the increase in input frequency resulted in the decreases in C_2H_2 and C_2H_4 formation rather than the decrease in H_2 formation. This led to the increase in H_2/C_2H_2 and H_2/C_2H_4 molar ratios, despite the decrease in the H_2 concentration (Figure 2.8b). With increasing input frequency, the C_2H_4/C_2H_2 molar ratio remained almost unchanged, implying that the tendency of C_2H_2 and C_2H_4 formation is in the same direction, which is consistent with the trend of H_2/C_2H_2 and H_2/C_2H_4 molar ratios. These results indicate that the oxidative dehydrogenation reactions, the electron-ethane collisions (Equations 19-21), and the coupling reactions of active species occur more preferentially at a low input frequency. For the H_2/CO molar ratio, it sharply decreased with increasing input frequency in the investigated range, probably resulted from the gradual decrease in H_2 concentration and the almost constant concentration of CO in the outlet gas stream (Figure 2.8b).

The effect of input frequency on the power consumptions is shown in Figure 2.9. It was clearly found that with increasing input frequency, both power consumptions per reactant molecule converted (E_C) and per H_2 molecule produced (E_{H2}) tended to increase. This is plausibly due to the decreases in quantities of converted reactants and of produced hydrogen when the input frequency increased. It was found that, with increasing input frequency, the intensity of the arc generated between the electrodes was reduced. This is

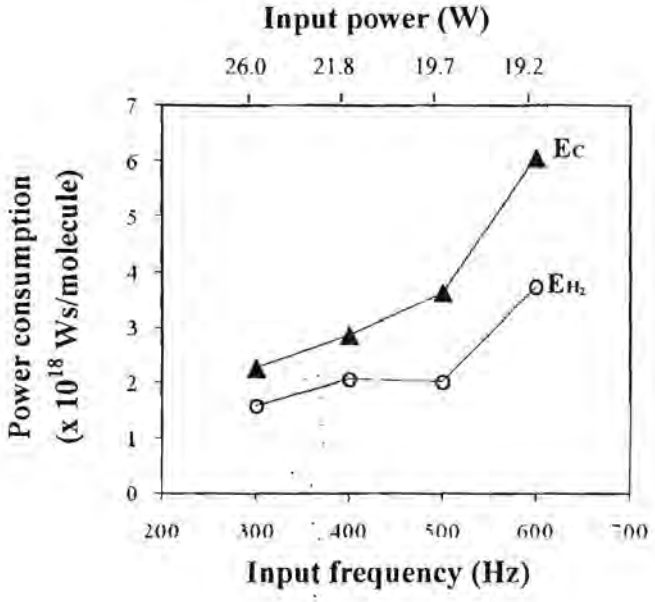

Figure 2.9 Effect of input frequency on power consumptions for the reforming of natural gas with steam (steam content, 10 mol%; total feed flow rate, 100 cm^3/min; applied voltage 13.5 kV; and electrode gap distance, 6 mm) (E_C: power per reactant molecule converted; E_{H2}: power per H_2 molecule produced).

likely because the larger number of sine-waveform cycles per second (high frequency) may require higher input energy to sufficiently sustain the gliding arc discharge, thereby reducing the intensity of the produced arc. From the overall experimental results, the operationable lowest frequency of 300 Hz was considered to be an optimum value for this investigated plasma system because it provided the highest H_2 yield, the lowest power consumptions per reactant molecule converted and per H_2 molecule produced, and the high stable plasma discharge during the system operation.

2.4 Conclusions

In this work, the reforming of CO_2-containing natural gas with steam was investigated under an AC gliding arc discharge system. The effects of hydrocarbons-to-steam molar ratio, total feed flow rate, applied voltage, and input frequency on the synthesis gas and C_2 hydrocarbon production were examined. The addition of steam content of 10 mol% to the simulated natural gas was found to greatly enhance the natural gas reforming performance in terms of reactant conversions, product yields, product selectivities, and power consumptions. All of the reactant conversions tended to increase with increasing applied voltage. However, in the applied voltage range of 13.5-18.5 kV, the decreases in both H_2 and C_2H_2 selectivities resulted from the direct observation of the rapidly increased amount of coke formed on the electrode surfaces. The increase in input frequency showed the negative effect on the reactant conversions, as well as the product yields. The optimum conditions of the investigated gliding arc discharge system were found at a hydrocarbons-to-steam molar ratio of 9/1 (a steam content of 10 mol%), a total feed flow rate of 100 cm^3/min, an applied voltage of 13.5 kV, and an input frequency of 300 Hz.

References

1. Wang B, Zhang X, Liu Y, Xu G. Conversion of CH_4, steam and O_2 to syngas and hydrocarbons via dielectric barrier discharge. J Nat Gas Chem 2009;18:94-7.
2. Sobacchi MG, Saveliev, Fridman AA, Kennedy LA, Ahmed S, Krause T. Experimental assessment of combined plasma/catalytic system for hydrogen production via partial oxidation of hydrocarbon fuels. Int J Hydrogen Energ 2002;27:635-42.
3. He JX, Han YY, Gao AH, Zhou YS, Lu ZG. Investigation on methane decomposition and the formation of C_2 hydrocarbons in DC discharge plasma by emission spectroscopy. Chin J Chem Eng 2004;12:149-51.
4. Nozaki T, Hattori A, Okazaki K. Partial oxidation of methane using a microscale non-equilibrium plasma reactor. Cataly Today 2009;98:607-16.
5. Kalra CS, Gutsol AF, Fridman AA. Gliding arc discharge as a source of intermediate plasma for methane partial oxidation. IEEE Trans Plasma Sci 2005;33:32-4.
6. Paulmier T, Fulcheri L. Use of non-thermal plasma for hydrocarbons reforming. Chem Eng J 2005;106:59-71.
7. Wang Y, Liu CJ, Zhang YP. Plasma methane conversion in the presence of dimethyl ether using dielectric-barrier discharge. Energ & Fuel 2005;19:877-81.
8. Ahmar E El, Met C, Aubry O, Khacef A, Cormier JM. Hydrogen enrichment of a methane-air mixture by atmospheric pressure plasma for vehicle applications. Chem Eng J 2009;116:13-8.

9 Bromberg L, Cohn DR, Rabinovich A, Alexeev N, Samokhin A, Hadidi K, et al. Onboard plasmatron hydrogen production for improved vehicles. MIT Plasma Sci & Fus Cent 2006;JA-06-3:1-173.

10 Petitpas G, Rollier JD, Darmon A, Gonzalez-Aguilar J, Matkemeijer R, Fulcheri L. A comparative study of non-thermal plasma assisted reforming technologies. Int J Hydrogen Energ 2007;32:2848-67.

11 Fridman A, Kennedy LA. Plasma Physics and Engineering. Taylor & Francis. New York; 2004.

12 Rueangjitt N, Akarawitoo C, Sreethawong T, Chavadej S. Reforming of CO_2-containing natural gas using an AC gliding arc system: Effect of gas component in natural gas. Plasma Chem Plasma Process 2007;27:559-76.

13 Rueangjitt N, Sreethawong T, Chavadej S. Reforming of CO_2-containing natural gas using an AC gliding arc system: effects of operational parameters and oxygen addition in feed. Plasma Chem Plasma Process 2008;28:49-67.

14 Supat K, Chavadej S, Lobban LL, Millinson GR. Combined steam reforming and partial oxidation of methane to synthesis gas under electrical discharge. Ind & Eng Chem Res 2003;42:1654-61.

15 Sugasawa M, Terasawa T, Futamura S. Effects of initial water content on steam reforming of aliphatic hydrocarbons with nonthermal plasma. J Electrostat 2010;68:212-7.

16 Dean JA. Lange's Handbook of Chemistry. McGraw-Hill. New York; 1999.

17 Sreethawong T, Thakonpatthanakun P, Chavadej S. Partial oxidation of methane with air for synthesis gas production in a multistage gliding arc discharge system. Int J Hydrogen Energ 2007;32:1067-79.

18 Zielinski T, Kijenski J. Plasma carbon black the new active additive for plastic. Composit Part A : Appl Sci Manufact 2005;36:467-71.

19 Opalinska T, Zielinski T, Schmidt-Szalowski K. Carbon black generation in gliding arc discharges. Polish J Chem 2003;77:1357-61.

20 Supat K, Kruapong A, Chavadej S, Lobban LL, Millinson GR, Mallinson RG. Synthesis gas production from partial oxidation of methane with air in AC electric gas discharge. Energ & Fuel 2003;17:471-81.

Part 3: Synthesis Gas Production from CO_2-Containing Natural Gas by Combined Steam Reforming and Partial Oxidation in an AC Gliding Arc Discharge (submitted to *Plasma Chemistry and Plasma Processing*)

3.1 Introduction and Survey of Related Literature

In the recent years, research on the natural gas conversion to synthesis gas and fuels by using reforming processes has been extensively investigated [1-6]. These studies have been based on the reforming of pure CH_4 while natural gas contains not only CH_4 but also significant amount of ethane (C_2H_6), propane (C_3H_8) and carbon dioxide (CO_2). It is known that most natural gas, with a high concentration of carbon dioxide, has been found in Asia [7]. Hence, the reforming of natural gas composed of various components without a separation process is of great interest since it can result in a reduction of the high cost of the separation process and the net emission of CO_2.

Several techniques, such as steam reforming and partial oxidation, have been developed for methane reforming; however, they still possess some problems and constraints. The most extensively investigated method for hydrogen (H_2)/synthesis gas production from methane is steam reforming. Methane reforming with steam is a direct reaction between steam and methane to achieve a gaseous product with a higher H_2 content (Equation 1). Since steam methane reforming is a highly endothermic reaction, a huge amount of supplied energy is required. The reaction normally takes place over a nickel catalyst at very high temperatures of about 425-550 °C [8].

$$CH_4 + H_2O \rightarrow CO + 3H_2 \qquad \Delta H^{\circ}_{298} = +206\ kJ\,mol \qquad (1)$$

The partial oxidation of methane is also an attractive alternative to converting

methane to H_2/synthesis gas. This reaction is an exothermic reaction (Equation 2); therefore, it can reduce the energy demand for the reforming reaction [9].

$$CH_4 + \frac{1}{2}O_2 \rightarrow CO + H_2 \qquad \Delta H^{\circ}_{298} = -36\ kJ\ mol \qquad (2)$$

Apart from the aforementioned conventional processes, non-thermal plasma is a new efficient technique, which can be used for successfully converting natural gas into synthesis gas as well as other valuable products. Under ambient temperature and pressure, it provides highly active species (electrons, ions, and free radicals), which can initiate natural gas reforming reactions [10]. The gliding arc discharge originates from an auto-oscillating phenomenon that develops between at least two diverging electrodes submerged in a laminar or turbulent gas flow. The discharge starts as thermal plasma, and it quickly becomes non-thermal plasma during the space and time evolution. This powerful and energy-efficient transition discharge combines the benefits of equilibrium and non-equilibrium discharge characteristics in a single discharge pattern. So far, there are several research studies reporting the utilization of plasma discharge for hydrocarbon reforming [11-21]; however, to our knowledge, there have been no report on the combination of steam reforming and partial oxidation of CO_2-containing natural gas by using the gliding arc discharge system.

Therefore, the main objective of this work was to determine the roles of the gliding arc discharge plasma, in conjunction with the combined steam and partial oxidation, on the CO_2-containing natural gas reforming to produce synthesis gas. The experiments were systematically carried out to investigate the effects of several operating parameters, including the hydrocarbons (HCs)-to-O_2 feed molar ratio, applied voltage, input frequency, and electrode gap distance, on reactant conversions, product selectivities

and yields, and power consumptions in order to obtain optimum conditions for maximum synthesis gas production.

3.2 Procedure

3.2.1. Reactant Gases

The simulated natural gas used in this work consisted of CH_4, C_2H_6, C_3H_8, and CO_2, with a CH_4:C_2H_6:C_3H_8:CO_2 molar ratio of 70:5:5:20, and oxygen (O_2) were specially manufactured by Thai Industry Gas (Public) Co., Ltd.

3.2.2. AC Gliding Arc Discharge System

The schematic of a low-temperature gliding arc system used in this work is shown in Figure 3.1.

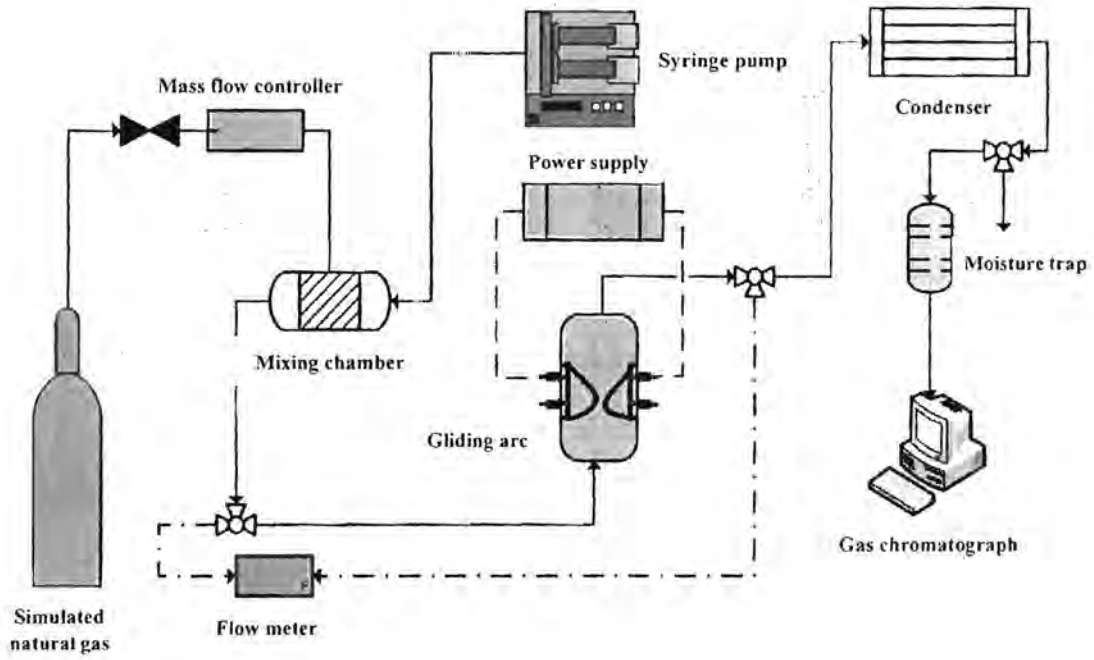

Figure 3.1 Schematic of gliding arc discharge system.

The detail of the gliding arc reactor configuration was described in our previous work [12]. A glass tube with 9 cm OD and 8.5 cm ID was used as the gliding arc reactor, which consisted of two diverging knife-shaped electrodes. The electrodes were made of stainless steel sheets with a 1.2 cm width. The gap distance between the pair of electrodes was fixed at 6 mm. The steam fed into the system was achieved by vaporizing water at a controlled temperature of 120 °C. A water flow rate was controlled by a syringe pump (Cole-Parmer). To prevent the water condensation in the feed line, the temperature of stainless tube from the syringe pump to a mixing chamber was maintained at 120 °C by using a heating tape. The flow rate of the simulated natural gas was controlled by a mass flow controller with a transducer (AALBORG). A 7-μm stainless steel filter was placed upstream of the mass flow controller in order to trap any solid particles in the reactant gas. The check valve was also placed downstream of the mass flow controller to prevent any backflow. The reactant gas and steam were well mixed in the mixing chamber controlled at 120 °C before being introduced upward into the reactor at atmospheric pressure. The compositions of the feed gas mixture and the outlet gas were quantitatively analyzed by an on-line gas chromatograph (HP, 5890) equipped with two separate columns, i.e. a Carboxen 1000 packed column and a PLOT Al_2O_3 "s" capillary column, which were adequate to detect all hydrocarbons, CO, CO_2, and H_2.

The power supply unit consisted of three steps. For the first step, the domestic AC input of 220 V and 50 Hz was converted to a DC output of 70 V by a DC power supply converter. For the second step, a 500 W power amplifier with a function generator was used to transform the DC into AC current with a sinusoidal waveform and different frequencies. For the third step, the outlet voltage was stepped up by using a high voltage transformer. The output voltage and frequency were controlled by the function generator.

The voltage and current at the low voltage side were measured instead of those at the high voltage side since the plasma generated is non-equilibrium in nature. The high side voltage and current were thereby calculated by multiplying and dividing by a factor of 130, respectively. A power analyzer was used to measure power, current, frequency, and voltage at the low voltage side of the power supply unit.

The feed gas mixture was first introduced into the gliding arc reactor without turning on the power supply unit for any studied conditions. After the compositions of outlet gas became invariant, the power supply unit was turned on. The flow rate of the outlet gas was also measured by using a bubble flow meter. The outlet gas was analyzed by the on-line GC every 30 min. After the plasma system reached steady state with invariant outlet gas concentrations, the outlet gas was taken for analysis at least a few times every hour. The average data were used to assess the process performance of the studied gliding arc discharge system.

3.2.3. Reaction Performance Calculation

The plasma system performance was evaluated from reactant conversions, product selectivities, H_2, CO, and C_2 yields, and power consumptions. The reactant conversion is defined as:

$$\% \text{ Reactant conversion} = \frac{(\text{Moles of reactant in} - \text{Moles of reactant out}) \times (100)}{\text{Moles of reactant in}} \qquad (1)$$

The selectivity of any C-containing product is defined on the basis of the amount of C-containing reactants converted to any specified product, as stated in Equation 2. The percentage of coke formed can be calculated from the difference between the total reactant conversions and total C-containing products, as given in Equation 3. In the

instance of the H_2 product, its selectivity is calculated based on the amount of H-containing reactants converted, as stated in Equation 4:

$$\% \text{ Selectivity for any hydrocarbon product} = \frac{[P](C_P)(100)}{\sum[R](C_R)} \quad (2)$$

$$\% \text{ Selectivity for hydrogen} = \frac{[P](H_P)(100)}{\sum[R](H_R)} \quad (3)$$

where [P] = moles of product in the outlet gas stream

[R] = moles of each reactant in the feed stream to be converted

C_p = number of carbon atoms in a product molecule

C_R = number of carbon atom in each reactant molecule

H_p = number of hydrogen atoms in a product molecule

H_R = number of hydrogen atoms in each reactant molecule

The yields of various products are calculated using the following equations:

$$\% \text{ } C_2 \text{ hydrocarbon yield} = \frac{[\Sigma(\% CH_4, \% C_2H_6, \% C_3H_8, \% CO_2 \text{ conversions})][\Sigma(\% C_2H_2, \% C_2H_4 \text{ selectivities})]}{(100)} \quad (4)$$

$$\% H_2 \text{ yield} = \frac{[\Sigma(\% CH_4, \% C_2H_6, \% C_3H_8 \text{ conversions})][\% H_2 \text{ selectivity}]}{(100)} \quad (5)$$

$$\% \text{ CO yield} = \frac{[\Sigma(\% CH_4, \% C_2H_6, \% C_3H_8, \% CO_2 \text{ conversions})][\% \text{ CO selectivity}]}{(100)} \quad (6)$$

The power consumption is calculated in a unit of Ws per C-containing reactant

molecule converted and Ws per hydrogen molecule produced using the following equation:

$$\text{Power consumption} = \frac{P \times 60}{N \times M} \quad (7)$$

where P = power (W)

N = Avogadro's number (6.02×10^{23} molecule g mole^{-1})

M = rate of converted carbon in the rate of produced hydrogen molecules (g mole min^{-1})

3.3 Results and Discussion

In order to obtain a better understanding of the chemical reactions in a plasma environment, the possibilities of all chemical pathways, which occurred by the collisions between electrons and all reactants introduced in to the feed to produce H_2 and various hydrocarbon species are hypothesized as the following reactions [8, 10]:

Electron-carbon dioxide collisions:

$$e^- + CO_2 \rightarrow CO + O^- \quad (9)$$

$$e^- + CO_2 \rightarrow CO + O + e^- \quad (10)$$

$$e^- + CO \rightarrow C + O + e^- \quad (11)$$

Electron-methane collisions:

$$e^- + CH_4 \rightarrow CH_3 + H + e^- \quad (12)$$

$$e^- + CH_3 \rightarrow CH_2 + H + e^- \quad (13)$$

$$e^- + CH_2 \rightarrow CH + H + e^- \quad (14)$$

$$e^- + CH \rightarrow C + H + e^- \quad (15)$$

$$H + H \rightarrow H_2 \quad (16)$$

Electron-ethane collisions:

$$e^- + C_2H_6 \rightarrow C_2H_5 + H + e^- \quad (17)$$

$$e^- + C_2H_5 \rightarrow C_2H_4 + H + e^- \quad (18)$$

$$e^- + C_2H_4 \rightarrow C_2H_3 + H + e^- \quad (19)$$

$$e^- + C_2H_3 \rightarrow C_2H_2 + H + e^- \quad (20)$$

$$e^- + C_2H_6 \rightarrow CH_3 + CH_3 + e^- \quad (21)$$

Electron-propane collisions:

$$e^- + C_3H_8 \rightarrow C_3H_7 + H + e^- \quad (22)$$

$$e^- + C_3H_7 \rightarrow C_3H_6 + H + e^- \quad (23)$$

$$e^- + C_3H_8 \rightarrow C_2H_5 + CH_3 + e^- \quad (24)$$

Electron-water collisions:

$$e^- + H_2O \rightarrow O^- + H_2 \quad (25)$$

$$e^- + H_2O \rightarrow OH^- + H \quad (26)$$

Under the presence of oxygen, several chemical reactions can be initiated in the plasma environment as follows:

Dissociative attachment:

$$e^- + O_2 \rightarrow 2O + e^- \rightarrow O^- + O \quad (27)$$

Attachment:

$$e^- + O_2 \rightarrow O_2^- \quad (28)$$

Dissociation:

$$e^- + O_2 \rightarrow 2O + e^- \quad (29)$$

Oxidative dehydrogenation reactions:

$$CH_4 + O\ (O^-, O_2^-) \rightarrow CH_3 + OH\ (OH^-, HO_2^-) \quad (30)$$

$$C_2H_6 + O\ (O^-, O_2^-) \rightarrow C_2H_5 + OH\ (OH^-, HO_2^-) \quad (31)$$

$$C_2H_5 + O\ (O^-, O_2^-) \rightarrow C_2H_4 + OH\ (OH^-, HO_2^-) \quad (32)$$

$$C_2H_4 + O\ (O^-, O_2^-) \rightarrow C_2H_3 + OH\ (OH^-, HO_2^-) \quad (33)$$

$$C_2H_3 + O\ (O^-, O_2^-) \rightarrow C_2H_2 + OH\ (OH^-, HO_2^-) \quad (34)$$

$$C_3H_8 + O\ (O^-, O_2^-) \rightarrow C_3H_7 + OH\ (OH^-, HO_2^-) \quad (35)$$

$$C_3H_7 + O\ (O^-, O_2^-) \rightarrow C_3H_6 + OH\ (OH^-, HO_2^-) \quad (36)$$

$$CH_4 + OH\ (O^-, O_2^-) \rightarrow CH_3 + H_2O\ (OH^-, HO_2^-) \quad (37)$$

$$C_2H_6 + OH\ (O^-, O_2^-) \rightarrow C_2H_5 + H_2O\ (OH^-, HO_2^-) \quad (38)$$

$$C_2H_5 + OH\ (O^-, O_2^-) \rightarrow C_2H_4 + H_2O\ (OH^-, HO_2^-) \quad (39)$$

$$C_2H_4 + OH\ (O^-, O_2^-) \rightarrow C_2H_3 + H_2O\ (OH^-, HO_2^-) \quad (40)$$

$$C_2H_3 + OH\ (O^-, O_2^-) \rightarrow C_2H_2 + H_2O\ (OH^-, HO_2^-) \quad (41)$$

$$C_3H_8 + OH\ (O^-, O_2^-) \rightarrow C_3H_7 + H_2O\ (OH^-, HO_2^-) \quad (42)$$

$$C_3H_7 + OH\ (O^-, O_2^-) \rightarrow C_3H_6 + H_2O\ (OH^-, HO_2^-) \quad (43)$$

All the active species formed from either electron collisions and oxidative reactions can further react to form various products as follows:

Coupling reactions of active species:

Ethylene (C_2H_4) formation;

$$CH_2 + CH_2 \rightarrow C_2H_4 \quad (44)$$

$$CH_3 + CH_3 \rightarrow C_2H_4 + H_2 \quad (45)$$

$$C_2H_5 + H \rightarrow C_2H_4 + H_2 \quad (46)$$

$$C_3H_7 + H \rightarrow C_2H_4 + CH_4 \quad (47)$$

Acetylene(C_2H_2) formation;

$$CH + CH \rightarrow C_2H_2 \quad (48)$$

$$CH_2 + CH_2 \rightarrow C_2H_2 + H_2 \quad (49)$$

$$CH_3 + CH \rightarrow C_2H_2 + H_2 \quad (50)$$

$$C_2H_5 + H \rightarrow C_2H_2 + H_2 + H_2 \quad (51)$$

$$C_3H_7 + H \rightarrow C_2H_2 + CH_4 + H_2 \quad (52)$$

Butane (C_4H_{10}) formation:

$$C_2H_5 + C_2H_5 \rightarrow C_4H_{10} \quad (53)$$

$$C_3H_7 + CH_3 \rightarrow C_4H_{10} \quad (54)$$

Carbon monoxide (CO) formation:

$$CH_3 + O \rightarrow HCHO + H \quad (55)$$

$$HCHO + O \rightarrow OH + CHO \quad (56)$$

$$CHO + O \rightarrow OH + CO \quad (57)$$

$$CHO + OH \rightarrow CO + H_2O \quad (58)$$

$$CHO + H \rightarrow H_2 + CO \quad (59)$$

3.3.1. Effect of the Hydrocarbons (HCs)-to-O_2 Feed Molar Ratio

Typically, the HCs-to-O_2 feed molar ratio in the natural gas feed mixture has a considerable impact on the plasma characteristics (i.e. breakdown voltage, electrical conductivity, and physical appearance) and the plasma stability, depending on the properties of each gas component. In this work, the experiments were initially performed by varying the O_2 content in the feed to obtain various HCs-to-O_2 feed molar ratios of 2/1, 3/1, 4/1, 6/1, and 9/1, while the other operating parameters were controlled at the base conditions (a steam content of 10 mol%, a total feed flow rate of 100 cm^3/min, an applied voltage of 13.5 kV, an input frequency of 300 Hz, and an electrode gap distance of 6 mm)

[23]. In this plasma system, a HCs-to-O_2 feed molar ratio lower than 2/1 was not investigated since it is close to the explosion zone.

Figure 3.2 shows the process performance of the studied gliding arc system as a function of the HCs-to-O_2 feed molar ratio. A decrease in the HCs-to-O_2 molar ratio (a lower HCs-to-O_2 feed molar ratio means a higher O_2 content) significantly enhanced both the conversions of all reactants (except CO_2) and the yields of H_2, CO, and C_2. The results can be explained by the fact that, when O_2 presents in the plasma system, it plays an important role in providing O_2 active species from the dissociative attachment reactions, as shown in Equations 27-29. These O_2 active species can further activate all reactants by oxidative dehydrogenation reactions (Equations 30-43), leading to an increase in the conversions of CH_4, C_2H_6, and C_3H_8, as well as the H_2, CO, and C_2 yields. An increase in O_2 content in the feed (decreasing HCs/O_2 feed molar ratio) results in the enhancement of a complete combustion reaction, leading to a decrease in CO_2 conversion.

As shown in Figure 3.2b, the CH_4, C_2H_6, and C_3H_8 concentrations in the outlet gas decrease significantly with decreasing HCs-to-O_2 feed molar ratios whereas the concentration of CO increases drastically with a slight increase in H_2 concentration. Interestingly, the CO_2 conversion decreased with the decreasing HCs-to-O_2 feed molar ratio. As mentioned before, when decreasing the HCs-to-O_2 feed molar ratio, the increase in oxygen provides a higher possibility for the oxidation of hydrocarbons to CO_2. Therefore, negative aspect of the CO_2 conversion at the lowest HCs-to-O_2 feed molar ratio of 2/1 suggests that the system provides a higher formation rate of CO_2 by the complete hydrocarbon oxidation than the CO_2 reduction rate by the reforming reactions [10]. In comparisons between the two cases of without and with O_2 addition in the feed,

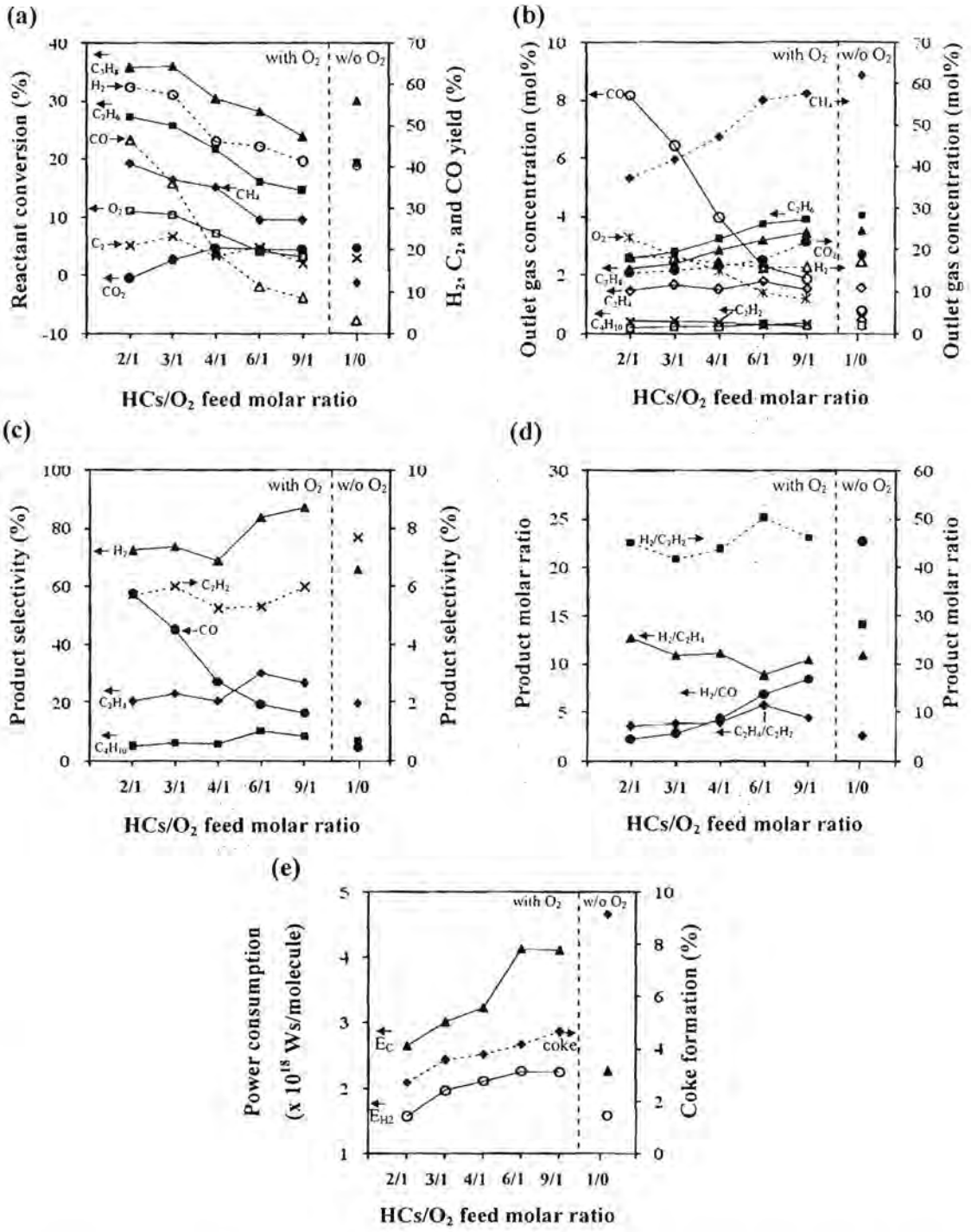

Figure 3.2 Effects of HCs-to-O_2 feed molar ratio on (a) reactant conversions and product yields, (b) concentrations of outlet gas, (c) product selectivities, (d) product

molar ratios, and (e) power consumptions and coke formation under studied conditions: steam content, 10 mol%; total feed flow rate, 100 cm^3/min; applied voltage, 13.5 kV; input frequency, 300 Hz; and electrode gap distance, 6 mm (E_c: power per reactant molecule converted; E_{H2}: power per H_2 molecule produced).

the O_2 addition in the feed with any HCs-to-O_2 feed molar ratio lower than 4/1 (high O_2 content range) potentially contributes to the positive effect of the enhancement of the reactant conversions, with the exception of the CO_2 conversion, and the H_2, CO, and C_2 yields, as well as the H_2 and CO selectivities.

The effect of the HCs-to-O_2 feed molar ratio on product selectivities is shown in Figure 3.2c. The selectivities for C_2H_4, C_4H_{10}, and H_2 tended to decrease with the decreasing HCs-to-O_2 feed molar ratio, whereas the CO selectivity increased drastically. As mentioned earlier, the higher the number of oxygen active species, the higher the opportunity for oxidative dehydrogenation reactions, consequently producing several intermediated species and water. Some of intermediate species (i.e. C_2H_5 and C_2H_3) can be further reacted to form C_2H_4 and C_2H_2 either by electron collisions (Equations 18, 20) and/or by oxidative dehydrogenation reactions (Equations 32, 34). In addition, the radicals of hydrocarbons and hydrogen derived from the earlier reactions may possibly react further to combine with one another via coupling reactions to form H_2, C_2H_2, C_2H_4, and C_4H_{10}, as shown in Equations 44-54. Hence, with the decreasing tendencies of the H_2, C_2H_2, C_2H_4, and C_4H_{10} selectivities with decreasing HCs-to-O_2 feed molar ratios infer that the opportunity for coupling reactions to form higher hydrocarbon molecules is less favorable at a lower HCs-to-O_2 feed molar ratio. The increase in the CO selectivity with decreasing HCs-to-O_2 feed molar ratio can be explained by the fact that the higher O and

OH active species may possibly provide a higher possibility of the partial oxidative pathways forming CO as an end product (Equations 55-59).

Figure 3.2d shows the effects of the HCs-to-O_2 feed molar ratio on various product molar ratios. The molar ratios of H_2/CO, H_2/C_2H_2, and C_2H_4/C_2H_2 tended to decrease with decreasing HCs-to-O_2 feed molar ratios, while the H_2/C_2H_4 molar ratio showed the opposite trend. These results correspond well to the decreases in the H_2, C_2H_4, and C_4H_{10} selectivities and the increase in the CO selectivity with the decreasing HCs-to-O_2 feed molar ratio. The increase in the H_2/C_2H_4 molar ratio with the increasing O_2 ratio in the system (decreasing the HCs-to-O_2 feed molar ratio) implies that the oxidative dehydrogenation reactions of hydrocarbons to form smaller hydrocarbon molecules have higher possibilities to simultaneously occur, as compared to the coupling reactions of active species to form large hydrocarbon molecules.

The effects of the HCs-to-O_2 feed molar ratio on power consumptions and coke formation are illustrated in Figure 3.2e. The power consumptions of both per reactant molecule converted and per H_2 molecule produced declined drastically with the decreasing HCs-to-O_2 feed molar ratio. The drop in both power consumptions can be explained by the increases in the CH_4, C_2H_6, and C_3H_8 conversions and H_2 yield (Figure 3.2a). Moreover, a decreasing tendency of coke deposition on the electrode surfaces and inner reactor glass wall could be observed at lower HCs-to-O_2 feed molar ratios (with higher O_2 contents). From the overall results, the optimum HCs-to-O_2 feed molar ratio of 2/1, which reasonably provided both higher H_2 yield and selectivity with extremely low power consumptions, was selected for further investigation. It is interesting to point out that the addition of oxygen cannot reduce the power consumption but it can significantly decrease coke formation.

3.3.2. Effect of Applied Voltage

In general, the applied voltage plays a significant role on plasma behaviors and subsequent plasma chemical reaction performance. For the investigated plasma system, the highest operating applied voltage of 20.5 kV was limited by the plasma instability and thereby the extinction of gliding arc discharges due to a very large amount of rapid coke deposited on the electrode surface. The lowest applied voltage (break-down voltage) to generate steady plasma was found at 13.5 kV. Hence, the experiments were carried out to investigate the effect of applied voltage in the range of 13.5-20.5 kV, while the other operating parameters were kept constant at a steam content of 10 mol%, a HCs-to-O_2 feed molar ratio of 2/1, a total feed flow rate of 100 cm^3/min, an input frequency of 300 Hz, and an electrode gap distance of 6 mm. The effects of applied voltage on the reactant conversions and product yields are demonstrated in Figure 3.3a. The conversions of CH_4, C_2H_6, C_3H_8, and O_2, as well as the H_2 and CO yields, steadily increased with increasing applied voltage. However, the CO_2 conversion remained almost unchanged in the studied range of applied voltage. These reactant conversion results were consistent with the decreases in the CH_4, C_2H_6, C_3H_8, and O_2 concentrations in the outlet gas, as well as the increases in H_2 and CO concentrations (Figure 3.3b). Fundamentally, an increase in the applied voltage for a plasma system directly corresponds to a stronger electric field strength across the electrodes, resulting in higher electron density or higher input energy (current) to the system [10], as indicated in Figure 3.3c. Increasing applied voltage leads to an increased opportunity for the occurrence of elementary chemical reactions by electron collision, by resulting in increases in all the conversions of CH_4, C_2H_6, C_3H_8, and O_2, as well as the H_2 and CO yields. The unchanged CO_2 conversion and CO_2

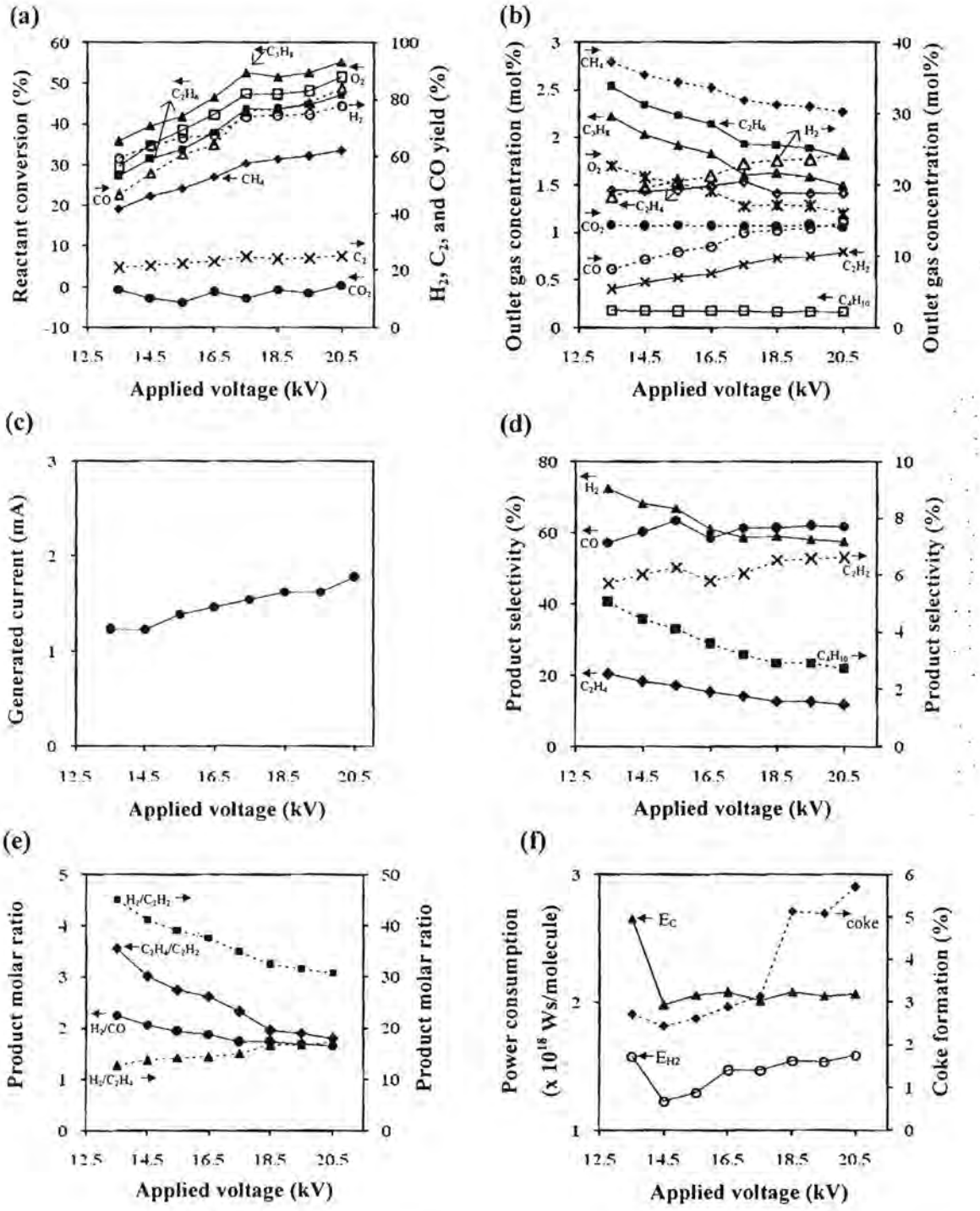

Figure 3.3 Effects of applied voltage on (a) reactant conversions and product yields, (b) concentrations of outlet gas, (c) generated current, (d) product selectivities, (e) product molar ratios, and (f) power consumptions and coke formation under studied

conditions: steam content, 10 mol%; HCs/O_2 feed molar ratio, 2/1; total feed flow rate, 100 cm^3/min; input frequency, 300 Hz; and electrode gap distance, 6 mm (E_c: power per reactant molecule converted; E_{H2}: power per H_2 molecule produced).

concentration in the product gas suggest that the rate of CO_2 reforming by plasma should be equal to the rate of CO_2 formation by the complete combustion reaction. In the applied voltage range of 18.5-20.5 kV, the slight increases in the CH_4, C_2H_6, C_3H_8, and O_2 conversions and the H_2 and CO yields can be credited to the increase in coke formation (as shown later), which was observed to be an obstacle to maintaining steady plasma behavior. Besides, it was found that increasing applied voltage had an insignificant impact on the C_2 yield, possibly, suggesting that the C_2 yield was independent of an applied voltage in the investigated range.

Figure 3.3d presents the effects of applied voltage on the product selectivities. The H_2, C_2H_4, and C_4H_{10} selectivities decreased with increasing applied voltage, whereas the C_2H_2 and CO selectivities tended to increase. These results imply that at a higher applied voltage, the carbon dioxide dissociation by electron collision (Equations 9 and 10) and oxidative dehydrogenation reactions of the hydrocarbons (Equations 30-43) occur more often than the coupling reactions of active species (Equations 44-54). According to the plasma behavior observed, a higher applied voltage can induce greater electron density and subsequently a higher number of active species, which can increased opportunity for both carbon dioxide dissociation and oxidative dehydrogenation reactions.

The effect of applied voltage on the product molar ratios is illustrated in Figure 3.3e. The molar ratios of H_2/CO, H_2/C_2H_2, and C_2H_4/C_2H_2 substantially decreased with

increasing applied voltage, while the H_2/C_2H_4 molar ratio showed the opposite trend. These results agree well with the decreased H_2, C_2H_4, and C_4H_{10} selectivities and the increased C_2H_2 and CO selectivities. The apparent decreases in the H_2/C_2H_2, H_2/CO, and C_2H_4/C_2H_2 molar ratios, and the opposite trend of the H_2/C_2H_4 molar ratio with increasing applied voltage, again confirm that the carbon dioxide dissociation by electron collision and oxidative dehydrogenation reactions are much more likely to occur than the coupling reactions of active species with increasing applied voltage.

Figure 3.3f shows the effects of applied voltage on power consumptions and coke formation. The power consumptions of both per reactant molecule converted and per H_2 molecule produced, decreased with increasing applied voltage (from 13.5 to 14.5 kV); however, with further increasing applied voltage to 20.5 kV, the power consumption per reactant molecule converted tended to be fairly constant, while the power consumption per H_2 molecule produced tended to only slightly increase. The initial decreases in both amounts of power consumptions can be explained by the increases in the CH_4, C_2H_6, and C_3H_8 conversions and the H_2 yield with increasing applied voltage. When considering the applied voltage range of 14.5-20.5 kV, the results reveal that the power consumption per H_2 molecule produced increased steadily with increasing applied voltage. The increase in H_2 yield with increasing applied voltage should indeed have led to lower power consumption per H_2 molecule produced. However, the opposite trend was experimentally observed, possibly because of the increase in coke formation. Generally, the formation of coke along the knife-shaped electrodes at high applied voltages not only decreases the efficiency of chemical reactions (i.e. decreasing reactant conversions and product yields) but also directly affects the gliding arc discharge stability. Particularly, an increase in a certain amount of coke can increase the conductivity of the system, leading to a decrease

in the uniformity of the plasma pattern. This phenomena resulted in a lowered probability of electron collision with reactant molecules to produce active gaseous species. From the results, a minimum of power consumptions were found at the applied voltage of 14.5 kV, while all ratios of hydrogen-to-other products were mostly high; therefore, the applied voltage of 14.5 kV was selected for further investigation.

3.3.3 Effect of Input Frequency

The input frequency parameter was next investigated by varying the range from 290-500 Hz, while the other operating parameters were controlled at a steam content of 10 mol%, a HCs/O_2 feed molar ratio of 2/1, a total feed flow rate of 100 cm^3/min, an applied voltage of 14.5 kV, and an electrode gap distance of 6 mm. It should be noted that the studied gliding arc system could not be operated lower than the lowest operating input frequency of 290 Hz. This is because a large amount of coke formation occurred on the surface of the electrodes as well as the extremely high current. For the input frequency greater than 500 Hz, the plasma system could not be operated because of the non-uniform plasma with a extremely small number of arcs produced. Figure 3.4 illustrates the effects of input frequency on the reactant conversions, product yields, concentrations of outlet gas, and power consumptions. The conversions of CH_4, C_2H_6, C_3H_8, and O_2, as well as the H_2, CO, and C_2 yields, tended to decrease with increasing input frequency (Figure 3.4a). These results correspond well to the increases in CH_4, C_2H_6, C_3H_8, and O_2 concentrations, as well as the decreases in H_2 and CO concentrations in the outlet gas (Figure 3.4b). In general, for any given applied voltage and electrode gap distance, the

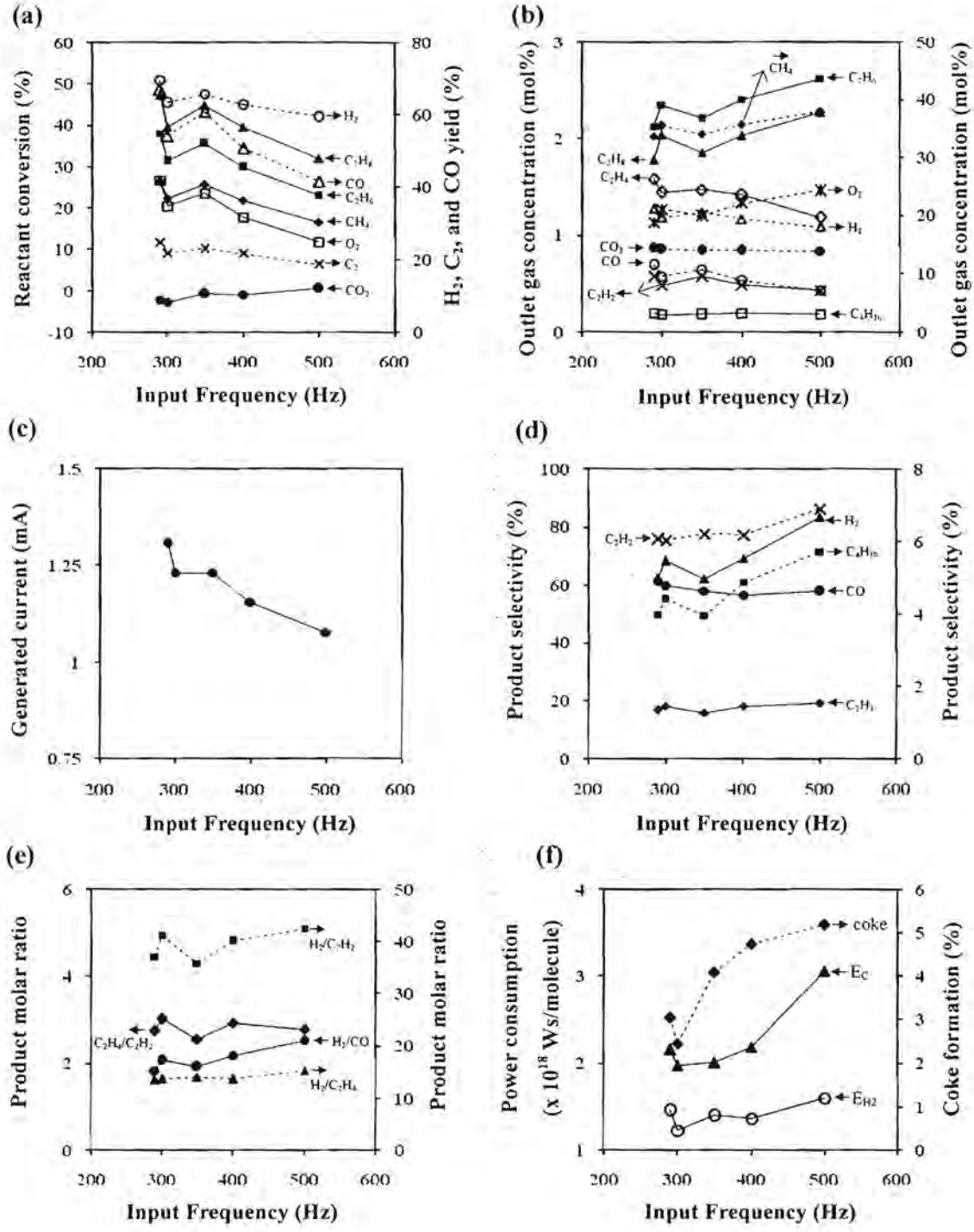

Figure 3.4 Effects of input frequency on (a) reactant conversions and product yields, (b) concentrations of outlet gas, (c) generated current, (d) product selectivities, (e) product molar ratios, and (f) power consumptions and coke

formation under studied conditions: steam content, 10 mol%; HCs/O_2 feed molar ratio, 2/1; total feed flow rate, 100 cm^3/min; applied voltage, 14.5kV; and electrode gap distance, 6 mm (E_c: power per reactant molecule converted; E_{H2}: power per H_2 molecule produced).

electric current required to sustain a discharge is reduced with increasing input frequency. Consequently, a lower current can be observed at a higher input frequency, as shown in Figure 3.4c. In accordance with the basic concept of the frequency effect as stated, the space charge (electrons and ions) characteristics of the alternating current discharge is the influential factor of frequency in changing the behaviors of arc discharge and reaction performance [8, 10, 24-25]. Therefore, increasing input frequency adversely causes a reduction in the number of electrons generated for initiating the chemically active species via the elementary plasma reactions by electron impact, resulting in lower reactant conversions and product yields.

The effect of input frequency on the product selectivities is shown in Figure 3.4d. The H_2, C_2H_2, and C_4H_{10} selectivities tended to increase with increasing input frequency from 290 to 500 Hz, whereas the C_2H_4 and CO selectivities tended to remain almost unchanged, implying that the C_2H_4 and CO selectivities were independent of input frequency. The present results do not agree with those in our previous work [10], in which the decreases in both H_2 and C_2H_2 selectivities were observed with increasing input frequency from 250-500 Hz. The difference in the experimental results could possibly be explained by the fact that the previous work used only simulated natural gas as a reactant feed, whereas the present work was conducted by adding both steam and oxygen to the simulated natural gas. Hence, the results imply that the presence of steam

and oxygen plays an important role in enhancing the electron-water collisions (Equations 25 and 26), as well as the dissociation reactions of oxygen (Equations 27-29), leading to increased oxidative dehydrogenation reactions (Equations 30-43) and coupling reactions of active species (Equations 44-54) to produce more H_2 and C_2H_2. As shown in Figure 4d, the increase in C_4H_{10} selectivity infers that the promotion of coupling reactions to form C_4H_{10} (Equations 53 and 54) can be achieved by increasing input frequency.

Figure 3.4e shows the effect of input frequency on the product molar ratios. The molar ratios of H_2/CO and H_2/C_2H_2 tended to increase with increasing input frequency. The increase in the H_2/CO molar ratio can be possibly described by the increase in the H_2 selectivity, while the CO selectivity remained almost unchanged with increasing input frequency. Interestingly, the simultaneous increases in the H_2/C_2H_2 molar ratio and the H_2 and C_2H_2 selectivities imply that the increase in the H_2 production rate is higher than that of the C_2H_2 production rate where the input frequency is increased. As a result, the number of electrons generated in the plasma system decreases with increasing input frequency, resulting in decreasing possibilities of secondary dehydrogenation reactions of hydrocarbon species (Equations 30-34 and 37-41) to produce C_2H_2. On the contrary, the H_2 selectivity increase with increasing input frequency is possibly due to the presence of steam, which provides a higher possibility of collision, between the electrons and water molecules (Equations 25-26). In addition, the C_2H_4/C_2H_2 molar ratio decreased slightly with increasing input frequency, whereas the H_2/C_2H_2 molar ratio remained almost unchanged. These results agree well with the increase in C_2H_2 selectivity and the invariant of C_2H_4 selectivity.

The effects of input frequency on power consumptions and coke formation are depicted in Figure 3.4f. The power consumptions of both per reactant molecule converted

and per H_2 molecule produced initially decreased with increasing input frequency from 290 to 300 Hz and then substantially increased with further increasing input frequency from 300 to 500 Hz. The initial decrease in both power consumptions was observed probably due to the decrease in current required to sustain the discharge (Figure 3.4c); whereas the further increase in input frequency from 300 to 500 Hz increased both power consumptions, probably resulting from the decreases in all reactant conversions and H_2 yield and selectivity (Figure 3.4a). Interestingly, power consumptions mirrored the coke formation profile, suggesting that coke deposition plays a significant role in affecting the power consumptions. From the results, lower power consumptions occurred with less coke formation were found at the input frequency of 300 Hz. It was selected as an optimum value for further investigation.

3.3.4. Effect of Electrode Gap Distance

For the investigation of the effect of electrode gap distance on the reforming reaction performance of the simulated natural gas, the electrode gap distance was varied in the range of 4-8 mm, while a steam content of 10 mol%, a HCs-to-O_2 feed molar ratio of 2/1, a total feed flow rate of 100 cm^3/min, an applied voltage of 14.5 kV, and input frequency of 300 Hz were used as the optimum conditions to operate the gliding arc system. The corresponding residence times at various electrode gap distances of 4, 6, 7, and 8 mm were 1.09, 1.37, 1.57, and 1.65 s, respectively. Beyond the highest electrode gap distance of 8 mm, the gliding arc system could not provide a steady discharge, whereas, at any electrode gap distance shorter than 4 mm, the system produced a large quantity of coke filaments across the two electrodes with in a relatively short operation period, causing a drastic drop of current and the termination of discharge.

The effects of the electrode gap distance on the reactant conversions and product yields are illustrated in Figure 3.5a. The conversions of CH_4, C_2H_6, C_3H_8, and O_2, as well as the H_2, CO, and C_2 yields, significantly increased with increasing electrode gap distance from 4 to 7 mm. The increase in the electrode gap distance simply increases the reaction volume and subsequently the residence time of gaseous species in the plasma zone increases. As a result, there is higher possibility of collisions between reactant molecules and electrons, leading to increases in all the reactant conversions (except CO_2) and product yields. These results are in good agreement with the significant decreases in the CH_4, C_2H_6, C_3H_8, and O_2 concentrations and the increases in the H_2 and CO concentrations in the outlet gas (Figure 3.5b). However, it was found that increasing the electrode gap distance in the range of 7-8 mm only slightly increased the CH_4, C_2H_6, C_3H_8, and O_2 conversions, as well as H_2, CO, and C_2 yields. It should be noted that there is another vital factor, apart from residence time, that affects the reactant conversions, product selectivities, and yields. When the electrode gap distance is varied, principally, the breakdown voltage required for initiating the plasma discharges and the power required for sustaining the discharges increase with increasing electrode gap distance [26]. However, if the electrode gap distance is too wide, the electric field strength weakens, resulting in a lower average electron energy, as well as a reduction in the number of electrons, which corresponds very well with the decreasing tendency of the generated current in the electrode gap distance range of 6 to 8 mm, as clearly shown in Figure 3.5c. Hence, all reactant conversions and product yields remained almost unchanged with increasing gap distance in this range, despite a longer residence time. Moreover, the results of the reactant conversions and product yields at different ranges of electrode gap

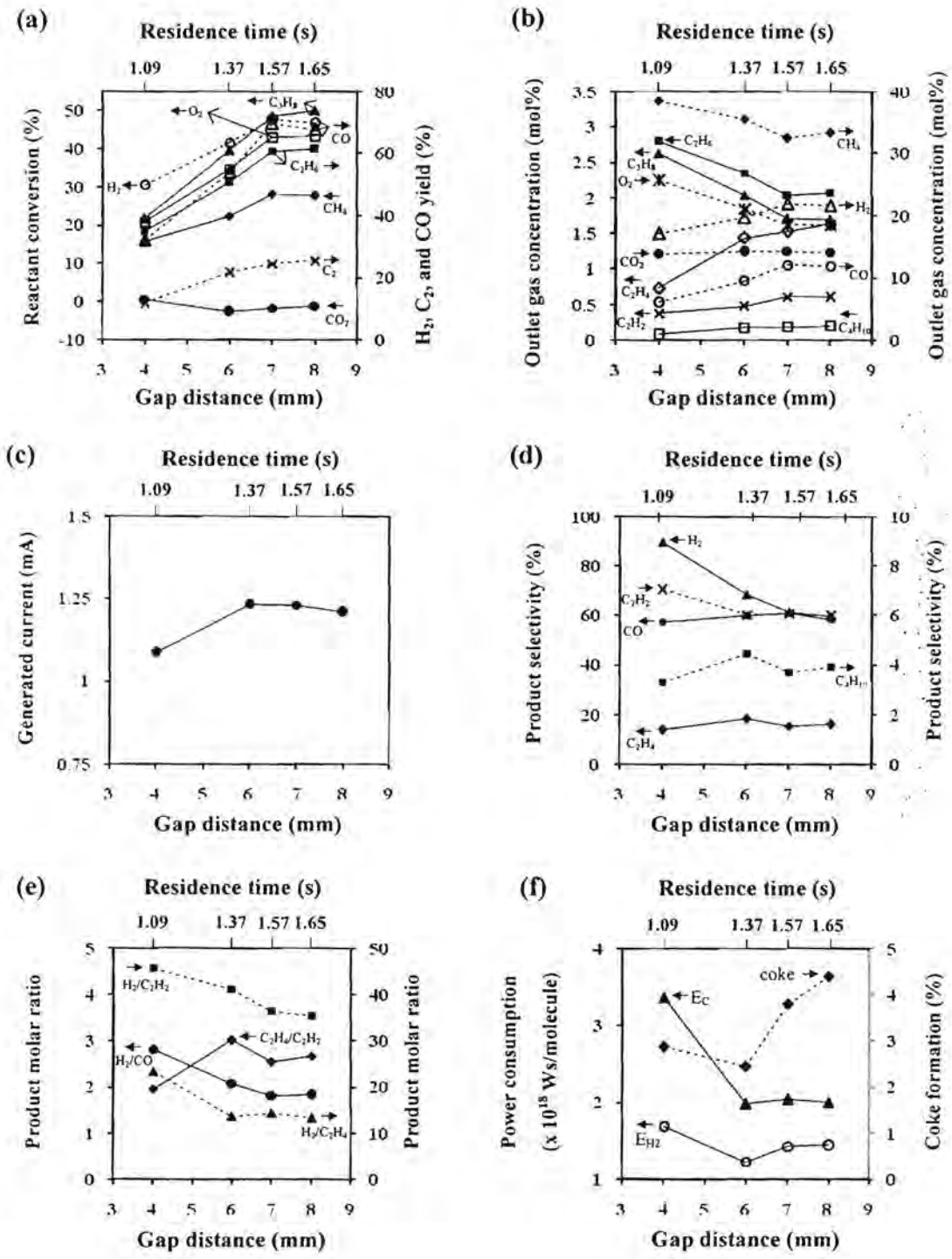

Figure 3.5 Effects of electrode gap distance on (a) reactant conversions and product yields, (b) concentrations of outlet gas, (c) generated current, (d) product selectivities, (e) product molar ratios, and (f) power consumptions and coke

formation under studied conditions: steam content, 10 mol%; HCs/O_2 feed molar ratio, 2/1; total feed flow rate, 100 cm^3/min; applied voltage, 14.5 kV; and input frequency, 300 Hz (E_c: power per reactant molecule converted; E_{H2}: power per H_2 molecule produced).

widths indicate that for the narrow electrode gap distance range of 4-6 mm, the residence time plays a dominant role in enhancing the plasma reforming performance, whereas, for the greater electrode gap distance range of 6-8 mm, the discharge characteristics have more significant impacts.

Figure 3.5d presents the effect of electrode gap distance on the product selectivities. The H_2 and C_2H_2 selectivities significantly decreased with increasing electrode gap distance. It may be implied that the increase in current by tapering electrode gap distance is responsible for the enhancement of the oxidative dehydrogenation reactions and the coupling reactions of the active species to form H_2 and C_2H_2. On the other hand, the C_2H_4 and C_4H_{10} selectivities tended to slightly increase with the expansion of electrode gap distance from 4 to 6 mm but beyond the electrode gap distance of 6 mm, they slightly decreased. These initial increases in both the C_2H_4 and C_4H_{10} selectivities suggest that the coupling reactions to obtain C_2H_4 and C_4H_{10} (Equations 44-47 and 53-54) more favorably occur than with the oxidative dehydrogenation reactions at a wider electrode gap distance (a longer residence time). A plausible explanation is that with wider electrode gap distance, the active species of hydrocarbons can further recombine via the coupling reactions due to the increase in residence time. However, when widening the electrode gap distance from 6 to 8 mm, all the product selectivities tended to slightly decrease probably due to both the decrease in

generated current, as described earlier, and the drastic increase in coke formation, as shown next. The CO selectivity varied slightly with a wider electrode gap distance, suggesting that the CO selectivity is independent of the electrode gap distance under the studied conditions.

Figure 3.5e illustrates the effect of the electrode gap distance on various product molar ratios. The molar ratios of H_2/CO, H_2/C_2H_2, and H_2/C_2H_4 greatly decreased with increasing electrode gap distance from 4 to 6 mm and then only slightly decreased with further widening of the electrode gap distance to 8 mm, whereas the C_2H_4/C_2H_2 molar ratio showed the opposite trend. These results again confirm that the coupling reactions of the active species more preferentially occur as secondary reactions than the dehydrogenation reactions when the system is operated at a longer residence time.

The power consumptions both per reactant molecule converted and per H_2 molecule produced decrease significantly with widening electrode gap distance from 4 to 6 mm and they tend to increase slightly with further widening of the electrode gap distance from 6 to 8 mm, as depicted in Figure 3.5f. The initial decrease in both power consumptions can be explained by the increases in the CH_4, C_2H_6, C_3H_8, and O_2 conversions, as well as the H_2 yield (Figure 3.5a). Beyond the electrode gap distance of 6 mm, which provided the minimum power consumptions, an increase in coke formation with further widening electrode gap distance is responsible for the increase in power consumptions.

3.3.5. Comparisons of CO_2-Containing Natural Gas Conversion Performances with Different Reforming Processes

Table 1 shows the comparisons of CO_2-containing natural gas conversion

performances, i.e. H_2 and CO selectivities and yields as well as power consumptions, with different reforming processes under their corresponding optimum conditions. It can be seen that the steam reforming process provided the highest H_2 selectivity of about 65.8%, but gave a very low CO selectivity of about 4.8%, as compared to the other reforming processes. Even though the highest H_2 selectivity was not obtained, the combined steam reforming and partial oxidation process gave acceptably high H_2 and CO selectivities of about 68.2% and 59.9%, respectively. As shown in Table 1, the significant enhancement of both the H_2 and CO selectivities for the combined steam reforming and partial oxidation process, as compared to all the other reforming processes. Both the steam and O_2 additions to the natural gas feed provides much higher number of oxygen active species, hydroxyl active species, and hydrogen active species (Equations 25-29). This enhances both the oxidative dehydrogenation reactions and coupling reactions (Equations 9-24, and 30-54). Interestingly, the combined steam reforming and partial oxidation process gives a very high CO production, as compared to the steam reforming process. This is because the added oxygen in the system can significantly suppress the coke formation, resulting in increased opportunities for CO formation (Equations 55-59). Hence, it can be clearly seen that the addition of both steam and oxygen can offer the acceptably highest synthesis gas production.

The power consumptions both per reactant molecule converted and per H_2 molecule produced are also given in Table 1. The results indicate that the presence of either oxygen (the combined reforming and partial oxidation process) or steam (the steam reforming process) in the natural gas feed could lower the power consumptions both per reactant molecule converted and per H_2 molecule produced, as compared to the case

Table 3.1 Comparison of the CO_2-containing natural gas conversion performances with different processes under their corresponding optimum conditions

Process	Operating conditions						Selectivity (%)		Yield (%)		Power consumptions ($\times 10^{18}$ s/molecule)	
	HCs/O_2 molar ratio	Steam content (mol%)	Total feed flow rate (cm^3/min)	Applied voltage (kV)	Input frequency (Hz)	Electrode gap distance (mm)	H_2	CO	H_2	CO	Per reactant molecule converted (E_C)	Per H_2 molecule produced (E_{H2})
Non-oxidative reforming[a]	-	-	125	15.5	300	6	24.5	2.9	12.2	-	6.34	3.58
Combined reforming and partial oxidation[b]	2/1	-	125	17.5	300	6	40.5	21.9	58.1	61.6	2.73	2.49
Steam reforming[c]	-	10	100	13.5	300	6	65.8	4.8	40.3	3.1	2.26	1.58
Combined steam reforming and partial oxidation[d]	2/1	10	100	14.5	300	6	68.2	59.9	63.4	54.0	1.98	1.22

[a][7], [b][10], [c][26], and [d]Present work

without the O_2 and steam addition (the sole reforming or non-oxidative reforming). The lowest power consumptions both per reactant molecule converted and per H_2 molecule produced were obtained from the combined steam reforming and partial oxidation process in the present work, suggesting that there is a synergistic effect of reduction in power consumption.

3.4 Conclusions

In this work, the combined steam reforming and partial oxidation of CO_2-containing natural gas was employed for the synthesis gas production from CO_2-containing natural gas in an AC gliding arc discharge system. The effects of the applied voltage, input frequency, and electrode gap distance significantly affected the reactant conversions, product selectivities, and product yields were investigated. The optimum conditions were found at a HCs/O_2 feed molar ratio of 2/1, an applied voltage of 14.5 kV, an input frequency of 300 Hz, and an electrode gap distance of 6 mm, which provided high CH_4 and O_2 conversions with high synthesis gas selectivity and very low power consumptions. Under these optimum conditions, the power consumptions were as low as 1.98×10^{-18} Ws (12.35 eV) per molecule of converted reactant and 1.22×10^{-18} Ws (7.64 eV) per molecule of produced hydrogen.

References

[1] SW. Yang, JN. Kondo, K. Hayashi, M. Hirono, K. Domen, H. Hosono. Partial oxidation of methane to syngas over promoted C12A7. Applied Catalysis A: General 227 (2004) 239-246.

[2] N.R. Bruke, DL. Trimm. Co-generation of energy and synthesis gas by partial oxidation of methane. Catalysis Today 117 (2006) 248-252.

[3] R.C. Vasant, C.M. Kartick. CO_2 reforming of methane combined with steam reforming or partial oxidation of methane to syngas over $NdCoO_3$ perovskite-type mixed metal-oxide catalyst. Applied Energy 83 (2006) 1024-1032.

[4] W. Yu, T. Ohmori, S. Kataoka, T. Yamamoto, A. Endo, M. Nakaiwa, N. Itoh. A comparative simulation study of methane steam reforming in a porous ceramic membrane reactor using nitrogen and steam as sweep gases. International Journal of Hydrogen Energy 33 (2008) 685-692.

[5] S. Ryi, J. Park, D. Kim, T. Kim, S. Kim. Methane steam reforming with a novel catalytic nickel membrane for effective hydrogen production. Journal of Membrane Science 339 (2009) 189-194.

[6] C.R.M. Santos, M. Laureanny, B.P. Fabio. The effect of the addition of Y_2O_3 to $Ni/\alpha\text{-}Al_2O_3$ catalysts on the autothermal. Catalysis Today 149 (2010) 401-406.

[7] N. Rueangjitt, C. Akarawitoo, T. Sreethawong, S. Chavadej. Reforming of CO_2-containing natural gas using an AC gliding arc system: Effect of gas component in natural gas. Plasma Chemistry and Plasma Processing 27 (2007) 559-576.

[8] T. Sreethawong, P. Thakonpatthanakun, S. Chavadej. Partial oxidation of methane

with air for synthesis gas production in a multistage gliding arc discharge system. International Journal of Hydrogen Energy 32 (2007) 1067-1079.

[9] J.A. Anderson, M.F. Garcia. Supported Metals in Catalysis. Imperial College Press, 2005.

[10] N. Rueangjitt, T. Sreethawong, S. Chavadej. Reforming of CO_2-containing natural gas using an AC gliding arc system: effects of operational parameters and oxygen addition in feed. Plasma Chemistry and Plasma Processing 28 (2008) 49-67.

[11] B. Wang, X. Zhang, Y. Liu, G. Xu. Conversion of CH_4, steam and O_2 to syngas and hydrocarbons via dielectric barrier discharge. Journal of Natural Gas Chemistry 18 (2009) 94-97.

[12] M.G. Sobacchi, A.V. Saveliev, A.A. Fridman, L.A. Kennedy, S. Ahmed, T. Krause. Experimental assessment of combined plasma/catalytic system for hydrogen production via partial oxidation of hydrocarbon fuels. International Journal of Hydrogen Energy 27 (2002) 635-642.

[13] J.X. He, Y.Y. Han, A.H. Gao, Y.S. Zhou, Z.G. Lu. Investigation on methane decomposition and the formation of C_2 hydrocarbons in DC discharge plasma by emission spectroscopy. Chinese Journal of Chemical Engineering 12 (2004) 149-151.

[15] T. Nozaki, A. Hattori, K. Okazaki. Partial oxidation of methane using a microscale non-equilibrium plasma reactor. Catalysis Today 98 (2004) 607-616.

[15] C.S. Kalra, A.F. Gutsol, A.A. Fridman. Gliding arc discharge as a source of intermediate plasma for methane partial oxidation. IEEE Transactions on Plasma Science 33 (2005) 32-4.

[16] T. Paulmier, L. Fulcheri. Use of non-thermal plasma for hydrocarbons reforming.

Chemical Engineering Journal 106 (2005) 59-71.

[17] Y. Wang, C.J. Liu, Y.P. Zhang. Plasma methane conversion in the presence of dimethyl ether using dielectric-barrier discharge. Energy & Fuels 19 (2005) 877-881.

[18] E. El Ahmar, C. Met, O. Aubry, A. Khacef, J.M. Cormier. Hydrogen enrichment of a methane-air mixture by atmospheric pressure plasma for vehicle applications. Chemical Engineering Journal 116 (2006) 13-18.

[19] G. Petitpas, J.-D. Rollier, A. Darmon, J. Gonzalez-Aguilar, R. Matkemeijer, L. Fulcheri. A comparative study of non-thermal plasma assisted reforming technologies. International Journal of Hydrogen Energy 32 (2007) 2848-2867.

[20] Y.C. Yang, B.J. Lee, Y.N. Chun. Characteristics of methane reforming using gliding arc reactor. Energy 34 (2009) 172-177.

[21] C. Liu, A. Marafee, B. Hill, G. Xu, R. Mallinson, L. Lobban. Oxidative coupling of methane with ac and dc corona discharges. Industrial & Engineering Chemistry Research 35 (1996) 3295-3301.

[22] N. Rueangjitt, W. Jittiang, K. Pornmai, J. Chamnanmanoontham, T. Sreethawong, S. Chavadej. Combined reforming and partial oxidation of CO_2-containing natural gas using an AC multistage gliding arc system: effect of number of plasma reactors. Plasma Chemistry and Plasma Processing 29 (2009) 433-453.

[23] K. Pornmai, H. Sekiguchi, S. Chavadej. Synthesis gas production from reforming of CO_2-containing natural gas with steam using an AC gliding arc discharge system: effects of steam addition in feed and operational parameters. Plasma Sources Science and Technology (In Contribution).

[24] T. Zielinski, J. Kijenski. Plasma carbon black the new active additive for plastic.

Composites Part A : Applied Science and Manufacturing 36 (2005) 467-471.

[25] T. Opalinska, T. Zielinski, K. Schmidt-Szalowski. Carbon black generation in gliding arc discharges. Polish Journal of Chemistry 77 (2003) 1357-1361.

[26] K. Supat, A. Kruapong, S. Chavadej, L.L. Lobban, G.R. Millinson. Synthesis gas production from partial oxidation of methane with air in AC electric gas discharge. Energy & Fuels 17 (2003) 471-481.

Appendix

Plasma Chem Plasma Process (2009) 29:433–453
DOI 10.1007/s11090-009-9191-1

ORIGINAL PAPER

Combined Reforming and Partial Oxidation of CO_2-Containing Natural Gas Using an AC Multistage Gliding Arc Discharge System: Effect of Stage Number of Plasma Reactors

Nongnuch Rueangjitt · Wariya Jittiang · Krittiya Pornmai · Jintana Chamnanmanoontham · Thammanoon Sreethawong · Sumaeth Chavadej

Received: 16 July 2009 / Accepted: 31 August 2009 / Published online: 19 September 2009

Abstract The effect of stage number of multistage AC gliding arc discharge reactors on the process performance of the combined reforming and partial oxidation of simulated CO_2-containing natural gas having a CH_4:C_2H_6:C_3H_8:CO_2 molar ratio of 70:5:5:20 was investigated. For the experiments with partial oxidation, either pure oxygen or air was used as the oxygen source with a fixed hydrocarbon-to-oxygen molar ratio of 2/1. Without partial oxidation at a constant feed flow rate, all conversions of hydrocarbons, except CO_2, greatly increased with increasing number of stages from 1 to 3; but beyond 3 stages, the reactant conversions remained almost unchanged. However, for a constant residence time, only C_3H_8 conversion gradually increased, whereas the conversions of the other reactants remained almost unchanged. The addition of oxygen was found to significantly enhance the process performance of natural gas reforming. The utilization of air as an oxygen source showed a superior process performance to pure oxygen in terms of reactant conversion and desired product selectivity. The optimum energy consumption of 12.05×10^{24} eV per mole of reactants converted and 9.65×10^{24} eV per mole of hydrogen produced was obtained using air as an oxygen source and 3 stages of plasma reactors at a constant residence time of 4.38 s.

Keywords Natural gas · Reforming · Partial oxidation · Gliding arc discharge · Plasma

N. Rueangjitt · W. Jittiang · K. Pornmai · J. Chamnanmanoontham · T. Sreethawong · S. Chavadej (✉)
The Petroleum and Petrochemical College, Chulalongkorn University, Soi Chula 12, Phyathai Road, Pathumwan, Bangkok 10330, Thailand
e-mail: sumaeth.c@chula.ac.th

T. Sreethawong · S. Chavadej
Center for Petroleum, Petrochemicals, and Advanced Materials, Chulalongkorn University, Bangkok 10330, Thailand

Introduction

In recent years, natural gas has become a versatile energy resource due to both environmental reason and due to its lower price as compared to petroleum. Therefore, the consumption of natural gas as an alternative fuel is currently increasing [1]. Generally, natural gas mostly contains a large amount of methane with lesser amounts of ethane, propane, and carbon dioxide, and its composition varies according to sub-geological conditions. Because methane is an inexpensive fuel, attempts at converting methane to more valuable hydrogen and higher hydrocarbons with new alternative technologies have been increasingly carried out. Moreover, the direct utilization of methane and carbon dioxide has been an area of great interest due to its environmentally friendly concept of decreasing greenhouse gas emissions. Nevertheless, methane reforming with carbon dioxide, as shown in Eq. 1, using conventional catalytic methods often encounters two main problems; it is a highly endothermic reaction consuming a large amount of energy, and the deactivation of catalysts due to coke deposition on the catalyst surface commonly occurs under various reaction conditions [2].

Methane reforming with carbon dioxide:

$$CH_4 + CO_2 \rightarrow 2CO + 2H_2 \quad \Delta H_{298K} = 247 kJ/mol \tag{1}$$

The second route for methane conversion to syngas is the steam reforming process, as shown in Eq. 2. This reaction is also highly endothermic, resulting in high energy consumption. Steam reforming reactors generally run with excess amounts of water in order to prevent coke deposition on the catalyst surface [3]. Methane reforming with steam has poor selectivity to CO and produces syngas with a high H_2/CO ratio, while methane reforming with carbon dioxide gives a higher CO selectivity and a lower H_2/CO ratio [4].

Steam reforming of methane:

$$CH_4 + H_2O \rightarrow CO + 3H_2 \quad \Delta H_{298K} = 206.2 kJ/mol \tag{2}$$

Another route used to produce syngas is the catalytic partial oxidation of methane, as shown in Eq. 3. This process gives high activity and selectivity, but cannot be easily controlled because of the generation of hot spots in the catalytic bed due to its exothermic nature [4].

Partial oxidation of methane:

$$CH_4 + 1/2\ O_2 \rightarrow CO + 2H_2 \quad \Delta H_{298K} = -38 kJ/mol \tag{3}$$

A combination of these reactions can potentially provide good and synergistic performance. For example, the combination of carbon dioxide reforming and steam reforming of methane can reduce coke deposition on the catalyst surface, resulting in a controlled and limited coke formation [5]. In addition, the combination of carbon dioxide reforming and partial oxidation of methane has a benefit in terms of balancing the heat load and reducing energy consumption [6, 7].

An attractive alternative for reforming hydrocarbon compounds is to use non-thermal plasma processes. The plasma contains highly active species (such as electrons, ions, and radicals), which can react with methane to produce various valuable products under ambient conditions. The electrical discharge produced also provides heat to the system, apart from generating radicals and excited species to initiate and enhance the plasma chemical reactions [8]. Furthermore, the plasma reforming processes can be operated at mild conditions with less energy consumption, and they have been employed for many applications [9–16].

Our previous works have addressed the reforming of simulated natural gas, which contained a CH_4:C_2H_6:C_3H_8:CO_2 molar ratio of 70:5:5:20, with and without partial oxidation, using a single gliding arc discharge plasma reactor [17, 18]. The addition of air was found to be superior to pure oxygen for hydrogen production with an optimum hydrocarbon-to-oxygen molar ratio of 2/1. In this present work, a multistage gliding arc plasma system comprising four gliding arc discharge plasma reactors connected in series was used for the investigation of a combined reforming and partial oxidation of the simulated natural gas to produce hydrogen and higher hydrocarbons. Initially, the effect of stage number of plasma reactors was systematically investigated to evaluate the process performance under two series of experiments with a fixed feed flow rate and a fixed residence time. Both pure oxygen and air were comparatively used as oxygen sources. A comparison of process performance between the systems, with and without partial oxidation, was finally made. The optimum stage number with corresponding low energy consumption was obtained.

Experimental

Reactant Gases

Simulated natural gas (containing methane, ethane, propane, and carbon dioxide, with a CH_4:C_2H_6:C_3H_8:CO_2 molar ratio of 70:5:5:20) was specially produced for this work by Thai Industry Gas (Public) Co., Ltd. Ultra-high purity oxygen and air zero used for performing the combined plasma reforming and partial oxidation of the simulated natural gas were also supplied by Thai Industry Gas (Public) Co., Ltd.

Setup of the Multistage Gliding Arc Discharge System

The experimental setup of the multistage AC gliding arc discharge system with 4 stages in series and the configuration of each reactor are shown in Figs. 1 and 2, respectively. The gliding arc reactors were made of a glass tube with 9 cm OD and 8.5 cm ID. Each reactor had two diverging knife-shaped electrodes that were fabricated from stainless steel sheets with a 1.2 cm width for each electrode. The gap distance between the pair of electrodes was fixed at 6 mm. Two Teflon sheets were placed at the top and bottom of the electrodes to force the feed gas to pass through the reaction zone. The flow rates of the reactant gases were regulated by a set of mass flow controllers and transducers supplied by SIERRA® Instrument, Inc. Stainless steel (7 μm) filters were placed upstream of all mass flow controllers in order to trap any solid particles in the reactant gases. The check valves were also placed downstream of the mass flow controllers to prevent any backflow. The simulated natural gas was well mixed with either pure oxygen or air to obtain a hydrocarbon-to-oxygen molar ratio of 2/1, which was the optimum ratio found in our previous work [18]. The mixed reactant gases were introduced upward into the first reactor at ambient temperature and atmospheric pressure. The compositions of the feed gas mixture and the effluent gases were analyzed by an on-line gas chromatograph (HP, 5890), equipped with a Carboxen 1000 packed column connected to a thermal conductivity detector (TCD) and a PLOT Al_2O_3 "S" capillary column connected to a flame ionization detector (FID).

For any studied conditions, the feed gas mixture was first introduced into the gliding arc system without turning on the power supply unit. After the composition of outlet gas was invariant with time, the power supply unit was turned on. The outlet gas composition was analyzed every 30 min by the on-line GC. After the system reached steady state, an analysis

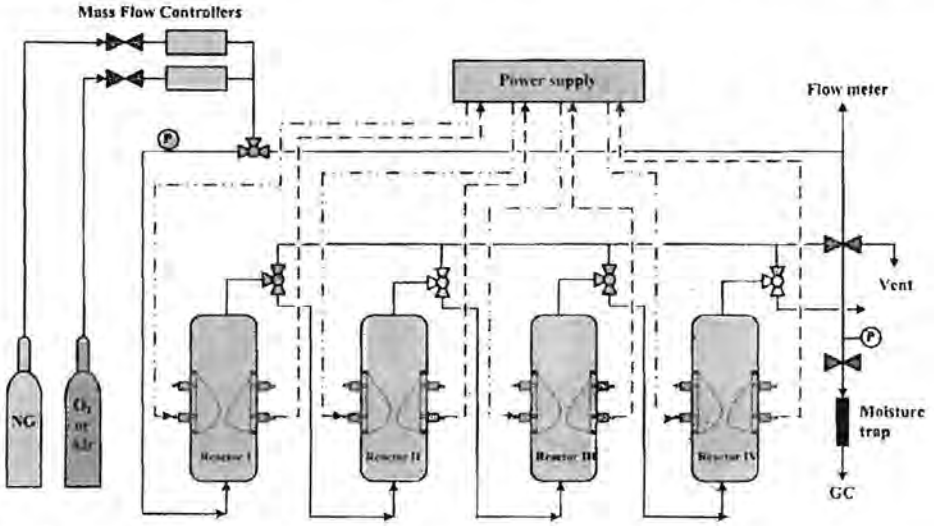

Fig. 1 Schematic of the multistage gliding arc discharge system

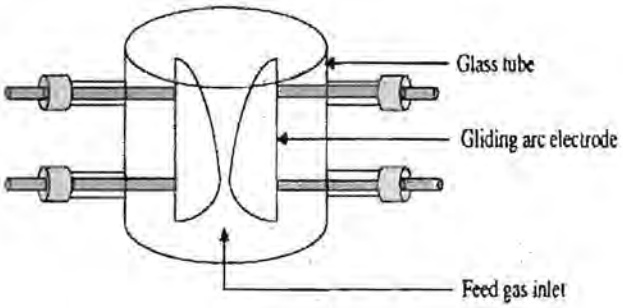

Fig. 2 Schematic of a gliding arc discharge reactor

of the outlet gas composition was taken at least few times every hour. The experimental data were averaged to evaluate the process performance. During the experiments, the temperature at the reactor wall was found to be in the range of 150–200°C. Since the volume of the reactor outlet zone was rather large, the outlet gas was cooled close to room temperature. It was observed that a small amount of water droplets appeared on the surrounding inner wall of the gliding arc reactor during the experiment. In the case of using air, a NO_X analyzer was employed to determine if there were any nitrogen oxides present in the effluent gas; none were detected. Therefore, under the studied conditions, nitrogen oxides were not produced by the plasma system. The flow rates of both the feed and the outlet gases were measured by using a digital bubble flow meter because of the gas volume change after the reaction.

The power supply unit used in this work was operated in three steps. For the first step, the domestic AC input of 220 V and 50 Hz was converted to a DC output of 70 V by a DC power supply converter. For the second step, a 500 W power amplifier with a function generator was used to convert the DC to AC with a sinusoidal waveform. For the final step, the output voltage was stepped up by using two transformers in series. The output voltage and frequency were controlled by the function generator. Since the plasma generated in

each plasma reactor is non-equilibrium in nature, it is not possible to measure the voltage across the electrodes of the reactor (high-side voltage). Therefore, the low-side voltage and current were measured instead, and the high-side voltage and current were then calculated by multiplying and dividing by a factor of 130, respectively. A power analyzer was used to measure power, frequency, and voltage at the low side of the power supply unit. Based on our previous work on the combined reforming and partial oxidation of CO_2-containing natural gas using a single-stage gliding arc discharge system [18], the obtained optimum operating conditions (an applied voltage of 17.5 kV, an input frequency of 300 Hz, and a hydrocarbon-to-oxygen molar ratio of 2/1) were used as the base conditions to operate the multistage gliding arc discharge system in this work.

Reaction Performance Evaluation

The reactant conversion is defined as:

$$\%\ \text{Reactant conversion} = \frac{(\text{moles of reactant } in - \text{moles of reactant } out)\,(100)}{(\text{moles of reactant } in)} \tag{4}$$

The selectivities for C-containing products are defined on the basis of the amount of C-containing reactants converted into any specified product, as stated in Eq. 5 below. In the case of the hydrogen product, its selectivity is calculated based on H-containing reactants converted, as stated below in Eq. 6:

$$\%\ \text{Selectivity for any hydrocarbon product} = [\text{P}]\,(\text{C}_\text{P})\,(100)/\Sigma\,[\text{R}]\,(\text{C}_\text{R}) \tag{5}$$

where

[P] = moles of product in the outlet gas stream
[R] = moles of each reactant in the feed stream to be converted
C_P = number of carbon atoms in the product molecule
C_R = number of carbon atoms in each reactant molecule

$$\%\ \text{Selectivity for hydrogen} = [\text{P}]\,(\text{H}_\text{P})\,(100)/\Sigma\,[\text{R}]\,(\text{H}_\text{R}) \tag{6}$$

where

H_P = number of hydrogen atoms in the product molecule
H_R = number of hydrogen atoms in each reactant molecule

The product yields are formulated as follows:

$$\%\ \text{C}_2\ \text{hydrocarbons yield} = \Sigma\,(\%\ \text{CH}_4,\ \text{C}_2\text{H}_6,\ \text{C}_3\text{H}_8, \text{CO}_2\ \text{conversion})\ \Sigma\,(\%\ \text{C}_2\text{H}_2,\ \text{C}_2\text{H}_4\ \text{selectivity})/(100) \tag{7}$$

$$\%\ \text{H}_2\ \text{yield} = \Sigma(\%\ \text{CH}_4,\ \text{C}_2\text{H}_6,\ \text{C}_3\text{H}_8\ \text{conversion})\,(\%\ \text{H}_2\ \text{selectivity})/(100) \tag{8}$$

$$\%\ \text{CO yield} = \Sigma\,(\%\ \text{CH}_4, \text{C}_2\text{H}_6,\ \text{C}_3\text{H}_8,\ \text{CO}_2\ \text{conversion})\,(\%\ \text{CO selectivity})/(100) \tag{9}$$

The specific energy consumption is calculated in a unit of electron (eV) per mole of C-containing reactants converted or per mole of hydrogen produced (eV/mol) using the following equation:

$$\text{Specific energy consumption} = (P)(60)/(M)\left(1.602 \times 10^{-19}\right) \quad (10)$$

where

P = power (W)

M = rate of converted carbon in the feed or rate of produced hydrogen molecules (g mol min^{-1})

1 eV = 1.602×10^{-19} W s

Results and discussion

Results of Natural Gas Reforming without Partial Oxidation

Effect of Stage Number on Reactant Conversion and Product Yield

Constant Residence Time The reactant conversions and product yields as a function of stage number of plasma reactors when varying feed flow rate at a constant residence time of 4.38 s are illustrated in Fig. 3a. For each stage of plasma reactors, the feed flow rate was controlled at 31.25, 62.50, 93.75, and 125 cm^3/min, respectively, in order to maintain the same residence time (4.38 s). The results show that only the conversion of C_3H_8 gradually increased with increasing stage number, whereas the conversions of the rest of the reactant components remained almost unchanged. It was also confirmed experimentally by the concentrations of outlet gases that the concentration of C_3H_8 sharply decreased, whereas the CH_4 concentration was nearly unchanged. The explanation is that the conversion of reactant gases depends upon the collision between the highly energetic electrons and the reactant gases, which is governed by both residence time and stage number of plasma reactors. Since the plasma operation in this experimental part was performed at a constant residence time, the process performance must be governed by the stage number. The results suggest that the formations of CH_4 and C_2H_6 are approximately equal to the

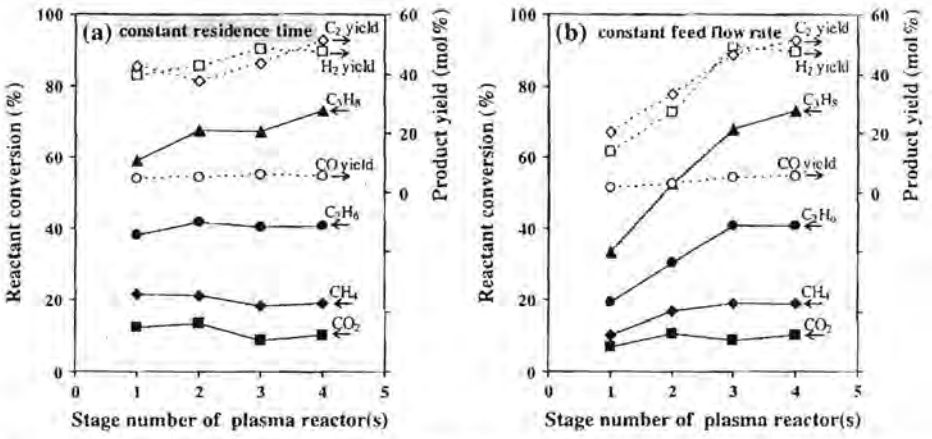

Fig. 3 Effect of stage number of plasma reactors on reactant conversions and product yields for the reforming of natural gas without O_2 or air addition: **a** at a constant residence time of 4.38 s and **b** at a constant feed flow rate of 125 cm^3/min (applied voltage, 17.5 kV; frequency, 300 Hz; and electrode gap distance, 6 mm)

conversions of these two reactants, leading to unchanged CH_4 and C_2H_6 conversions. Another reason is due to their different bond dissociation energies, which are 4.33, 4.35, 4.55, and 5.52 eV, for propane, ethane, methane, and CO_2, respectively [19]. Moreover, the H_2 and C_2 yields only slightly increased with increasing stage number of plasma reactors, whereas the CO yield remained almost unchanged (Fig. 3a). The results suggest that the coupling reactions of the active species and oxidative dehydrogenation reactions may not be significantly affected by the stage number.

Constant Feed Flow Rate The reactant conversions and product yields as a function of stage number of plasma reactors at a constant feed flow rate of 125 cm^3/min are illustrated in Fig. 3b. The residence time of the single stage, 2, 3, and 4 stages was controlled at 1.09, 2.19, 3.29, and 4.38 s, respectively. The conversions of all hydrocarbons, except CO_2, increased considerably with increasing stage number because of the longer residence time. Beyond 3 stages, only the propane conversion increased, but the other reactant conversions remained almost unchanged. Comparatively, the propane conversion increased rapidly with increasing stage number of plasma reactors, whereas the methane conversion tended to slightly increase. The conversions of all reactant gases were in the following order: propane > ethane > methane > CO_2. The same reasons as mentioned above can be used to explain the different conversions of all reactants. For the H_2 and C_2 yields, the increase in residence time due to the increase in the stage number of plasma reactors enhances the conversion of all reactants, as aforementioned, and consequently leads to increasing the production yields. However, the CO yield only slightly increased with increasing stage number of plasma reactors, possibly because the system was operated at an oxygen-deficient condition (a hydrocarbon-to-oxygen molar ratio of 2/1).

Effect of Stage Number on Product Selectivity and Product Molar Ratio

Constant Residence Time The effect of stage number of plasma reactors on the selectivities for H_2, C_2H_2, C_2H_4, C_4H_{10}, and CO at a constant residence time of 4.38 s is depicted in Fig. 4a. The selectivities for H_2 and C_2H_4 tended to slightly increase with increasing stage number from 1 to 3 stages, and the selectivities for CO and C_4H_{10} remained almost unchanged. The results are relevant to the molar ratios of H_2/C_2H_2 and C_2H_4/C_2H_2, as also shown in Fig. 4a, while the molar ratio of H_2/C_2H_4 gradually decreases. This implies that the increase in the C_2H_4 selectivity exceeds the increase in the H_2 selectivity, resulting in the gradually decreasing H_2/C_2H_4 ratio. It should be noted, therefore, that the hydrogenation of C_2H_2 more favorably occurs than the coupling reaction of hydrocarbon active species with increasing stage number of plasma reactors from 1 to 3 stages, leading to the consumption of H_2 to some extent to produce C_2H_4. At 3 stages of plasma reactors, the maximum selectivity for H_2 was obtained at approximately 38.2%. From this point of view, it could be concluded that the increase in stage number of plasma reactors from 1 to 3 stages assists in improving the H_2 selectivity.

Constant Feed Flow Rate The effect of stage number of plasma reactors on the product selectivities at a constant feed flow rate of 125 cm^3/min is shown in Fig. 4b. The results reveal that the selectivities for H_2 and C_2H_2 markedly increased with increasing stage number of plasma reactors, whereas those for C_2H_4, C_4H_{10}, and CO remained almost unchanged. This implies that the oxidative dehydrogenation preferably occurs at a high residence time. The H_2/C_2H_4 ratio increased with increasing stage number of plasma

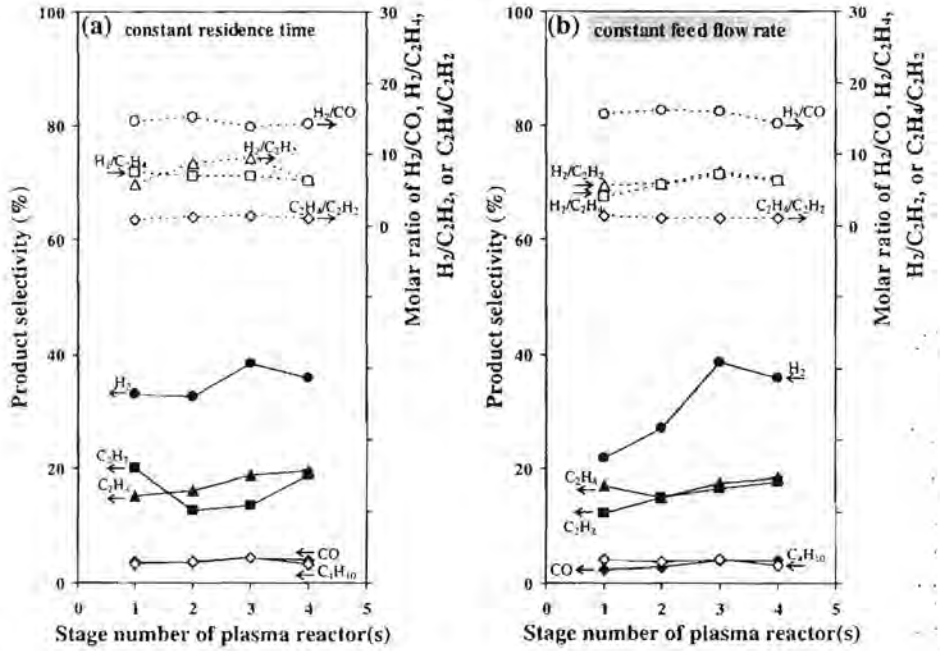

Fig. 4 Effect of stage number of plasma reactors on product selectivities and product molar ratios for the reforming of natural gas without O_2 or air addition: **a** at a constant residence time of 4.38 s and **b** at a constant feed flow rate of 125 cm^3/min (applied voltage, 17.5 kV; frequency, 300 Hz; and electrode gap distance, 6 mm)

reactors from 1 to 3 stages, whereas the molar ratio of C_2H_4/C_2H_2 slightly decreased, suggesting that the dehydrogenation of C_2H_4 is likely to occur when the stage number of plasma reactors is increased. Moreover, the coupling reaction of hydrogen radicals can occur, and results in the great increase in the selectivity for H_2 at 3 stages of plasma reactors. In contrast, the selectivities for C_2H_4, C_4H_{10}, and CO remained almost unchanged. From these experimental results, it can be concluded that the rate of dehydrogenation increases with increasing stage number of plasma reactors when the multistage system is operated at a constant feed flow rate.

Effect of Stage Number on Energy Consumption

Constant Residence Time The effect of stage number of plasma reactors on energy consumption per mole of reactants converted and per mole of hydrogen produced at the constant residence time is shown in Fig. 5a. The energy consumption per mole of hydrogen produced sharply declined from 1 to 2 stages of plasma reactors and then gradually decreased with increasing stage number from 2 to 4 stages, while the energy consumption per mole of reactants converted also decreased in the same manner as the energy consumption per mole of hydrogen produced when the stage number increased from 1 to 2 stages but became almost unchanged with further increasing stage number up to 4 stages. The minimum energy consumption was about 1.03×10^{25} eV per mole of reactants converted and 1.28×10^{25} eV per mole of hydrogen produced at 4 stages of plasma reactors.

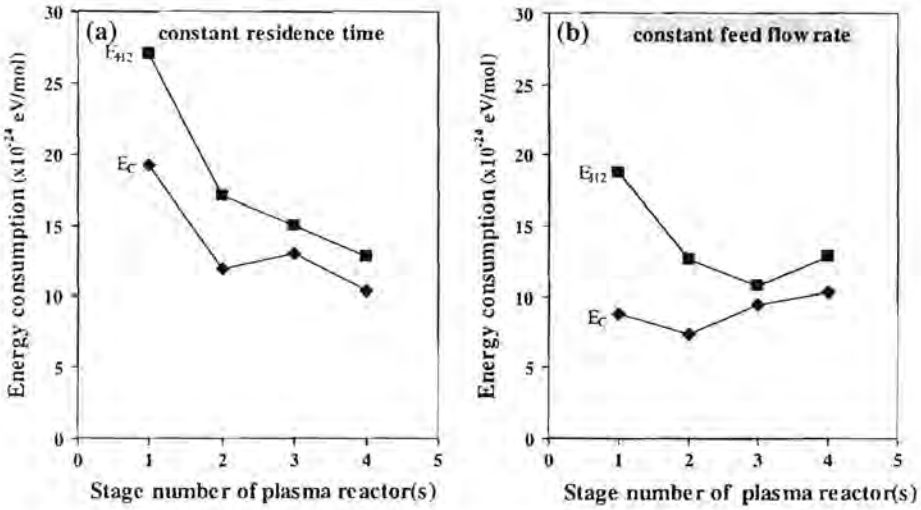

Fig. 5 Effect of stage number of plasma reactors on energy consumption (E_C = energy consumption per mole of reactants converted and E_{H2} = energy consumption per mole of hydrogen produced) for the reforming of natural gas without O_2 or air addition: **a** at a constant residence time of 4.38 s and **b** at a constant feed flow rate of 125 cm^3/min (applied voltage, 17.5 kV; frequency, 300 Hz; and electrode gap distance, 6 mm)

Constant Feed Flow Rate The effect of stage number of plasma reactors on energy consumption per mole of reactants converted and per mole of hydrogen produced at the constant feed flow rate is depicted in Fig. 5b. The energy consumption per mole of hydrogen produced substantially decreased when the stage number of plasma reactors increased from 1 to 3 stages, but the energy consumption per mole of reactants converted was insignificantly changed. At 3 stages, a minimum energy consumption of about 1.07×10^{25} eV per mole of hydrogen produced was achieved.

Results of Natural Gas Reforming with Partial Oxidation

For the combined plasma reforming and partial oxidation of the simulated natural gas, the effects of residence time and feed flow rate were also systematically investigated to determine whether or not the addition of oxygen to the natural gas feed could improve the system performance by using two different oxygen sources: pure oxygen and air.

Results of Natural Gas Reforming with Partial Oxidation Using Pure Oxygen

Effect of Stage Number on Reactant Conversion and Product Yield

Constant Residence Time The effect of stage number of plasma reactors of the system operated at a constant residence time of 4.38 s and a hydrocarbon-to-oxygen ratio of 2/1 is shown in Fig. 6a. All of the reactant conversions only slightly increased with increasing stage number from 1 to 3 stages. Beyond 3 stages, they remained almost unchanged. The H_2, C_2, and CO yields gradually increased with increasing stage number of plasma reactors; however, the H_2 and CO yields reached the maximum values at 3 stages. The values of H_2 and CO yields were somewhat greater than 100% due to the complexity of the

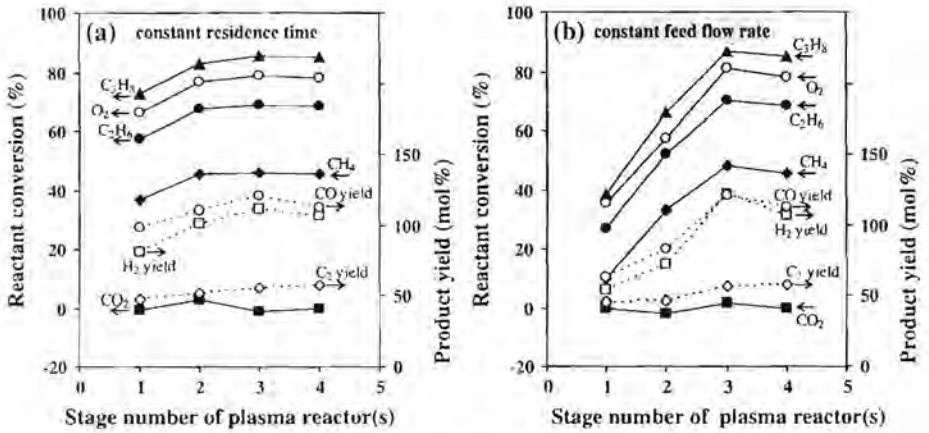

Fig. 6 Effect of stage number of plasma reactors on reactant conversions and product yields for the reforming of natural gas with pure O_2 addition: **a** at a constant residence time of 4.38 s and **b** at a constant feed flow rate of 125 cm^3/min (hydrocarbon-to-oxygen molar ratio, 2/1; applied voltage, 17.5 kV; frequency, 300 Hz; and electrode gap distance, 6 mm)

reactions, of which both forward and backward reactions simultaneously occurred in the plasma reactors. From the experimental observation, the outlet concentrations of all reactants decreased with increasing stage number of plasma reactors except that the outlet concentration of CO_2 remained unchanged, which might result from its high bond dissociation energy, as mentioned above.

Constant Feed Flow Rate As shown in Fig. 6b, at the constant feed flow rate, the conversion of all reactants, except CO_2, considerably increases when the stage number of plasma reactors increases from 1 to 3 stages, and all the reactant conversions remain almost unchanged with further increasing stage number to 4 stages. This is probably due to a small amount of oxygen molecules left in the fourth plasma reactor, as indicated by the oxygen conversion profile. For the CO_2 conversion, a minus value was observed. This can be explained in that the formation rate of CO_2 by the hydrocarbon oxidation is higher than the CO_2 consumption rate by the reforming reactions with partial oxidation [18]. The H_2 and CO yields also significantly increased with increasing stage number of plasma reactors to reach the maximum values at 3 stages, and after that they tended to decrease, as also observed in the case of the constant residence time. In the meantime, the C_2 yield slightly increased with increasing stage number. Moreover, the H_2 yield was found to be much higher than the C_2 yield. The most significant difference between H_2 and C_2 yields was noticed at 3 stages of plasma reactors. This implies that at a higher stage number of plasma reactors, up to 3 stages, the H_2 production via the dehydrogenation reactions occurs more favorably than the C_2 production via the coupling reactions. However, at 4 stages, less H_2 production due to less reactant conversion, as well as higher hydrogen consumption for the hydrogenation reactions, may simultaneously occur instead.

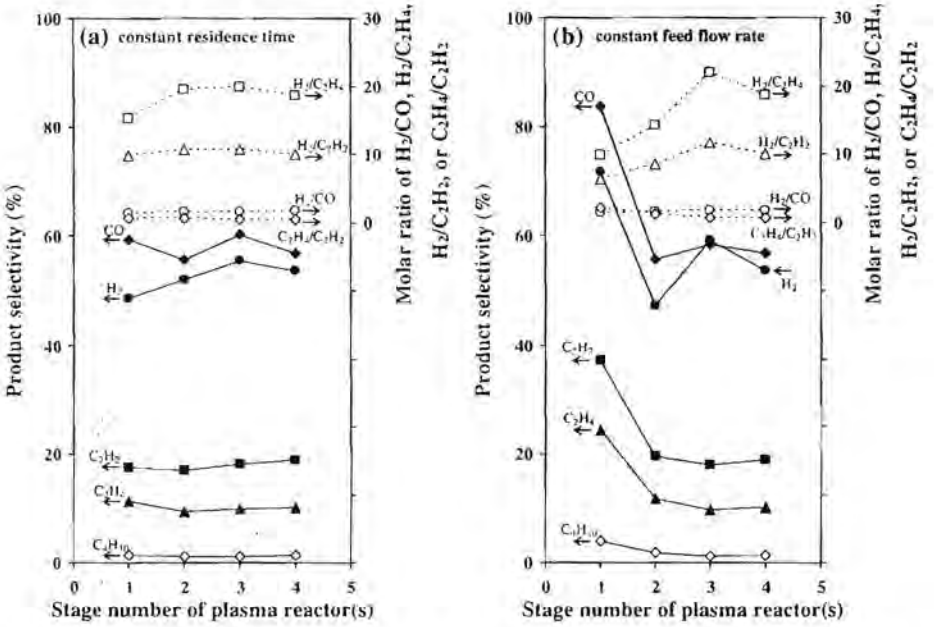

Fig. 7 Effect of stage number of plasma reactors on product selectivities and product molar ratios for the reforming of natural gas with pure O_2 addition: **a** at a constant residence time of 4.38 s and **b** at a constant feed flow rate of 125 cm^3/min (hydrocarbon-to-oxygen molar ratio, 2/1; applied voltage, 17.5 kV; frequency, 300 Hz; and electrode gap distance, 6 mm)

Effect on Product Selectivity and Product Molar Ratio

Constant Residence Time Most of the product selectivities do not significantly change when the stage number of plasma reactors increases at the constant residence time, except that the selectivity for H_2 tends to increase (Fig. 7a). The molar ratio of H_2/C_2H_4 increased as the number of plasma reactors increased from 1 to 2 stages and then remained almost unchanged with further increasing stage number, whereas the other product molar ratios were almost constant. This can be explained in that both the dehydrogenation reactions and the coupling reaction of hydrogen radicals to produce H_2 have a high possibility of occurring due to the greater opportunity to collide with the active species present at the early stages of plasma reactors at the residence time of 4.38 s.

Constant Feed Flow Rate All of the product selectivities gradually decrease with increasing stage number of plasma reactors at the constant feed flow rate, especially from single stage to two stages, as illustrated in Fig. 7b. The decreased selectivities for all the products are due to the fact that with an increasing stage number of plasma reactors, the residence time is also increased. The sharp decline of all product selectivities, except for CO_2, when increasing stage number from 1 to 2 stages results from a large quantity of oxygen-active species available in the system. However, the outlet concentration of CO_2 was experimentally found to be almost unchanged, probably because of the equivalent rates of formation and reduction of CO_2. The molar ratio of H_2/C_2 products increased

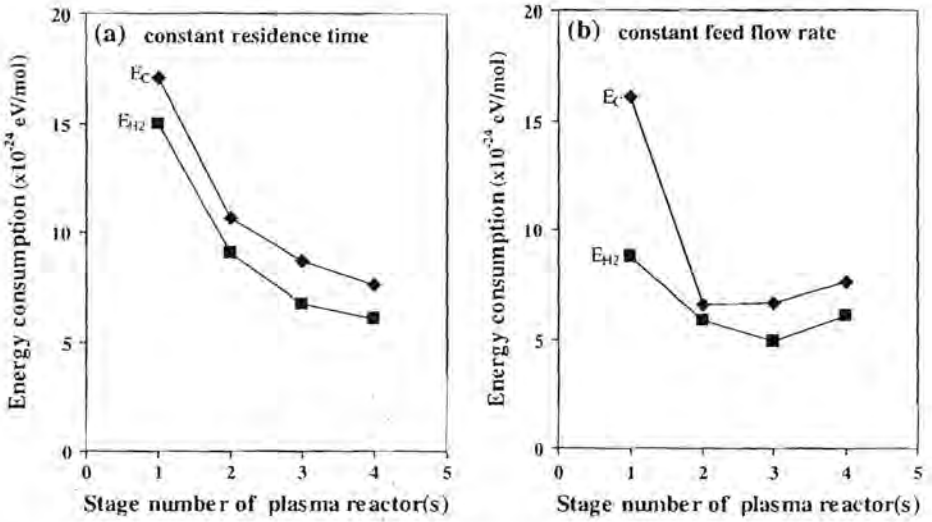

Fig. 8 Effect of stage number of plasma reactors on energy consumption (E_C = energy consumption per mole of reactants converted and E_{H2} = energy consumption per mole of hydrogen produced) for the reforming of natural gas with pure O_2 addition: **a** at a constant residence time of 4.38 s and **b** at a constant feed flow rate of 125 cm^3/min (hydrocarbon-to-oxygen molar ratio, 2/1; applied voltage, 17.5 kV; frequency, 300 Hz; and electrode gap distance, 6 mm)

with increasing stage number from 1 to 3 stages and then decreased when the stage number was further increased, whereas the H_2/CO molar ratio did not vary much. This also implies that the dehydrogenation and coupling reactions were favorable to take place at a higher residence time and to reach maximum levels at a very high residence time.

Effect of Stage Number on Energy Consumption

Constant Residence Time As shown in Fig. 8a, the sharp decreases in the energy consumption per mole of both reactants converted and hydrogen produced with increasing stage number of plasma reactors were observed at the constant residence time, especially from 1 to 2 stages, as observed above. The minimum energy consumption was 7.58×10^{24} eV per mole of reactants converted and 6.07×10^{24} eV per mole of hydrogen produced at 4 stages of plasma reactors operated with partial oxidation, which were both significantly lower than those of the system without partial oxidation (Fig. 5a).

Constant Feed Flow Rate For the multistage plasma system operated at the constant feed flow rate, the energy consumption per mole of reactants converted rapidly declines with increasing stage number of plasma reactors from 1 to 2 stages, and after that it remains almost constant, as depicted in Fig. 8b. Moreover, the energy consumption per mole of hydrogen produced decreased until reaching 3 stages, and then it slightly increased at 4 stages. The minimum energy consumption was observed to be about 6.58×10^{24} eV per mole of reactants converted at 2 stages of plasma reactors and 4.90×10^{24} eV per mole of hydrogen produced at 3 stages of plasma reactors, also being much lower than those of the system without partial oxidation (Fig. 5b).

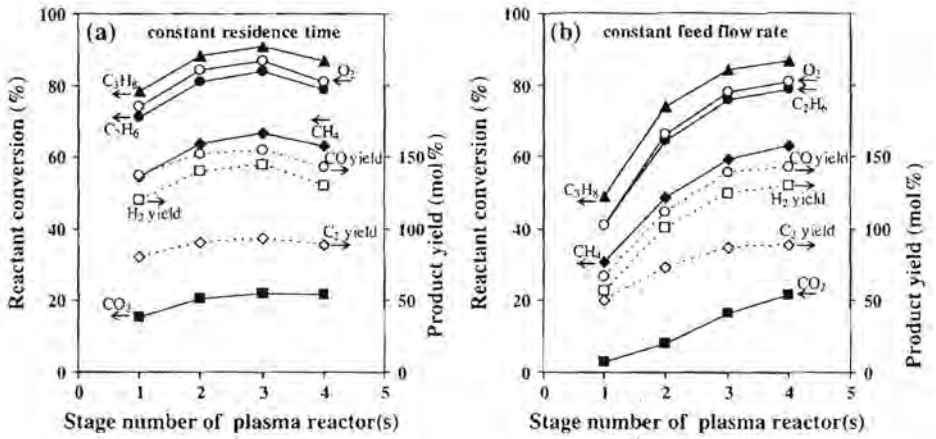

Fig. 9 Effect of stage number of plasma reactors on reactant conversions and product yields for the reforming of natural gas with air addition: **a** at a constant residence time of 4.38 s and **b** at a constant feed flow rate of 125 cm^3/min (hydrocarbon-to-oxygen molar ratio, 2/1, applied voltage, 17.5 kV; frequency, 300 Hz; and electrode gap distance, 6 mm)

Results of Natural Gas Reforming with Partial Oxidation Using Air

Effect of Stage Number on Reactant Conversion and Product Yield

Constant residence time As shown in Fig. 9a, similar to the case of pure oxygen, the conversions of all reactants and the yields of H_2 and C_2 slightly increase with increasing stage number from 1 to 3 stages. The same explanation as in the case of pure oxygen can be used for the case of air for the partial oxidation at the constant residence time. However, at 4 stages, the conversions remained almost constant in the case of air, whereas they adversely decreased in the case of pure oxygen (Fig. 6a). It may be proposed that the backward reactions of some products and/or the coupling reactions may take place. Interestingly, the CO_2 conversion also increased with increasing stage number of plasma reactors when using air as an oxygen source, which is in contrast with the use of pure oxygen, as discussed later.

Constant Feed Flow Rate As depicted in Fig. 9b, at the constant feed flow rate, all the reactant conversions and the product yields markedly increase as the stage number of plasma reactors increases up to 4 stages. It can be hypothesized that the higher stage number of plasma reactors, or longer residence time, allows more opportunity for highly energetic electrons to collide with reactant molecules, especially oxygen molecules in air, for subsequent reactions, leading to higher reactant conversions and product yields. It can be noticed that the H_2 yield became much higher than the C_2 yield at a higher stage number of plasma reactors, indicating that the dehydrogenations and oxidative dehydrogenations to produce hydrogen are more favorable to occur than the coupling reactions at a longer residence time.

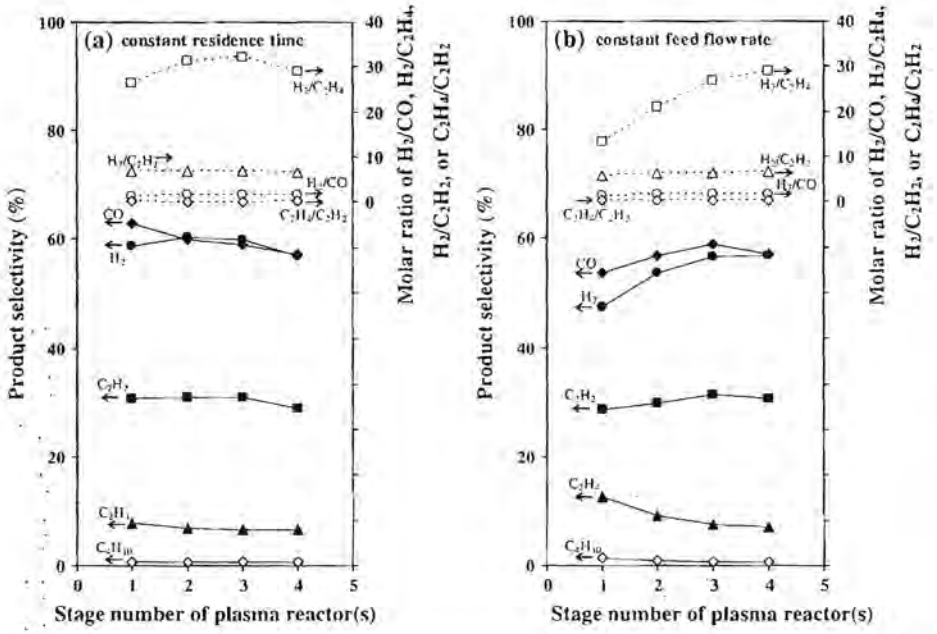

Fig. 10 Effect of stage number of plasma reactors on product selectivities and product molar ratios for the reforming of natural gas with air addition: **a** at a constant residence time of 4.38 s and **b** at a constant feed flow rate of 125 cm^3/min (hydrocarbon-to-oxygen molar ratio, 2/1; applied voltage, 17.5 kV; frequency, 300 Hz; and electrode gap distance, 6 mm)

Effect of Stage Number on Product Selectivity and Product Molar Ratio

Constant Residence Time For the constant residence time, the selectivities for C_2H_2, C_2H_4, and C_4H_{10} remain nearly unchanged, while the selectivity for CO slightly declines with increasing stage number of plasma reactors, as shown in Fig. 10a. This can be explained in that increasing the stage number of plasma reactors results in a greater opportunity for CO oxidation. The molar ratio of H_2/C_2H_4 increased with increasing stage number of plasma reactors from 1 to 3 stages; however, after that it tended to decrease. This suggests that oxidative dehydrogenation of C_2H_4 is likely to occur, leading to an increase in the H_2 selectivity with increasing stage number of plasma reactors from 1 to 3 stages.

Constant Feed Flow Rate The selectivities for CO, H_2, and C_2H_2 increase with increasing stage number of plasma reactors, whereas the selectivity for C_2H_4 tends to decrease, and the selectivity for C_4H_{10} remains unchanged for the constant feed flow rate, as shown in Fig. 10b. Figure 10b also shows the rapid increase in the molar ratio of H_2/C_2H_4, while the molar ratios of the others were nearly unchanged. These results can be explained in that with increasing stage number of plasma reactors, the dehydrogenation reactions more favorably occur, as mentioned above.

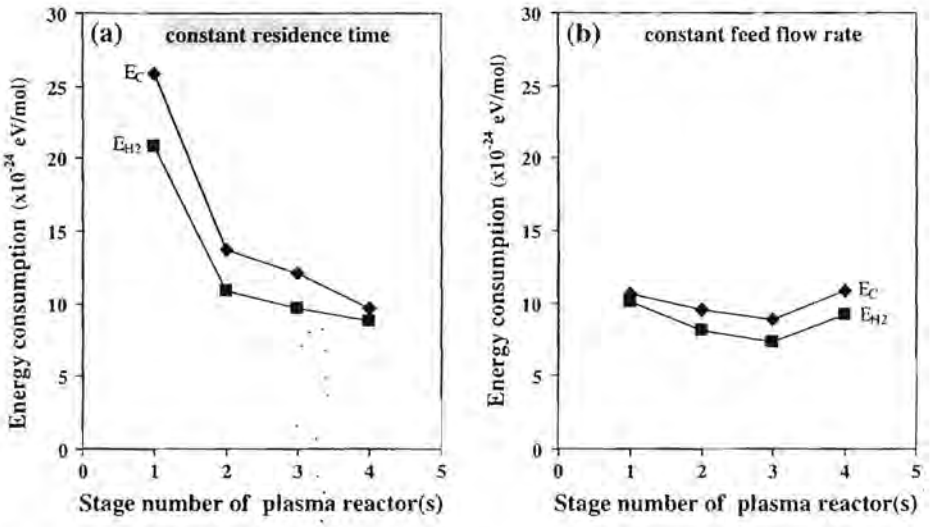

Fig. 11 Effect of stage number of plasma reactors on energy consumption (E_C = energy consumption per mole of reactants converted and E_{H2} = energy consumption per mole of hydrogen produced) for the reforming of natural gas with air addition: **a** at a constant residence time of 4.38 s and **b** at a constant feed flow rate of 125 cm^3/min (hydrocarbon-to-oxygen molar ratio, 2/1; applied voltage, 17.5 kV; frequency, 300 Hz; and electrode gap distance, 6 mm)

Effect of Stage Number on Energy Consumption

Constant Residence Time The same tendency of the energy consumption per mole of reactants converted and per mole of hydrogen produced for the constant residence time was found (Fig. 11a), as also observed in the previous case of pure oxygen addition, that they tended to rapidly decline from 1 to 2 stages, but after that only gradually decreased.

Constant Feed Flow Rate For the constant feed flow rate, the energy consumption both per mole of hydrogen produced and per mole of hydrocarbons converted decreases with increasing stage number of plasma reactors from 1 to 3 stages, but beyond 3 stages, it conversely increases, as shown in Fig. 11b. The minimum energy consumption was 7.38×10^{24} eV per mole of hydrogen produced and 8.87×10^{24} eV per mole of reactants converted at 3 stages of plasma reactors. At 4 stages, the higher energy consumption was observed due to less reactant conversions, despite higher H_2 production, as compared to the 3 stages of plasma reactors.

Comparisons of Reforming of Natural Gas with and without Partial Oxidation

Two systems with a constant residence time and a constant feed flow rate were so far investigated. From an engineering point of view, the systems operating at a constant residence time under different feed flow rates with and without oxygen addition are more meaningful for making a comparison. Figures 12, 13, 14, and 15 show the comparative results of the CO_2-containing natural gas reforming with and without the addition of either pure oxygen or air using the multistage plasma system under the operating conditions of a constant residence time of 4.38 s, an applied voltage of 17.5 kV, a frequency of 300 Hz, an electrode gap distance of 6 mm, and a hydrocarbon-to-oxygen molar ratio of 2/1.

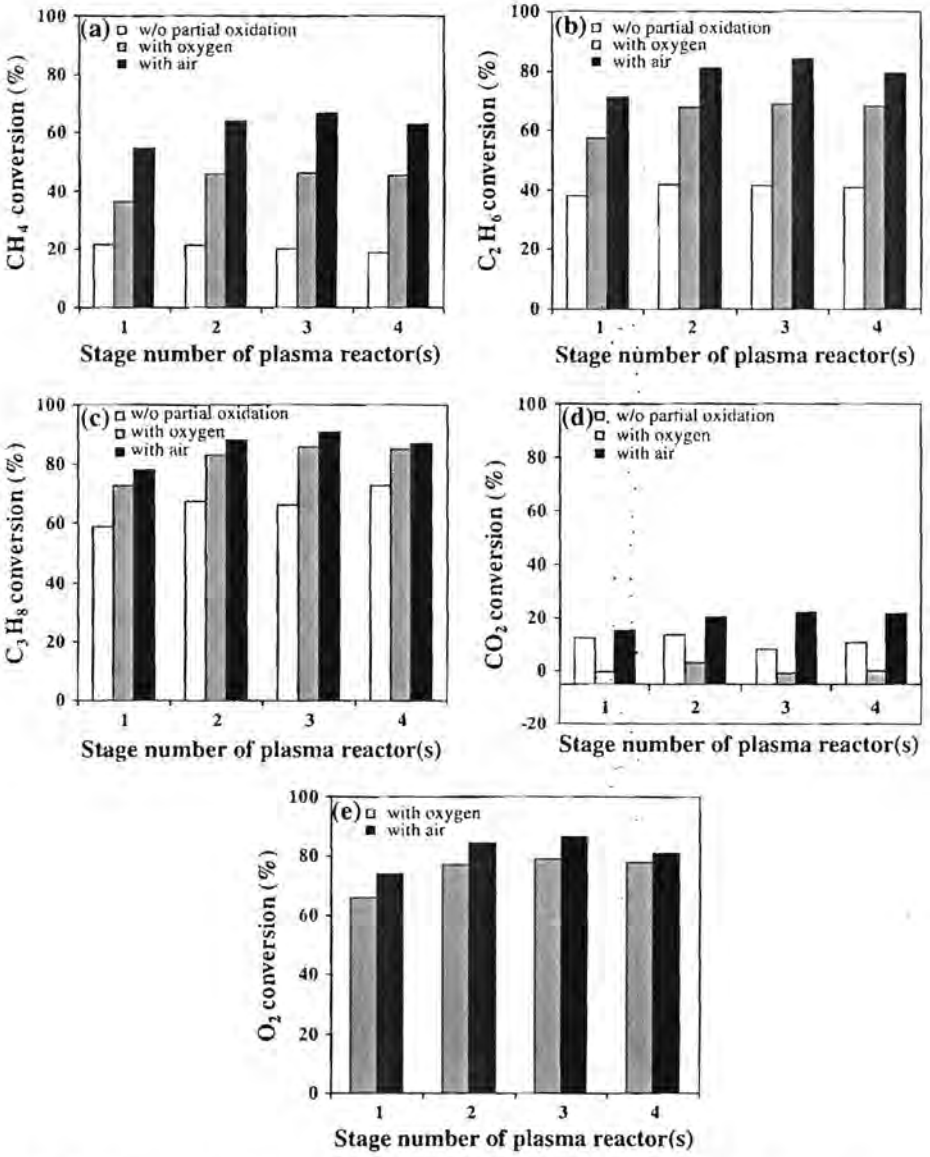

Fig. 12 Comparisons of conversions of **a** CH_4, **b** C_2H_6, **c** C_3H_8, **d** CO_2, and **e** O_2 of the reforming of natural gas with and without partial oxidation at different stage numbers of plasma reactors (applied voltage, 17.5 kV; frequency, 300 Hz; electrode gap distance, 6 mm; residence time, 4.38 s; and hydrocarbon-to-oxygen molar ratio, 2/1)

The conversions of all reactants, except CO_2, increase substantially in the presence of oxygen compared to that without the partial oxidation (Fig. 12). This may be because oxygen molecules assist in improving the performance of the reactions, especially via the oxidative dehydrogenation to produce hydrogen [18]. For a comparison between the two oxygen sources, the air system provided a higher process performance in terms of reactant conversions than the pure oxygen system. The results reveal that the addition of air in the

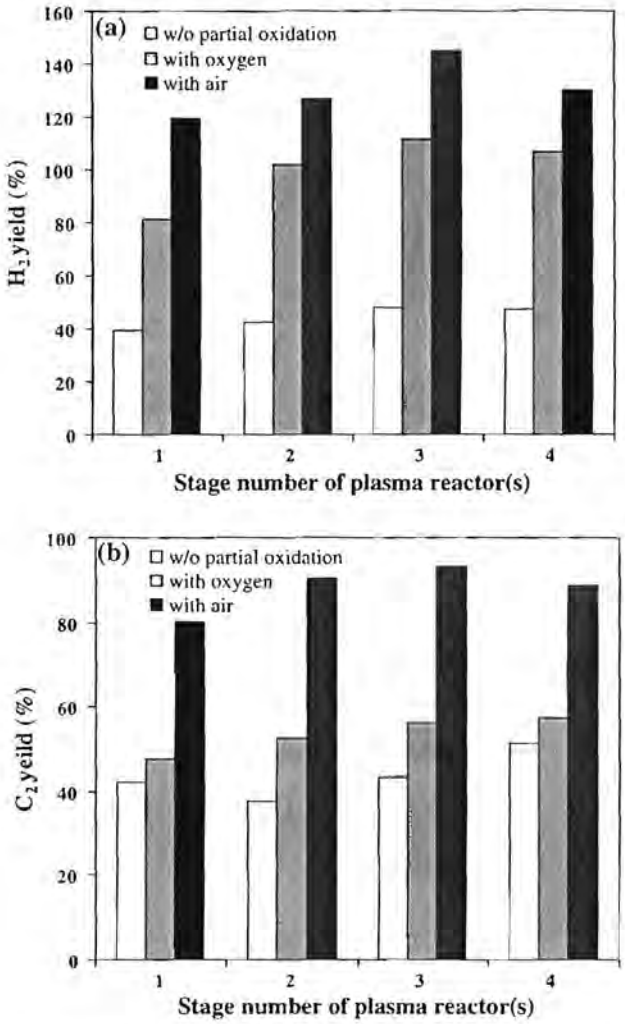

Fig. 13 Comparisons of yields of **a** H_2 and **b** C_2 of the reforming of natural gas with and without partial oxidation at different stage numbers of plasma reactors (applied voltage, 17.5 kV; frequency, 300 Hz; electrode gap distance, 6 mm; residence time, 4.38 s; and hydrocarbon-to-oxygen molar ratio, 2/1)

feed potentially contributes the positive effect to the activation of reactant gases for the reforming of CO_2-containing natural gas. Surprisingly, the CO_2 conversion in the case of adding pure oxygen exhibited comparatively lower values that those of the air system at all stages of plasma reactors. This can be explained in that the nitrogen molecules in air possibly act as the third body to facilitate chemical reactions by altering the dielectric properties of the system and/or by reducing the activation energies of some chemical reactions [20]. From the results, the highest reactant conversions were attained at 3 stages of plasma reactors when using air as an oxygen source.

As shown in Fig. 13, the system with oxygen addition provided much higher H_2 and C_2 yields than the system without oxygen addition because the oxygen molecules can be easily activated by the plasma to form several oxygen active species for extracting the H

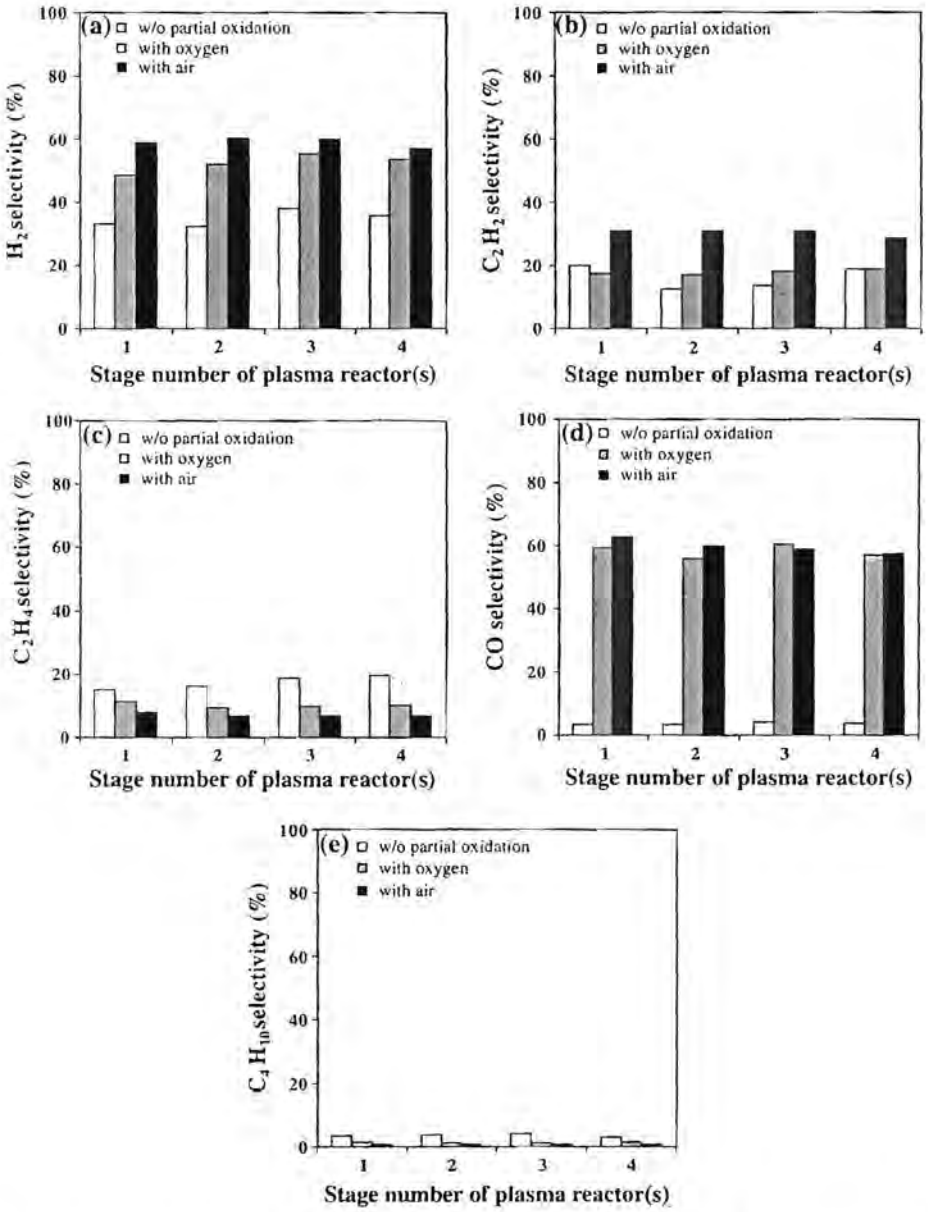

Fig. 14 Comparisons of selectivities for **a** H_2, **b** C_2H_2, **c** C_2H_4, **d** CO, and **e** C_4H_{10} of the reforming of natural gas with and without partial oxidation at different stage numbers of plasma reactors (applied voltage, 17.5 kV; frequency, 300 Hz; electrode gap distance, 6 mm; residence time, 4.38 s; and hydrocarbon-to-oxygen molar ratio, 2/1)

atoms from the hydrocarbon molecules, as mentioned above. Interestingly, for the case of oxygen addition, the use of air as an oxygen source also provided significantly higher product yields than that of pure oxygen. These can be explained in that nitrogen molecules in air can possibly act as the third body to facilitate the reactions, as also mentioned above.

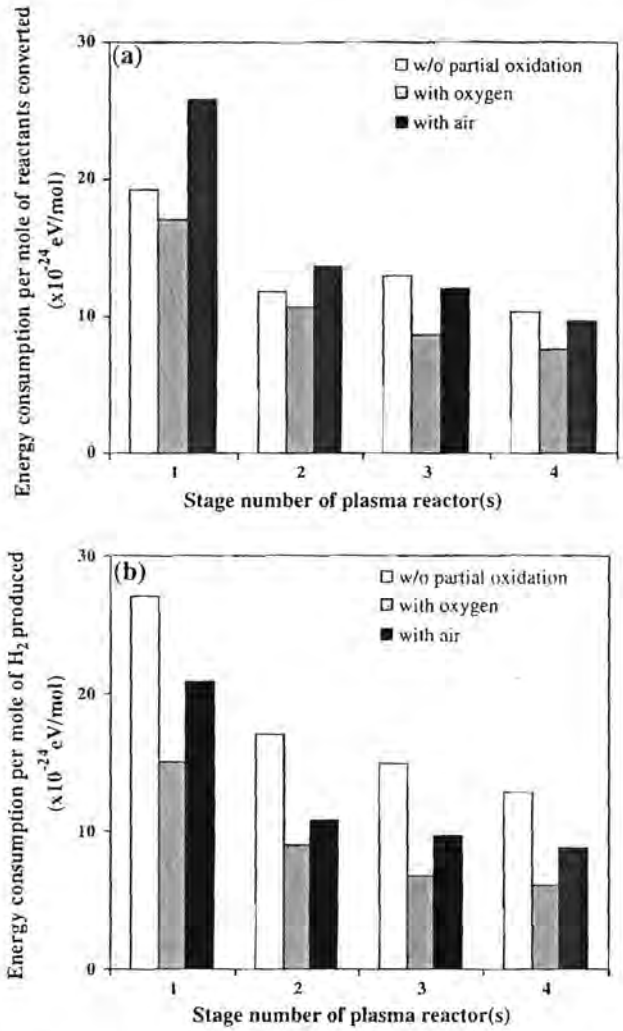

Fig. 15 Comparisons of energy consumption for the reforming of natural gas with and without partial oxidation at different stage numbers of plasma reactors: **a** energy consumption per mole of reactants converted (E_C) and **b** energy consumption per mole of hydrogen produced (E_{H2}) (applied voltage, 17.5 kV; frequency, 300 Hz; electrode gap distance, 6 mm; residence time, 4.38 s; and hydrocarbon-to-oxygen molar ratio, 2/1)

Moreover, 3 stages of plasma reactors were clearly found to provide the highest yields of H_2 and C_2, in addition to the highest reaction conversions, for both systems (i.e. with pure oxygen and air addition).

The product selectivities are shown comparatively in Fig. 14. Most of the product selectivities, except for the C_2H_4 and C_4H_{10} selectivities, significantly increased, especially for the CO selectivity, when adding both oxygen sources to the system. However, the addition of oxygen provided negative effect on the C_2H_4 and C_4H_{10} selectivities because the oxygen active species generated by the plasma are responsible for the oxidative dehydrogenations of both reactants and intermediates to form H_2 and C_2H_2 products instead

of more saturated C_2H_4 and C_4H_{10} products. Moreover, when comparing the ability of pure oxygen and air to induce the H_2 formation, it was clearly observed that using air as an oxygen source provided the superior performance.

The energy consumption of the investigated systems is shown comparatively in Fig. 15. The energy consumption per mole of reactants converted of the systems with oxygen addition tended to become lower than that without oxygen addition at any given stage number of plasma reactors. However, the energy consumption per mole of hydrogen produced of the systems with oxygen addition was clearly lower than that without oxygen addition at all stage numbers of plasma reactors. When considering the energy consumption at high stage numbers in the cases of both the pure oxygen and the air additions, even though using the pure oxygen as an oxygen source consumed less energy for the plasma system operation, the system with the pure oxygen addition showed lower energy consumption both per mole of reactants converted and per mole of hydrogen produced than that with the air addition. Moreover, since no other works have been performed to investigate the reforming of natural gas by using any gliding arc discharge systems, the energy consumption in this present work cannot be evaluated for making a comparison. However, from our previous work [13], the energy consumption of the gliding arc discharge system was found to be lower than that of the corona discharge system for the reforming of methane with partial oxidation. This verifies the high efficiency of the gliding arc discharge system.

From these comparisons, it can be concluded that the addition of oxygen (pure oxygen or air) provided positive effects on the reforming of CO_2-containing natural gas with not only enhancing the reactant conversions, the desired product yields, and the desired selectivities, but also on consuming comparatively less energy for producing hydrogen, as compared to the system without the oxygen addition. In addition, the use of air as the oxygen source assists in improving the reforming of CO_2-containing natural gas more effectively than pure oxygen in terms of both higher reactant conversions and higher product yields and selectivities, which are more advantageous from an economic viewpoint, even though the energy consumption is slightly higher for the system with air addition. Finally, from the overall results, it can also be reasonably concluded that 3 stages of plasma reactors are sufficient to achieve a satisfactorily high process performance.

Conclusions

The combined reforming and partial oxidation of CO_2-containing natural gas was investigated under two systems with a constant residence time and a constant feed flow rate by using a multistage gliding arc discharge system. The major products were mainly hydrogen and C_2 hydrocarbons. For the system without partial oxidation operated at a constant feed flow rate, all reactant conversions, except CO_2 conversion, as well as product yields and product selectivities, increased with increasing stage number of plasma reactors. For the system operated at a constant residence time, the stage number of plasma reactors only slightly affected the reactant conversions, product yields, and product selectivities. For the system with partial oxidation, the stage number of plasma reactors provided positive effects on the reactant conversions, product yields, and product selectivities, and also energy consumption was also lower compared to the system without partial oxidation. The addition of air as the oxygen source provided better process performance for the reforming of CO_2-containing natural gas than that of pure oxygen in terms of higher selectivities and yields, with reasonably low energy consumption. Moreover, the plasma system with 3 stages of plasma reactors led to good process performance with acceptably high reactant conversions and desired product yield.

Acknowledgments The authors would like to thank the Ratchadapisek Somphot Endowment Fund, Chulalongkorn University, Thailand; the Commission on Higher Education, Thailand; the National Research Council of Thailand (NRCT); the Sustainable Petroleum and Petrochemicals Research Unit, Center for Petroleum, Petrochemicals, and Advanced Materials, Chulalongkorn University, Thailand; and the Petrochemical and Environmental Catalysis Research Unit under the Ratchadapisek Somphot Endowment Fund, Chulalongkorn University, Thailand.

References

1. Jeong HK, Kim SC, Han C, Lee H, Song HK, Na BK (2001) Korean J Chem Eng 18:196–201
2. Li MW, Xu GH, Tian YL, Chen L, Fu HF (2004) J Phys Chem A 108:1687–1693
3. Hwang BB, Yeo YK, Na BK (2003) Korean J Chem Eng 20:631–634
4. Xu H, Shi K, Shang Y, Zhang Y, Xu G, Wei Y (1999) J Mol Catal A: Chem 147:41–46
5. Effendi A, Zhang ZG, Hellgardt K, Honda K, Yoshida T (2002) Catal Today 77:181–189
6. Supat K, Chavadej S, Lobban LL, Millinson RG (2003) Ind Eng Chem Res 42:1654–1661
7. Supat K, Kruapong A, Chavadej S, Lobbon LL, Mallinson RG (2003) Energ Fuel 17:418–474
8. Paulmier T, Fulcheri L (2005) Chem Eng J 106:59–71
9. Eliasson B, Hirth M, Kogeischatz U (1987) J Appl Phys 20:1421–1437
10. LA Rosacha, GK Anderson, LA Bechtold, JJ Coogan, HG Heck, M Kang, WH McCulla, RA Tennant, PJ Wantuck (1993) NATO ASI Series, Part B 34
11. Krawczyk K, Młotek M (2001) Appl Catal B: Environ 30:233–245
12. Chavadej S, Kiatubolpaiboon W, Rangsunvigit P, Sreethawong T (2007) J Mol Catal A: Chem 263:128–136
13. Sreethawong T, Thakonpatthanakun P, Chavadej S (2007) Int J Hydrogen Energ 32:1067–1079
14. Chavadej S, Saktrakool K, Rangsunvigit P, Lobban LL, Sreethawong T (2007) Chem Eng J 132 345–353
15. Sreethawong T, Suwannabart T, Chavadej S (2008) Plasma Chem Plasma Process 28:629–642
16. Chavadej S, Tansuwan A, Sreethawong T (2008) Plasma Chem Plasma Process 28:643–662
17. Rueangjitt N, Akarawitoo C, Sreethawong T, Chavadej S (2007) Plasma Chem Plasma Process 27: 559–576
18. Rueangjitt N, Sreethawong T, Chavadej S (2008) Plasma Chem Plasma Process 28:49–67
19. Dean JA (1999) Lange's handbook of chemistry, 5th edn. McGraw-Hill, New York
20. Indarto A, Choi JW, Lee H, Song HK (2006) Energy 31:2650–2659